Posttranslational Regulation of Copper Transporters

Peter V.E. van den Berghe

Coverdesign: Erwin & Peter van den Berghe
(oude sluizen Hansweert 1967)
ISBN: 978-90-786-7560-0
Printed by: F&N Eigen Beheer, Amsterdam

The research presented in this thesis was performed in the Department of Metabolic and Endocrine Diseases, and the Netherlands Metabolomics Center, Wilhelmina Children's Hospital of the University Medical Center Utrecht, The Netherlands. This work was financially supported by the Dutch Organization for Scientific Research (NWO 912-04-106).

The printing of this thesis was financially supported by contributions from de J.E. Jurriaanse Stichting, de Nederlandse Vereniging voor Hepatologie, Biolegio B.V., Eurogentec B.V., de Universiteit Utrecht, and the department of Metabolic and Endocrine diseases.

Posttranslational Regulation of Copper Transporters

Posttranslationele Regulatie van Kopertransporters

(met een samenvatting in het Nederlands)

Proefschrift

ter verkrijging van de graad van doctor aan de Universiteit Utrecht
op gezag van de rector magnificus, prof.dr. J.C. Stoof, ingevolge het
besluit van het college voor promoties in het openbaar te verdedigen
op dinsdag 28 april 2009 des middags te 2.30 uur

door

Petrus Victor Eppo van den Berghe

geboren op 3 januari 1980,
te Reimerswaal

Promotor: Prof.dr. R. Berger

Co-promotor: Dr. L.W.J. Klomp

Voor Opa Vic

Table of contents

4-PBA	4-phenylbutyric acid
A-domain	actuator domain
ATP7A	copper-transporting P1B-type ATPase 7A
ATP7B	copper-transporting P1B-type ATPase 7B
BCS	bathocuproinedisulfonic acid
CTR	copper transporter
CTR1	copper transporter 1
CTR2	copper transporter 2
DFO	desferrioxamine
DMEM	Dulbecco's modified Eagle's medium
DMT1	divalent metal transporter 1
eGFP	enhanced green fluorescent protein
EGS	ethylene glycolbis(succinimidylsuccinate)
ER	endoplasmic reticulum
ERAD	ER-associated protein degradation
EV	empty vector
FCS	fetal calf serum
FRET	foster-resonance energy transfer
GABA	gamma-aminobutyric acid
GSH	Glutathione
GST	Glutathione S transferase
hCTR	human CTR
HEK-293T	human embryonic kidney cell expressing the large T-antigen of SV40
HSPs	heat shock proteins
LAMP	lysosome-associated membrane protein
M-domain	transmembrane domain
MBD	metal binding domain
MBS	metal binding site
MEF	mouse embryonic fibroblast
MD	Menkes disease
MT	metallothionein
MTF-1	metal-responsive transcription factor-1
MTT	3-(4,5-dimethylthiazol-2-yl)-2,5-diphenyl-2H-tetrazolium bromide
MRE	metal-responsive element
N-domain	nucleotide binding domain
OHS	occipital horn syndrome
P-domain	phosphorylation domain
PEI	polyethyleneimine
PFIC2	progressive familial intrahepatic cholestasis Type 2
qRT-PCR	quantitative Reverse Transcriptase Polymerase Chain Reaction
RLU	relative light units
ROS	reactive oxygen species
SV40	simian virus 40
TfR	transferrin receptor
TGN	trans-Golgi network
UPR	unfolded protein response
vsvG	vesicular-stomatitis-virus glycoprotein
WD	Wilson disease
WT	wild type

PREFACE

The transition metal copper is essential for all organisms that require oxygen. Copper can occur in two redox states, the oxidized Cu^{1+} and the reduced Cu^{2+}. This ability makes copper a versatile cofactor for many redox-active enzymes. However, this same feature enables the generation of toxic reactive oxygen species (ROS). To circumvent the deleterious consequences of copper deficiency and copper overload, organisms have evolved intricate mechanisms, performed by highly conserved proteins, to balance copper uptake, distribution and export on both the systemic and cellular level. Perturbations of these mechanisms underlie severe genetic disorders of copper homeostasis in humans. The fatal neurodevelopmental disorders Menkes disease is caused by systemic copper deficiency, due to mutations in the *ATP7A* gene on the X-chromosome. In contrast, patients with Wilson disease develop toxic hepatic copper accumulation due to autosomal recessive mutations in the *ATP7B* gene. ATP7A and ATP7B are homologous and functionally equivalent copper-transporting P_{1B}-type ATPases, which are expressed in distinct tissues in the human body and required for cellular copper export. In lower unicellular eukaryotes like the yeast *Saccharomyces cerevisiae*, copper homeostasis is achieved mainly by copper-dependent transcriptional regulation of copper transport proteins, including the yeast homologue of ATP7A and ATP7B. Unlike yeast cells, mammalian cells exert homeostatic control of copper metabolism predominantly by posttranscriptional mechanisms that control the activity of cellular copper import and export proteins. These mechanisms may comprise activating or inactivating posttranslational protein modifications, regulated protein-protein interactions, copper-dependent regulation of subcellular localization, and regulation of protein synthesis, stabilization and degradation. Although many of the transport proteins responsible for copper uptake and export in mammalian cells have been cloned and characterized, our knowledge about the regulation of cellular copper uptake and export is far from complete. **The aim of this thesis is therefore to unravel posttranslational mechanisms that regulate cellular copper uptake and export in relation to the molecular pathogenesis of Wilson disease.** As an important tool to investigate copper uptake and export in mammalian cells, we developed a new genetically-encoded copper sensor. This sensor enabled us to quantitatively measure bioavailable copper and allowed us to delineate the effects of copper import and export proteins on cytoplasmic copper availability.

The first part of this thesis contains a detailed introduction of the current knowledge on copper transporter biology in mammalian cells. The regulation of dietary copper uptake is reviewed and introduced in **chapter 1**. Here, I focus on the contribution of the intestine to the regulation of body copper homeostasis. The regulatory functions of enterocytes with respect to cellular copper uptake, intracellular distribution, and cellular copper export are reviewed. Regulation of cellular copper export by P_{1B}-type ATPases ATP7A and ATP7B is introduced in **chapter 2**. In this chapter, the structural and functional similarities and differences between these copper transporting P-type ATPases are discussed with respect to regulation of subcellular localization, biological function, protein-protein interactions and known posttranslational modifications. In addition, the clinical and pathophysiological consequences of hereditary mutations in these genes, leading to the copper homeostasis disorders Menkes disease and Wilson disease, respectively, are briefly introduced. The distinction between copper uptake and export as carried out in the introductory part of this thesis is maintained in the subsequent experimental chapters.

In the second part of this thesis, the mechanisms of cellular copper uptake are further explored in **chapters 3 and 4**. Cellular copper uptake is highly conserved in evolution and copper uptake is mainly mediated by members of the SLC31 superfamily of copper transporters (CTR), comprising hCTR1 and hCTR2 in humans. Previous studies in our laboratory and those of others had identified hCTR1 as an essential high-affinity copper import protein. These studies had also identified a CTR1-independent copper uptake activity in mammalian cells. In **chapter 3**, we set out to characterize the protein responsible for this CTR1-independent copper uptake activity, we identified hCTR2 as a novel human copper transporter with low affinity compared to hCTR1. hCTR1 localized to both the plasmamembrane and to intracellular organelles, whereas hCTR2 was exclusively localized into intracellular vesicular structures, suggesting that these distinct human CTR proteins may mobilize different copper pools. Next, we studied the structural requirements for CTR-dependent copper import. CTR proteins are thought to form aqueous copper-permeable channels by assembling in oligomeric complexes comprising three CTR subunits. The necessity of this oligomerization process with respect to functional copper uptake *in vitro* is addressed in **chapter 4**. Here, we adopted a dominant-negative approach, using a non-functional mutant of hCTR1, to provide compelling evidence that hCTR1-mediated copper import requires assembly of hCTR1 subunits in a homo-oligomeric complex. Parallel studies using non-functional hCTR2 subunits yielded similar results, indicating that the requirement to form oligomers is a common property of CTR proteins.

In the third part of this thesis, we addressed the posttranslational regulatory mechanisms of copper export. The strategy of our experiments was inspired by aberrant copper export as observed in Wilson disease patients. In **chapter 5,** we investigated the molecular consequences of mutations in functional P_{1B}-type ATPase consensus domains as well as Wilson disease-associated mutations in *ATP7B* with respect to protein expression, function, subcellular localization and protein-protein interactions. The fact that most missense mutations in ATP7B caused protein misfolding enabled us to asses a novel treatment strategy using pharmacological folding chaperones that are known to improve protein folding and consequently protein expression and functional recovery.

In the summarizing discussion in **chapter 6**, our results obtained in **chapters 3-5** are discussed and integrated in a model describing our current knowledge on the posttranslational regulation of mammalian copper homeostasis in health and disease.

CHAPTER 1

Regulation of Intestinal Copper Absorption

Peter V.E. van den Berghe
Leo W.J. Klomp

Review, in preparation

Abstract

The transition metal copper is an essential trace element involved in many enzymatic processes that require redox-chemistry. The redox-activity of copper is potential harmful, and misbalance of copper homeostasis is therefore associated with severe hereditary disorders. Copper is acquired from our diet by intestinal copper absorption and subsequent distribution throughout the body. However, the regulatory role of the intestine in body copper homeostasis is currently poorly understood. In this review we evaluate novel findings regarding intestinal copper uptake. The role of recently identified transporters in enterocyte copper uptake and excretion into the portal circulation is described, and we discuss the regulation of dietary copper uptake during physiological and pathophysiological conditions.

Introduction

Trace elements, such as iron, zinc and copper, are needed in only small quantities, but are absolutely required to sustain life. It is estimated that more than one billion people worldwide suffer from nutritional trace element deficiency, either isolated or combined. Trace element deficiency thus represents a major global health problem, which necessitates detailed understanding of the mechanisms by which trace metals are handled in humans.

Copper homeostasis is balanced around a remarkable paradox: copper is an essential transition metal for all organisms that require oxygen for life. Copper is a cofactor for multiple redox enzymes involved in respiratory oxidation, neurotransmitter synthesis, iron metabolism and other processes. Excessive copper is very harmful, because copper can catalyze the Fenton reaction that generates the superoxide anion. These superoxide anions together with hydrogen peroxide act as a substrate for the Haber-Weiss reaction that generates harmful reactive hydroxyl radicals [1]. This copper homeostasis paradox is clearly illustrated by two human genetic disorders Wilson disease (WD) (OMIM 277900) and Menkes disease (MD) (OMIM 309400), which are associated with hepatolenticular copper overload or systemic copper deficiency, respectively. To maintain body copper homeostasis within narrow boundaries, copper uptake, distribution and excretion are strictly regulated.

In the gut, copper is absorbed by enterocytes prior to distribution of copper throughout the body (Figure 1). The daily copper absorption in the gut is approximately 0.6 to 1.6 mg/day. Approximately 4.5 mg/day is excreted into the gastrointestinal tract in fluids like saliva, gastric juice, pancreatic juice (approx. 2 mg/day) and bile (approx. 2.5 mg/day) [2]. Absorption of copper mainly occurs in the stomach and duodenum. Only 0.5 to 2.5 mg/day is cleared from the body by defecation, indicating that most of the secreted copper is reabsorbed [2]. Newly absorbed copper is transported by the portal vein and is largely taken up by hepatocytes. The liver also excretes excessive copper into the bile. The bile has been shown to contain a copper pool that is not subject to reabsorption, and since the proportion of copper excreted in urine is negligible under physiological conditions, biliary excretion is the main mechanism to discard excessive copper from the body [2-4]. Copper homeostasis can also be regulated at the point of copper entry. Dietary copper absorption is affected by several parameters like age, sex, the type of food (plant versus animal proteins), the amount of copper in the diet, and the use of oral contraceptives, as was demonstrated by copper tracer studies in humans and monkeys [5-14]. Currently, the role of the intestine in the regulation of body copper homeostasis is poorly understood, but recent exciting studies have uncovered some of the transporters involved in intestinal copper uptake. In this review we focus on the regulation of intestinal copper uptake and transcellular transport into the blood stream during physiological and pathophysiological conditions. Detailed insight into these processes should assist in designing improved therapeutic strategies in the treatment of copper homeostasis disorders.

Physiology and pathophysiology of copper homeostasis

Current models describe copper distribution throughout the body as a biphasic process (Figure 1). In the first phase, dietary copper is absorbed by enterocytes and is readily exported into

the portal venous system for subsequent distribution throughout the body. The absorption of dietary copper is dependent of the amount of dietary copper. Studies in young men with stable ^{65}Cu isotopes revealed that a daily copper uptake of only 0.8 mg copper is enough to maintain body copper homeostasis [10]. Copper absorption is higher in women (71%) compared to men (64%) aged 20 - 59 years using radioactive ^{67}Cu measurements [8], but the net copper absorption was not different. These data suggest that the copper requirement is different for men and women. Within the age of 20 - 59 years, copper absorption was also not different. However, weanling and suckling rats rely mainly on diffusion or paracellular transport for copper uptake, as the absorption is only copper concentration dependent [15]. In contrast, adolescent rats and mice developed a saturable copper uptake system with a K_m of approximately 10 - 13 μM [15, 16], indicating that intestinal copper absorption is altered during development. The difference in copper absorption mechanisms does not imply that adaptation is absent in suckling rats. Copper absorption was increased by copper supplementation in the milk, but serum levels in these animals remained unaffected as a result of increased copper retention in the intestine [17, 18]. In adults, the amount of copper absorption is inversely correlated with dietary copper intake: high dietary copper intake results in low copper absorption (as low as 12% from food diet), whereas copper absorption can reach approximately 65% from food diet when dietary copper concentrations are low [10-12]. Copper absorption is also dependent on the bioavailability of dietary copper. Copper absorption from a plant protein diet was 33.8% compared to 41.2% from an animal protein diet that was labeled with stable ^{65}Cu [13]. The net copper absorption was higher compared to the non-vegetarian diet as a result of the higher copper content in the vegetarian diet [7], but the absorption of copper was less efficient. In conclusion, both the amount of copper and other components in the diet affect copper absorption. The net copper uptake is increased by high dietary copper intake, suggesting that the intestine is an important, but not the only organ that regulates copper homeostasis.

After copper absorption, copper is delivered into the blood compartment. Here, copper is bound to small molecules such as Histidine, and to serum proteins like α2-macroglobulin and albumin (Figure 1) [19]. Copper bound to serum proteins is exchangeable, and this copper pool in the portal venous system enters the liver where copper is imported into hepatocytes [20]. Hepatic copper can be redistributed throughout the body by excretion into the blood. Approximately 65 - 90% [2, 20, 21, 22] of all copper present in plasma is intrinsic to the blue copper oxidase ceruplasmin, which is mainly synthesized and excreted by the liver, thus marking the second phase of the biphasic copper distribution in the body (Figure 1). The remaining plasma copper appears to be exchangeably bound to α2-macroglobulin (appr. 12%), albumin (appr. 18%), small peptides and amino acids [2, 21, 22], but the exact mechanisms of copper transport through the plasma, and how this exchangeable copper pool is presented to target cells, remain largely elusive. Ceruloplasmin is a ferroxidase and the six copper atoms bound to the ceruloplasmin molecule serve a catalytic role. Importantly, these copper atoms are non-exchangeable, precluding a role of ceruloplasmin as a classic copper transport protein in plasma (reviewed by [20]). Consistent with this notion, patients with hereditary loss-of-function mutations in the ceruloplasmin gene and ceruloplasmin knockout mice suffer from iron accumulation in the brain without clear defects in copper homeostasis [23, 24]. Completely desialylated ceruloplasmin is eventually endocytosed by

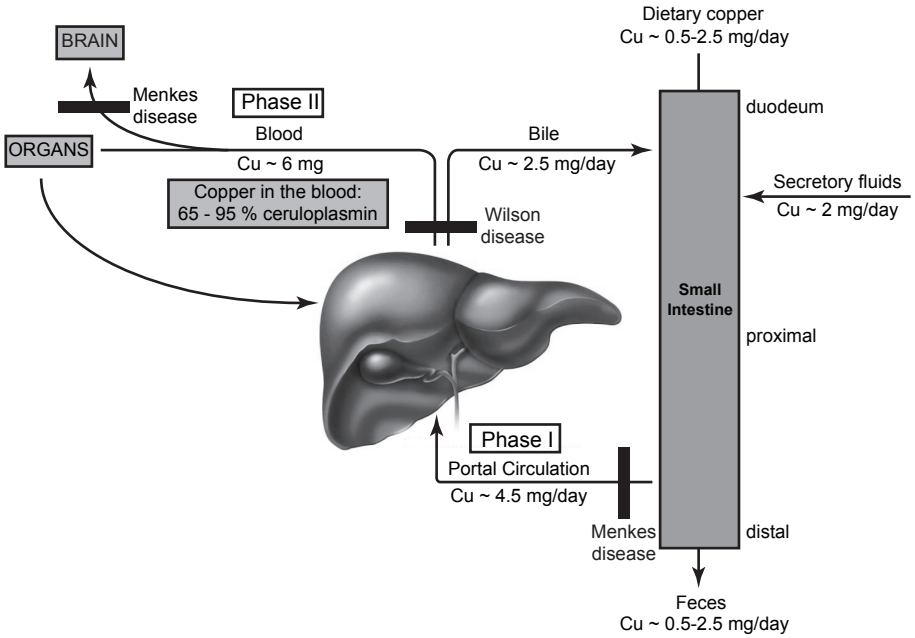

Figure 1. Schematic overview of copper body copper homeostasis
Dietary copper is predominantly absorbed in the duodenum and small intestine. The first phase of copper uptake and distribution is marked by copper transport to the portal venous circulation where virtually all copper is bound to serum proteins. Patients with MD have a block in copper uptake, caused by mutations in ATP7A resulting in a systemic copper deficiency. Most of the copper is absorbed by the liver, and is incorporated in apoceruloplasmin. The second phase of copper distribution is marked by the excretion of holoceruloplasmin into the blood. Excessive copper is excreted by the liver into the bile, and this copper is discarded from the body by defecation. Patients with WD suffer from copper toxicosis in the liver due to mutations in ATP7B.

hepatocytes by means of the asialoglycoprotein receptors [25, 26]. Following degradation of internalized ceruloplasmin in lysosomes, the copper is released. To maintain body copper homeostasis, hepatocytes excrete excessive copper into the bile to remove copper from the body (approximately 2.5 mg/day) (Figure 1). This biliary copper pool is bound to components, like bile salts, that immobilize copper, thus preventing reabsorption of copper [3, 4]. Copper excreted by the liver therefore leaves the body, which underscores the major role of the liver in the regulation of body copper excretion.

The necessity of a well-regulated copper export system is clearly illustrated by WD (Figure 1). WD patients have autosomal recessive mutations in the gene encoding ATP7B, a copper-transporting P_{1B}-type ATPase. The disorder has an incidence between 1:30,000 to 1:100,000 [27], and over three hundred different mutations have been identified [28]. ATP7B is predominantly expressed in the liver and to some extent in the brain, placenta, kidney, and mammary tissue [29-31]. WD patients suffer from toxic copper accumulation in different tissues, primarily in the liver and the brain. These patients present with a spectrum of clinical symptoms, but no clear genotype-phenotype correlation exists. Hepatic abnormalities like liver cirrhosis, chronic liver inflammation and fulminant liver failure are frequently seen. Neurological manifestations including Parkinsonian movement disorders, seizures, personality changes, depression and psychosis may also be characteristic clinical

abnormalities. Copper deposits are found in several tissues. For instance, copper can accumulate in the cornea, resulting in the typical Kayser-Fleisher ring. Treatment of WD is dependent on the manifestation of the symptoms. Fulminant liver failure requires liver transplantation, but the less severely affected patients benefit from the reduction of both copper uptake and increased copper excretion. Excretion can be promoted by treatment with copper chelating agents like penicillamine [32], trientine [32] and ammonium tetramolybdate [33, 34]. An additional strategy is zinc supplementation in the diet, which results in decreased copper absorption from the diet [35].

The necessity of copper is clearly illustrated in the fatal neurodevelopmental disorder MD (Figure 1). MD is a recessive X-linked disorder in which the gene encoding the P_{1B}-type ATPase ATP7A is mutated. The prevalence of MD is between 1:40,000 and 1:350,000 [36-38]. Mutations in *ATP7A* can results in classical MD, a less severe MD, and occipital horn syndrome (OHS; also known as X-linked cutis laxa, or Ehlers-Danlos syndrome type IX) that is allelic to MD [36]. Classical MD is typically characterized by neurological defects (neurodegeneration, severe mental retardation, and seizures), growth retardation, hypopigmentation, hypothermia, laxity of skin and joints, and peculiar 'kinky' or 'steely' hair [39-41]. Symptoms arise within 2-3 months after birth, and the average life-span is approximately three years. Patients with mild MD have less profound neurological symptoms and an increased average life-span [42-44]. *ATP7A* is homologous to *ATP7B*, and expression of ATP7B in skin-derived fibroblasts of MD patients functionally restores their copper-phenotypes, suggesting that these proteins have similar functions [45]. In contrast to ATP7B, ATP7A is ubiquitously expressed, including in the intestine, thus explaining why MD leads to generalized copper deficiency. Therapeutic strategies are therefore focused on the bypass of the copper uptake block in the intestine. The only strategy that fulfils this task to some extent is copper replacement therapy, which involves subcutaneous injection of copper-histidine [46]. Although this treatment is not effective for every patient, significant improvement was observed in patients with the milder variant of MD [46]. Unfortunately, the prognosis remains poor for patients with classical MD.

Intestinal copper absorption

Enterocytes are fully-differentiated polarized epithelial cells that line the intestinal track and are the gatekeepers that facilitate and regulate uptake of nutrients from the diet. Like any other cell, enterocytes are faced with the challenge to balance copper metabolism between essential and toxic levels. In fact, the enterocytes require substantial amounts of copper as a cofactor in the multicopper oxidase hephaestin, which serves as a ferroxidase with an essential role in the dietary uptake of iron [47, 48]. At the same time, sufficient copper must be made available by transcellular transport to provide the rest of the body with adequate amounts of the metal. The sequence of transport events by which dietary copper is moved from the intestinal lumen into the portal circulation is currently largely unknown and how this process is regulated is even more elusive. Several transmembrane transporters, intracellular copper chaperones and putative cupric reductases that may contribute to cellular copper uptake by enterocytes have been identified and this has provided important insight into the mechanisms of directional copper movement through the intestinal mucosa. Strong

evidence has recently accumulated that dietary copper uptake is absolutely dependent on at least two transport proteins, the high-affinity copper transporter 1 (CTR1) and ATP7A. In addition, the copper chaperone ATOX1 is essential for dietary copper uptake. More controversial or circumstantial evidence has implicated the divalent metal transporter 1 (DMT1) and the low-affinity copper transporter 2 (CTR2) within this process (Figure 2). Below, we discuss these molecules and integrate recent findings into a working-model of dietary copper uptake.

Enterocyte copper export

Dietary copper absorption is dependent on ATP7A, as is illustrated by the severe copper deficiency in patients with MD [39-41]. ATP7A is a copper-transporting P-type ATPase with a dual function. It translocates cytosolic copper into the biosynthetic pathway (i.e. Golgi network) for subsequent incorporation into cuproproteins that are ultimately secreted or membrane-bound. In addition, ATP7A is necessary for copper excretion from cells, to limit cellular copper stores and as a means to directionally transport copper over epithelial barriers. This dual function of ATP7A in copper metabolism has been well-conserved throughout evolution. As an example, the yeast homologue of ATP7A, Ccc2p makes copper available for incorporation into the transmembrane multicopper oxidase Fet3p, which utilizes the redox chemistry of copper to oxidize iron as a necessary step in yeast iron uptake [49]. In addition, Ccc2p is essential for excessive copper excretion, and yeast lacking Ccc2p are therefore hypersensitive to copper [49]. Other organisms, including plants and zebrafish are equally dependent on their ATP7A orthologues for copper homeostasis [50, 51]. The structure-function relationship of ATP7A has been extensively reviewed elsewhere [52, 53]. Briefly, ATP7A contains eight transmembrane domains that form an aqueous pore and several functional signature domains characteristic of P-type ATPases, like the nucleotide-binding-domain and the actuator-domain. Copper-transporting P-type ATPases have multiple consecutive metal-binding motifs in their cytoplasmic N-terminal domains (six in the case of ATP7A) and two conserved copper coordination sites in the transmembrane pore [54, 55]. Thus, ATP7A transports copper across cellular membranes at the cost of ATP hydrolysis.

ATP7A is more or less ubiquitously expressed. ATP7A mRNA expression is highest in placental tissue, and substantial expression was detected in heart, brain, intestine, testis and other tissues [56, 57]. Hardly any detectable mRNA expression was observed in the liver and spleen. Even in some tissues that predominantly express the homologous ATP7B, like the liver, placenta, mammary tissue and some areas in the brain, ATP7A may be expressed and may perform an analogous, but slightly different function as ATP7B [29, 31, 58]. ATP7A is highly expressed in the duodenum and upper jejunal part of the intestine in mice [59]. To date, no evidence for copper-induced gene expression of *ATP7A* exists, except for a slight increase in *Atp7a* expression in mouse pups when expressed to high dietary copper [18]. Under normal conditions ATP7A is localized in the *trans*-Golgi network (TGN) of cells (Figure 2), consistent with its function to transport copper into the secretory pathway [60-62]. Specifically, this perinuclear Golgi localization has also been observed in polarized intestinal cells *in vitro* as well as in mouse intestine [17, 59]. An increase in intracellular copper results in the specific and rapid relocalization of ATP7A to intracellular organelles

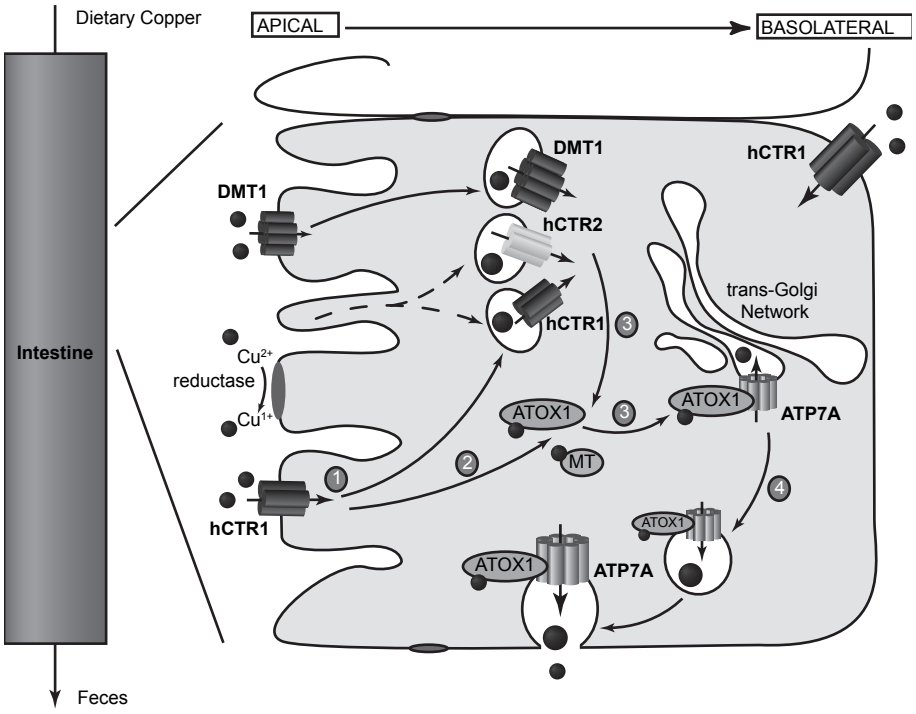

Figure 2. Model for the regulation of copper homeostasis in the enterocyte
Dietary copper in the gut is absorbed by enterocytes. Metalloreductases presumably reduce copper to Cu^{1+} prior to cellular uptake. The copper import protein hCTR1 is located in intracellular organelles and at the apical and basolateral membrane (1). Excessive copper induces hCTR1 internalization, but it is unclear if uptake from these intracellular organelles occurs. Besides hCTR1, DMT1 and hCTR2 might be involved in cellular copper uptake. Imported copper is bound to cytosolic proteins (2). Metallothioneins can act as a buffer system to scavenge cytosolic copper, and copper chaperones, like ATOX1 bind cytosolic copper and deliver copper to target proteins in the cell (3). Copper bound to ATOX1 is targeted to the ATP7A, which transports copper into the trans-Golgi network. Elevated cellular copper levels result in translocation of ATP7A to the basolateral membrane for copper export to the circulation (4).

that are distinct from the Golgi-apparatus and are localized in the periphery of the cell (Figure 2) [17, 59, 60, 63, 64]. In addition, ATP7A is detected on the basolateral membranes of enterocytes in response to elevated copper concentrations [59, 65]. In fact, it is likely that the intracellular and plasma membrane localization reflect a highly dynamic, continuously recycling pool of ATP7A, whose predominant location in the cell may be adapted to specific needs by changing the rates of exocytosis and endocytosis of these molecules. Consistent with this notion, the copper-dependent localization to the plasma membrane of ATP7A is reversed when copper levels decrease [60, 63]. In one study, both apical and basolateral membrane localization of ATP7A in the rat duodenum was observed after prolonged copper administration (Figure 2) [65]. The apical localization of ATP7A might be a way for the enterocyte to discard excessive copper back into the intestinal lumen. In contrast, other work demonstrated that ATP7A predominantly localized near the basolateral plasmamembrane, but hardly any co-localization with the membrane itself was observed [59]. Taken into the context of dietary copper absorption, it is believed that the copper-dependent localization of ATP7A near or at the basolateral membrane is a means to export the excessive copper from

the cell into the bloodstream and interstitional fluids (Figure 2) [60, 66, 67], resulting in net transport across the epithelial layer. As such ATP7A-dependent transport over the basolateral membrane forms the last step in dietary copper uptake at the level of the intestine. This notion would imply the transient presence of copper in the cytosol of the enterocyte during the copper uptake process.

Intracellular copper distribution in enterocytes

Imported copper is instantaneously bound upon entering the cell by small peptides and proteins in order to scavenge the potential harmful copper atoms. It has been estimated that virtually all copper in a cell is bound, and that each cell contains less than one free copper atom [68]. Copper-dependent enzymes and proteins therefore need accessory factors to compete with the vast excess of copper chelators that sequester essentially all intracellular free copper. To this end, cells express copper metallochaperones, like ATOX1, CCS, and Cox17 [69]. As defined by O'Halloran *et al.*, copper chaperones transiently bind copper with high affinity and utilize copper-dependent protein-protein interactions to ensure specific delivery of the metal ion to its proper intracellular destination while protecting the precious cargo from adventitious reactions and a multitude of alternative binding sites [70]. ATOX1 is the copper chaperone for ATP7A (Figure 2) [60, 62]. ATOX1 delivers copper to this protein by a copper-dependent protein-protein interaction between ATOX1 and the metal binding domains (MBDs) in the aminoterminal tail of ATP7A [71-77] or directly to the transmembrane copper-binding site [78]. This suggested that copper export by ATP7A is dependent on ATOX1 expression. Analysis of Atox1 knockout mice confirmed this hypothesis, as these mice have a copper deficiency phenotype that is similar to MD [79]. Also the copper-dependent localization of ATP7A as described above is impaired in Atox1-deficient cells (Figure 2) [80]. Arguello *et al.* recently proposed that conformational changes in the aminoterminus as a result of copper binding act as a molecular switch that regulates ATP7A activity in an ATOX1-dependent manner [54, 55]. Taken together, these observations indicate that ATOX1 is essential for ATP7A-dependent copper export and thus dietary copper absorption. ATOX1 is probably not directly involved in cellular copper uptake as ATOX1-deficient cells accumulate copper similar to MD cells, suggesting that other chaperones or molecules accept copper directly after uptake.

Copper uptake in enterocytes

Dietary copper absorption is dependent on CTR1, which constitutes the prime candidate for copper uptake in enterocytes. CTR proteins form a family of highly conserved proteins expressed in eukaryotic cells, and their function in copper uptake has been established in several experimental models including the yeast *Saccharomyces cerevisiae* and *Arabidopsis thaliana* [81-83]. Deletion of the two high-affinity copper transporters yCtr1p and its homologue yCtr3p resulted in a dramatic copper deficiency in yeast [83]. The single human high-affinity copper transporter (hCTR1) was first identified by functional complementation of this deficient yeast strain [84]. Overexpression of hCTR1 in several cell lines resulted in a substantial, specific and saturable induction of cellular copper import [85-87] (chapter 3 and 4; van den Berghe et al, unpublished data). Genetic knockout of Ctr1 in mice established the necessity of Ctr1 for cellular copper uptake in mammals. Mice that lack Ctr1 die during

mid-gestation, indicating an essential role for Ctr1 in embryonic development [88, 89]. This is not necessarily an effect of reduced copper uptake as Ctr1 affects cell morphogenesis and embryonic stem cell fate by transducing fibroblast growth factor signals in the developing embryo [90]. However, depletion of copper during embryogenesis in zebrafish severely impaired the embryonic development [51]. $Ctr^{+/-}$ mice survived embryonic stages, and displayed copper deficiencies in brain tissue, which indeed provided evidence that Ctr1 is indispensable for copper transport in mammals [88]. Mouse embryonic fibroblasts isolated from these Ctr1 knockout mice have a substantial defect in copper uptake and copper incorporation into cuproenzymes [91]. Finally, analysis of conditional knockout mice that lack Ctr1 expression specifically in hepatocytes or in intestinal epithelial cells, revealed a relatively minor contribution of Ctr1 to liver copper uptake [92], but an essential role for Ctr1 in intestinal copper uptake. Intestine-specific Ctr1 knockout mice displayed a copper deficiency phenotype comparable to MD due to hampered copper uptake in the gut [93]. Together with the observation that a single intraperitoneal injection of copper in these mice rescued the copper deficiency phenotypes, these observations indicated that Ctr1 is necessary for dietary copper uptake, and that no clear redundant systems compensated for loss of intestinal Ctr1. A detailed understanding of the structure, function, localization and regulation of intestinal CTR1 should therefore provide valuable information on dietary copper uptake.

Ctr1 (SLC31A) is a member of the solute carrier superfamily and has been characterized as a high-affinity copper transporter with a K_m of approximately 1-5 μM [85-87] (chapter 3 and 4). Studies in yeast and mammalian cells revealed that CTR1 proteins are integral membrane proteins, which contain three transmembrane domains. Extensive experimental evidence supports a topological model of CTR1 [64, 86, 94, 95]. Their carboxytermini extrude in the cytosol, while their amino-termini are located at the extracytoplasmic side of the membrane. The aminoterminus of CTR1 contains a number of conserved methionine and histidine residues, arranged in so-called Mets-motifs. These motifs likely contribute the sulfhydryl ligands that coordinate copper for subsequent transport. Whereas only the penultimate methionine in these motifs is absolutely required for copper transport, their presence highly increases copper transport affinity [96]. The aminoterminus is substituted with N-linked and O-linked oligosaccharides [95, 97]. The function of the N-glycosylation is not completely clear, but the O-linked glycans are likely involved in the stability of the protein [97]. Biochemical cross-linking experiments revealed that CTR1 forms oligomeric complexes [86]. Recent co-immunoprecipitation data indicated that hCTR1 monomers interacted with themselves, suggesting that hCTR1 forms homo-oligomers (chapter 4). Homo-oligomerization may involve mutual interactions of the aminotermini of hCTR1, as was suggested by yeast-two-hybrid experiments [95], but a cysteine residue in the carboxyterminus [98] and a Gly-Xaa-Xaa-Xaa-Gly sequence in the second transmembrane domain [99, 100] have also been implicated in hCTR1 oligomerization. The latter sequence is well-known to support interactions between transmembrane domains in multiple proteins [101, 102]. Together, these data support the notion that multiple domains within CTR1 proteins contribute to the formation of oligomeric transporters. In elegant work done by the Unger laboratory, recombinant hCTR1 was reconstituted in native phospholipid bilayers to generate 2D protein crystals. These crystals were subjected to electron microscopic

crystallography, which permitted determination of the structure of the hCTR1 oligomer at approximately 6-Å resolution. These studies revealed that CTR1 formed compact trimeric complexes containing nine transmembrane domains [99, 100]. Indeed, this structural information was supported by recent genetic evidence that functional copper uptake is dependent on homo-oligomerization of Ctr1 (chapter 4). Together this work provided the structural basis for our current hypothesis that hCTR1 forms an aqueous, copper permeable channel. Formation of such a channel would permit copper transport by initial binding of the metal to the aminoterminal Mets motifs and subsequent coordination of copper by a series of six methionine residues buried within the transmembrane domains of the hCTR1 trimer. Indeed, all CTR proteins have a characteristic conserved Met-Xaa-Xaa-Xaa-Met motif in the second transmembrane region that is essential for copper transport [96]. Finally, the cytoplasmic carboxyterminal domain of hCTR1 contains a conserved His-Cys-His motif. The cytosolic part of the hCTR1 trimer therefore contains nine high-affinity copper ligand residues, which may generate the thermodynamic energy that drives copper import and which may prevent unregulated entry of "free" copper into the cytosol. This copper "sink" may be the target for interactions with copper chaperones to transfer copper for intracellular distribution. Many questions remain unsolved. It is unknown if hCTR1 transport Cu^{1+} or Cu^{2+}, if copper transport is coupled to co-transport of other ions, and what provides the energy for copper transport. It also remains to be determined if the formation of trimeric hCTR1 copper channels *in vivo* is a default process or is subject to regulation. Such a mechanism would provide an elegant mechanism to control copper uptake by regulation Ctr1 oligomerization, analogous to the formation of functional STIM1 oligomers after Ca^{2+}-depletion to activate calcium uptake [103] or the disassembly of GABAB receptor upon capsaicin stimulation to reduce signaling by the neurotransmitter gamma-aminobutyric acid (GABA) [104].

The cellular localization of CTR1 is different in cell types and is, at least in part, dependent on the copper concentration in the medium. In all cell types hCTR1 is predominantly localized in intracellular organelles that are located in the perinuclear area. Dependent on the cell type, a smaller or larger proportion of hCTR1 is exposed on the plasma membrane (Figure 2) [86, 105]. hCTR1 constitutively recycles between this intracellular compartment and the plasma membrane [105]. It is unclear to what extent intracellular hCTR1 directly contributes to copper import, or just represents a rapidly mobilizable pool of copper transporters. Interestingly, the cell surface pool of hCTR1 is rapidly internalized upon treatment with extracellular copper (Figure 2) [64, 105], which is dependent of the Mets motifs in the aminoterminus of Ctr1 [94]. This phenomenon was induced by relatively low extracellular copper concentrations within the (physiological) range of the K_m of copper transport by hCTR1. This endocytosed hCTR1 was directed away from the recycling pool, and was degraded. Together, these findings could indicate that hCTR1 is constitutively expressed in intracellular organelles where it could transport pinocytosed copper or copper liberated from cuproproteins by lysosomal degradation, and simultaneously form a pool of transporters that can be rapidly recruited to the plasma membrane in case of cellular copper deficiency.

In order to translate such a model to enterocytes, it is imperative to consider the cellular localization of hCTR1 in the context of polarized cells. Experiments to address this issue have resulted in contradicting evidence. Intestinal copper uptake seems to be restricted to

the stomach and the proximal part of the intestine [106], but northern blot analysis revealed that Ctr1 is expressed throughout the entire intestine [84]. Based on immunohistochemical evidence, murine Ctr1 was observed in an intracellular compartment [93], and at the apical membrane in duodenal enterocytes [17, 93, 107]. Consistent with these findings, dietary copper uptake is critically dependent on Ctr1 expression in the gut [93]. Together, these data are best explained by a model in which Ctr1 functions to transport copper from the intestinal lumen into the cytoplasm of the enterocyte. This model does not explain, however, why enterocytes of intestine-specific $Ctr1^{-/-}$ mice accumulate excessive copper in a pool that is apparently not bioavailable [93]. In apparent contrast to this model, hCTR1 was localized in intracellular organelles and on the (basolateral) membrane of Caco2 cells, a well-characterized model of intestinal enterocytes [95, 108]. Zimnicka *et al.* also observed a predominant basolateral localization of hCTR1 in polarized Caco2 cells by basolateral surface biotinylation and immunofluorescence microscopy [108]. This localization was confirmed by immunohistochemistry of the mouse intestine. Basolateral copper uptake kinetics in polarized Caco2 cells was typical around the K_m of hCTR1 and uptake was inhibited by Ag^{1+}, whereas apical copper uptake appeared to be independent of hCTR1. The latter suggests that CTR1-dependent dietary copper uptake might not directly occur by apical membrane localization of this protein. In our opinion, apical localization of CTR1 protein has not been conclusively demonstrated, nor has this possibility been conclusively eliminated. Based on the current data, we propose that the basolateral CTR1 pool takes up copper from the interstitial space for the copper requirement of the enterocyte itself. On the other hand, we speculate that dietary copper in the lumen of the intestine is made available to the intracellular CTR1 pool by a currently unknown mechanism that could either involve pinocytosis or the presence of (an) additional copper transport protein(s). In any case, this hypothesis would predict the exciting existence of different copper pools in enterocytes that are separately created and regulated. Taken together, CTR1 has an essential role in dietary copper uptake, but how exactly this occurs is unknown. This question should receive priority in defining novel research aimed at delineating the molecular mechanisms of dietary copper acquisition.

Are there other proteins besides CTR1 that could contribute to uptake of dietary copper in enterocytes? Copper uptake experiments in mouse embryonic fibroblasts derived from the Ctr1 knockout mouse suggested that other low-affinity import mechanisms may contribute to cellular copper uptake [91]. One such a candidate for an alternative copper uptake route is CTR2 (Figure 2). Northern blot analysis of human tissues revealed that human CTR2 (hCTR2) is ubiquitously expressed, but intestinal mRNA expression is rather low compared to hCTR1 [84]. hCTR2 is homologous to hCTR1, and has a similar predicted structure and topology as hCTR1. However, hCTR2 lacks the Mets domains that are essential for high-affinity copper transport present in the aminoterminus of hCTR1, and the characteristic His-Cys-His motif in the carboxyterminal tail of hCTR1. Nevertheless, recent observations revealed that hCTR2 facilitated cellular copper uptake *in vitro* with an approximately 20-fold reduced affinity compared to hCTR1 (chapter 3 and [87, 109]). hCTR2 is exclusively localized in intracellular organelles that are reminiscent of late endocytic and lysosomal compartments. However, observations by Bertinato *et al.* in the monkey Cos7 cell line also revealed some endogenous CTR2 localization at the plasmamembrane [109]. However, this

antibody was raised against human CTR2 and this epitope is not conserved between species. In our opinion, the localization of endogenous CTR2 should be assessed by specific antibodies directed to species-specific epitopes in the CTR2 protein. Future research will benefit from specific antibodies and Ctr2 knockout mouse models to explore the physiological role and site of action of CTR2 in copper homeostasis.

An additional candidate for dietary copper uptake is the divalent metal transporter 1 (DMT1), which facilitates iron uptake from the diet (Figure 2). DMT1 is a protein with twelve transmembrane regions that transports divalent metals (Fe^{2+}, Cd^{2+}, Co^{2+}, Cu^{2+}, Ni^{2+}, Mn^{2+}, Pb^{2+} and Zn^{2+}) across membranes by exchanging protons in an energy-dependent manner [110]. DMT1 is expressed in the brush border of duodenal enterocytes [110, 111]. Several reports have shown that DMT1 can facilitate copper uptake in different model systems and organisms. A mutation in *Malvolio*, the DMT1 homologue in *Drosophila melanogaster*, resulted in increased sensitivity to copper limitation and excessive copper [112]. Mutations in the *Drosophila* orthologue of CTR1, dCtr1B, resulted in a similar phenotype suggesting that both Malvolio and dCTR1B contribute to copper uptake and distribution with only partial redundancy [113, 114]. Partial knockdown of DMT1 in the Caco2 cell line demonstrated that copper uptake was reduced in knockdown cells, although the knockdown was not very robust [115]. In contrast with these observations, Belgrade rats that harbor an inactivating mutation in *Dmt1* resulting in microcytic hypochromic anemia due to peripheral iron deficiency have no copper deficiency [116]. Similar Fe-deficient microcytic anemia phenotypes were observed in human patients with hereditary mutations in *DMT1* [117-119]. Taken together, the lack of a copper phenotype in DMT1-deficient patients and in Belgrade rats, and the lack of apparent redundant copper uptake systems in the intestine-specific Ctr1 knockout mice, suggests that Ctr1 mediates the major copper uptake route in enterocytes. However, further research is needed to characterize putative contribution of copper uptake proteins like CTR2 and DMT1 on cellular and dietary copper uptake.

The role of putative cupric reductase activity in intestinal copper uptake

Most copper in the presence of oxygen is present as Cu^{2+}, whereas intracellular copper is present in the reduced Cu^{1+} form. Copper uptake by CTR1 is specific for Cu^{1+}, and treatment with ascorbate markedly improved copper uptake [86]. This implies that copper needs to be reduced before copper uptake by CTR1 is possible. Dietary components like ascorbate might generate this Cu^{1+} pool in the intestinal lumen. On the other hand, metalloreductases could be required to reduce copper before absorption. Recently, a novel class of metalloreductases - the STEAP proteins, which were localized to intracellular organelles and the plasma membrane - were able to reduce both iron and copper, and were able to induce uptake of these metals [120]. Another metalloreductase that localized to the plasmamembrane of intestinal enterocytes, dCytb, is involved in iron uptake and is a cupric reductase *in vitro* [121, 122]. The need for a cupric reductase system is currently only established in *in vitro* models [86, 91, 123]. It is tempting to speculate that the existence of such a cupric reductase system is yet another step in regulation of intestinal copper uptake by modulating the availability or proper localization of these reductases.

The enterocyte as a regulator of intestinal copper uptake

As detailed above, dietary copper absorption is strictly regulated during development and adapts to the amount of bioavailable copper in the diet [5-14]. Although the proteins involved in intestinal copper uptake are mostly known, it is currently incompletely understood how these are coordinately regulated to permit control of copper intake. Many questions remain to be answered in future research. Do intestinal cells fundamentally differ from other epithelial cell types with respect to copper homeostasis? Are adaptations to copper concentrations transient in response to acutely changing copper concentrations, or do intestinal cells manifest a prolonged adaptive response to slowly changing total body requirements? How do enterocytes sense that dietary copper is high; in other words, how do enterocytes perceive differences in copper supply at their apical surfaces? How, if at all, does the enterocyte sense the copper requirement of the body as a whole and how does it respond to changes in copper availability at its basolateral surface? How do enterocytes balance the necessity to strictly regulate cell-intrinsic copper homeostasis with total body copper requirement? Without having the answers to these questions, we speculate on some of these notions below.

Comparison of regulation of copper homeostasis in different epithelia might open new avenues in understanding the regulation of copper absorption by enterocytes. In both the placenta and mammary tissue, copper transport is a regulated process across an epithelial barrier similar to the intestinal barrier. In mammary tissue, lactogenic hormones triggered ATP7B localization to the apical plasma membrane region to initiate copper export into the milk [31]. Furthermore, prolactin induced localization of both ATP7A and hCTR1 to the basolateral membrane, which correlated with increased copper levels in the milk [58]. Comparable hormonal regulation by both insulin and estrogen in the placenta resulted in localization of ATP7B in the TGN, whereas ATP7A trafficked to the basolateral membrane [29]. Currently, no hormones have been characterized that alter localization or expression of copper transport proteins in enterocytes, but it is tempting to speculate that crosstalk between different organs mediated by hormones also dictates copper dietary absorption (Figure 3A, 3B). A clear precedence for such a regulatory mechanism is the hepatic hormone hepcidin that forms a central player in the regulation of intestinal iron uptake. Hepcidin inhibited apical iron uptake in enterocytes by decreasing the expression of the apical iron uptake protein ferroportin [124-126]. Consistent with these finding, hereditary mutations in the genes encoding hepcidin and ferroportin result in uncontrolled iron uptake from the diet and cause hereditary hemochromatosis type 2B (OMIM 602390) type 4 (OMIM 606069), respectively.

Responses to acute changes in copper homeostasis in enterocytes are most probably mediated by posttranslational regulation of copper transporter localization in a manner similar to what has been described for other cell types. CTR1 is rapidly internalized and degraded following increased copper availability (Figure 3B). Apparently, cells decrease CTR1 expression to reduce cellular copper uptake. This mechanism could account for rapid limitation of dietary copper uptake if CTR1 is located in brush border membranes [17, 93]. In contrast, basolateral CTR1 [108] would implicate exposure of CTR1 to copper in the bloodstream. Its rapid endocytosis under high copper conditions could be responsible

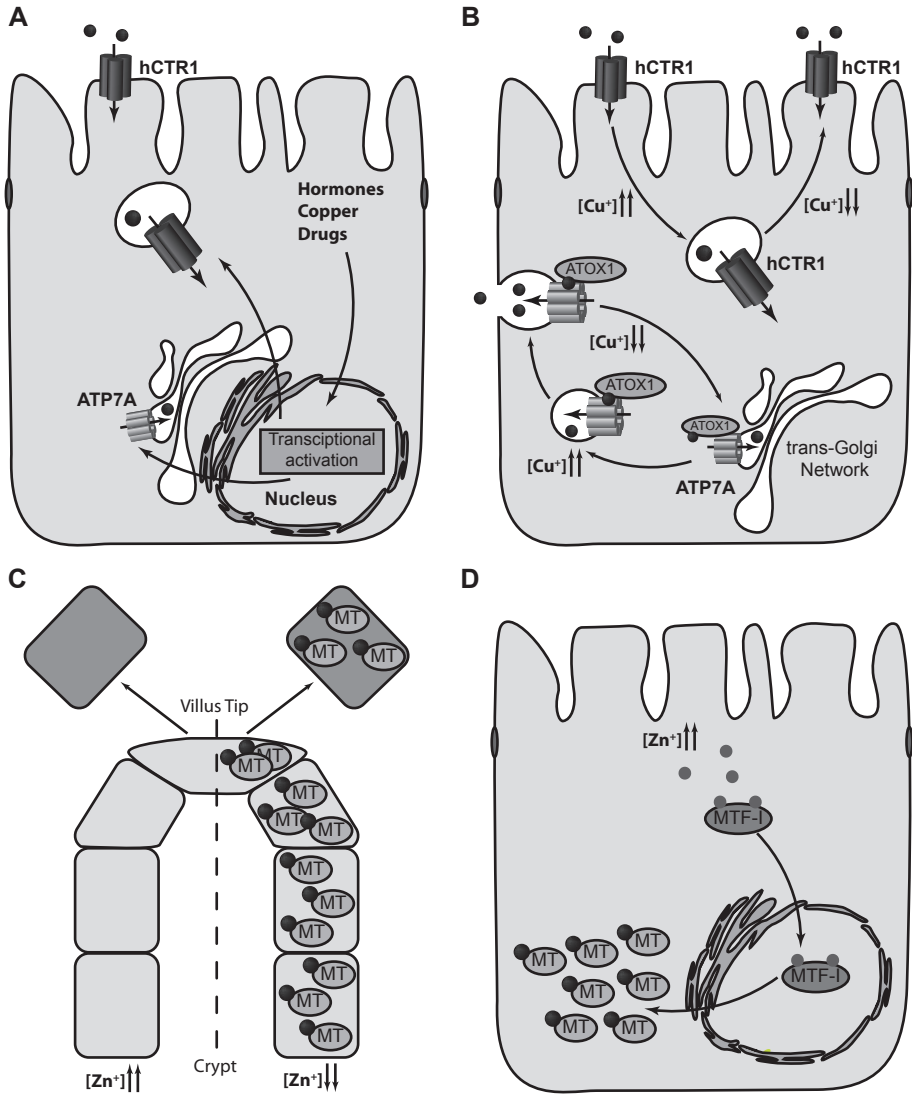

Figure 3. Different regulation strategies of copper uptake in the intestine
The intestine has the availability of several strategies to regulate copper uptake, distribution and cellular homeostasis. (A) Prolonged incubation with copper or extracellular stimuli like hormones can affect expression of copper transport proteins. (B) Increased extracellular copper, stimulation by hormones, or drugs can affect the subcellular localization of copper transporting proteins. Both CTR1 and ATP7A localization are copper-dependent. (C) Cells can become primed resulting in a coordinated adaptation of the whole tissue with respect to copper absorption. (D) To buffer intracellular copper and reduce copper export from enterocytes, metallothionein (MT) expression can be induced by metals like zinc and copper. When intracellular zinc concentrations are increased, zinc activates the metal-responsive transcription factor I (MTF-I). Activated MTF-I induces MT gene expression. Copper bound to MT is not directly available for ATP7A-dependent copper export, resulting in decreased copper uptake from the diet. In combination with induced MT expression, copper uptake can be prevented by shedding cells that were loaded with copper (C).

to protect intestinal cells from peripheral copper excess in a cell autonomous way. Bauerly *et al*. reported reduced copper uptake and apical to basolateral transport in response to excess copper in the medium of polarized Caco-2 cells grown on transwell filters [17]. Given the dissimilar results on hCTR1 localization, it seems imperative to re-examine these results by interrogating whether excessive copper from the basolateral or from the apical medium would result in reduced copper uptake.

Localization of ATP7A is also affected by extracellular copper concentrations. ATP7A was retained in the TGN during copper depleted conditions, and excessive copper induced ATP7A trafficking from the TGN to vesicular organelles near the basolateral membrane [66]. This is in concordance with the observed copper-dependent trafficking of ATP7A in different cell types [17, 59, 60, 63, 64] (Figure 3B). Relocalization of ATP7A in response to copper excess taken up from the diet would ensure rapid and complete transcellular copper flux. In apparent contrast, ATP7A localization to the plasmamembrane caused by increased copper taken up from the basolateral surface may help to protect enterocytes from toxic copper overload. A role for ATP7B in intestinal copper uptake is unlikely, given the lack of expression of ATP7B in this tissue and the normal copper uptake in untreated patients with Wilson Disease. Finally, Leary *et al.* recently proposed the existence of a novel signal transduction pathway involving cross-talk between copper-dependent redox chemistry in mitochondria with posttranslational regulation of copper excretion by ATP7A [127]. Whether there is a direct role for mitochondria in dietary copper uptake remains to be established.

Little is known about the prolonged effects on intestinal protein expression or localization of copper transports in response to chronic differences in copper exposure. Most genes involved in copper homeostasis, except metallothionein genes, were not regulated at the transcriptional level in response to copper in HepG2 cells, Caco2 cells and in adult mice [18, 128, 129], which suggested that intestinal copper absorption in adults is not or only moderately regulated by modulation of gene transcription. However, decreased Ctr1 protein expression was observed in mice that were fed with a high copper diet for a prolong period [107] (Figure 3B). Suckling rats displayed transcriptional induction of both Ctr1 and Atp7a mRNA and protein expression upon prolonged treatment with dietary copper [17, 18] (Figure 3A). Possibly, transcriptional regulation of dietary copper intake, if at all biologically relevant, is restricted to young animals, and posttranslational regulation is more predominant in older animals. The existence of prolonged effects on dietary copper absorption became apparent from studies with WD patients. Dietary copper absorption in WD patients is reduced by dietary zinc supplementation. When this treatment was discontinued, the beneficial effects lasted for almost eleven days [130] Figure 3C). The average life span of an enterocyte is approximately four days, suggesting that the cell population low in the intestinal crypt was primed to produce mature enterocytes that react in a coordinated manner. This enabled the beneficial effect to last longer due to renewal of enterocytes by the primed cells in the crypt. Supplementation with dietary zinc resulted in increased metallothionein (MT) expression in both liver and intestine (Figure 3D) [131, 132]. MTs are small proteins that scavenge potential toxic heavy metals that enter the cytosol [133]. Increased MT expression can scavenge imported copper, thereby preventing its excretion into the circulation and diverting copper into a largely non exchangeable pool [132, 134-136]. This results in reduced copper

excretion by ATP7A as can be observed in WD patients treated with zinc. The accumulated copper is lost in the feces when the enterocytes are sloughed off into the intestinal lumen (Figure 3C).

Conclusions and perspectives

The intestine is a key organ in the absorption and distribution of copper. Enterocytes comprise the gateway for copper uptake. The current dogma in literature that regulation of copper homeostasis is achieved by the liver might be oversimplified. Enterocytes affect copper absorption from the diet by regulation of MT expression, and by regulating the expression and localization of both CTR1 and ATP7A. Interesting directions for future research in this respect are the contribution of other copper transporting proteins in copper uptake. More importantly, our current understanding of regulation of copper homeostasis lacks the potential influence of blood-to-enterocyte signaling. Further studies are warranted to help define novel intervention strategies towards treatment of hereditary copper homeostasis disorders in selected patients, as well as mild copper deficiency and copper overload at the population level.

CHAPTER 2

Posttranslational regulation of P-type ATPases ATP7A and ATP7B in relation to Menkes disease and Wilson disease

Peter V.E. van den Berghe
Leo W.J. Klomp

Journal of Biological Inorganic Chemistry, invited review, in preparation

Introduction

Copper homeostasis is a strictly regulated process that balances the cellular need with the potential toxic nature of copper. Copper is a transition metal that can switch from the oxidized cupric (Cu^{2+}) to the reduced cuprous (Cu^{1+}) form by accepting or donating an electron. Due to this redox-activity, copper is an essential cofactor in many enzymatic pathways including respiratory oxidation, neurotransmitter synthesis, iron metabolism, pigmentation and others. This same redox-activity can catalyze the Fenton reaction resulting in formation of superoxide anions, which react with hydrogen peroxide yielding harmful reactive oxygen species [1]. The necessity of copper homeostasis is clearly illustrated by two genetic disorders in humans in which the cellular copper export machinery is severely impaired. The genes encoding homologous copper-transporting P_{1B}-type ATPases ATP7A and ATP7B are mutated in Menkes disease (MD) (OMIM 309400) and Wilson disease (WD) (OMIM 277900), respectively. Under basal copper conditions, ATP7A and ATP7B are localized in the *trans*-Golgi network (TGN) area [60, 62, 137], and ATP7A and ATP7B traffic to the cell periphery or to the plasmamembrane when cells are exposed to increased copper levels [60, 138-144] to excrete cellular copper. Mutation in either *ATP7A* or *ATP7B* results in cellular copper accumulation, but MD and WD have very different clinical presentations due to tissue specific expression of these genes.

Mutations in *ATP7A* result in a systemic copper deficiency due to a block in dietary copper absorption. MD is a fatal X-linked neurodevelopmental disorder with a prevalence between 1:40,000 and 1:350,000 [36-38]. Patients present with neurological defects, growth retardation, hypopigmentation, hypothermia, laxity of skin and joints, and peculiar 'kinky' or 'steely' hair [39-41]. Patients with a severe form of MD have an average life-span of approximately three years, whereas patients with a milder form present with less profound neurological symptoms and an increased average life-span [42-44]. WD is characterized by hepatolenticular copper overload as a result of mutations in *ATP7B*. WD is relatively rare with an incidence of about 1:30,000 to 1:100,000 [27], and to date over 300 different mutations have been described [28]. ATP7B is mainly expressed in the liver and in some regions of the brain, and to some extent in placenta, kidney, and mammary tissue [29-31]. As a copper-transporting P-type ATPase, ATP7B mediates copper transport across membranes at the cost of ATP hydrolysis, and therefore mutations in ATP7B result in toxic copper accumulation in ATP7B-expressing tissues. The clinical presentation of WD is variable and symptoms can start at different ages of onset. WD can manifest as a predominant hepatic disorder comprising liver cirrhosis, chronic liver inflammation and fulminant liver failure due to toxic copper accumulation, whereas neurological manifestations include Parkinsonian movement disorders, seizures, personality changes, depression and psychosis. Despite the many described mutations, it is difficult to make clear genotype-phenotype correlations [145, 146].

To maintain cellular copper homeostasis within narrow boundaries, cells have evolved an intricate system of copper import, intracellular distribution, and copper export. In contrast to other organisms, hardly any transcriptional regulation of genes primarily involved in copper homeostasis exists [128]. In this review, we discuss the posttranslational regulation of copper export by ATP7A and ATP7B with respect to protein structure, regulation of

ATPase activity, copper-dependent and copper-independent trafficking, and the role of modifications and interacting proteins are systematically discussed.

ATP7A and ATP7B are copper transporters

ATP7A and ATP7B have dual functions, depending on the cellular copper status. As Golgi-resident proteins, they mediate copper transport into the biosynthetic pathway for subsequent incorporation in cuproenzymes. After relocalization to the plasma membrane under conditions of copper overload, these proteins are essential for cellular copper export. The latter became apparent from cell culture studies in skin fibroblasts isolated from MD patients that accumulate intracellular copper. This phenotype was reversed by introduction of either ATP7A or ATP7B in these cells [45]. The former was concluded from experiments using the *ΔCcc2* yeast strain, in which the orthologue of ATP7A and ATP7B, Ccc2p is deleted. Here, copper incorporation into a ferroxidase, Fet3p, was also rescued by introduction of either ATP7A or ATP7B [137, 147]. Furthermore, overexpression of ATP7A or ATP7B resulted in decreased copper accumulation and retention in several cell lines [148-150]. Finally, the copper export capacity of ATP7A and ATP7B was demonstrated by translocation of ^{64}Cu into isolated membrane organelles [151-153], which was dependent on ATP7A or ATP7B expression. This finding was supported by reconstitution of ATP7A in soybean asolectin liposomes, which resulted in ATP7A-, ATP- and Mg^{2+}-dependent copper transport into these liposomes [151-153]. Taken together, these date suggest that both ATP7A and ATP7B are copper-transporting P-type ATPases.

Structural characteristics of copper-transporting P-type ATPases

ATP7A and ATP7B are quite homologous (approximately 54%) and both belong to the heavy metal transporting P_{1B}-type ATPase subfamily. The overall topology of ATP7A and ATP7B is therefore comparable. ATP7A and ATP7B have eight transmembrane domains and their aminotermini and carboxytermini protrude into the cytosol (Figure 1). Extracellular loops of ATP7A were substituted with N-linked glycan chains [62], whereas consensus glycosylation sites at relevant extra-cytoplasmic domains are absent in ATP7B. Another significant difference between ATP7A and ATP7B are two inserts present in ATP7A. One small peptide is inserted in the first extracellular loop, and an insert in the third cytosolic loop after the nucleotide binding domain (N-domain) (Figure 1). However, the function of these inserts is currently unknown. ATP7A and ATP7B have several conserved motifs that are essential for their ATPase activity, and which are characteristic of the P-type ATPase protein family [154]. These include the N-domain, the phosphorylation domain (P-domain), and the actuator domain (A-domain), which will be further explained below (Figure 1). Furthermore, copper-transporting P-type ATPases contain several specific motifs that are essential for copper transport. Six metal binding domains (MBDs) are present in the aminoterminal domain of ATP7B and ATP7A, which contain one typical Met-Xaa-Cys-Xaa-Xaa-Cys copper-binding sites each (Figure 1). Structural analysis by NMR spectroscopy and X-ray spectroscopy revealed that these MBDs adopt a conserved βαββαβ ferredoxin fold [155-162]. The copper-binding sites are surface exposed and thus accessible for copper

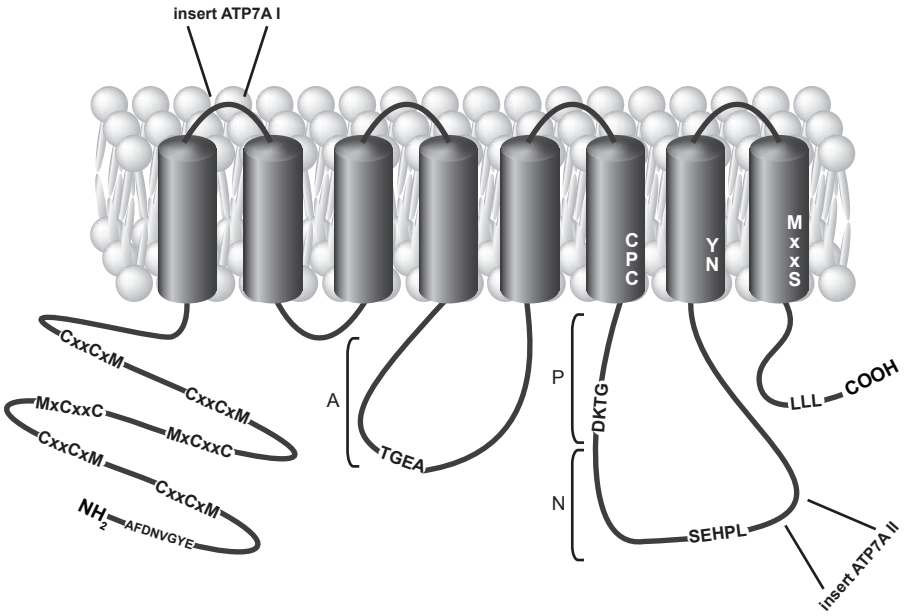

Figure 1. Membrane topology and structural elements of copper-transporting P-type ATPases
The P1B-type ATPase ATP7B is a transmembrane protein with eight transmembrane helices. several characteristic domains for P-type ATPases are involved in the catalytic cycle that mediates ion transport at the cost of ATP hydrolysis: the nucleotide binding domain (N) with the conserved SEHPL motif; the phosphorylation domain (P) with the invariant aspartic acid in the DKTG motif; and the actuator domain (A) with the TGEA motif. Typical for the copper-transporting P-type ATPases are the CPC, the YN, and the MXXS metal binding sites in the membrane domain (M domain) that bind copper as part of the copper exporting cycle in the 6th, 7th and 8th transmembrane helices, respectively. The amino-terminal peptide contains six highly conserved copper-binding sites containing the MXCXXC motif that binds copper and accepts copper from the copper chaperone ATOX1, which contains a similar MXCXXC motif. The extreme amino-terminal part contains the F_{37}AFDNVGYE$_{45}$ sequence that is involved in trafficking of ATP7B to the apical membrane, whereas a di/tri-leucine motif in the carboxyterminus is involved in retrograde transport to the TGN.

binding. These copper-binding sites can coordinate Cu^{1+}, the form that copper adopts in the reducing environment of the cytosol, in a stoichiometry of 0.5-1 atom per copper-binding site [163, 164]. MBDs are highly conserved in evolution. Besides the copper-transporting P-type ATPases, other proteins, including the copper chaperone ATOX1 contain a similarly folded MBD [71]. The MBD structure enabled copper-dependent dimerization of these motifs [77]. As discussed above, copper-dependent dimerization allows copper transfer between the copper-binding sites of ATOX1 and both copper-transporting P-type ATPases. The interaction between ATOX1 and ATP7A or ATP7B is essential for copper-dependent localization and copper translocation by ATP7A and ATP7B [60, 72, 73, 76, 80, 147, 165-175]. Strikingly however, bacterial and yeast orthologues of ATP7A and ATP7B only contain one or two (and sometimes four) MBDs, indicating that the six MBDs in ATP7A and ATP7B might be partially redundant.

To enable copper translocation across the membrane, P-type ATPases have a metal binding site (MBS) in the transmembrane domain (M-domain) [154]. Copper coordination in the M-domain is essential for ATPase-dependent copper transport, and therefore three transmembrane helices contain invariant residues that coordinate copper in M-domain (Figure 1); Cys-Pro-Cys (CPC) motif in helix 6 [162], the Asp, Tyr (YN) motif in helix 7,

and the Met-Xaa-Xaa-Ser (MXXS) motif in helix 8 were able to coordinate copper in the M-domain [52, 54, 176, 177]. Furthermore, several domains have been characterized that involve copper-dependent trafficking of ATP7A and ATP7B that will be discussed below in further detail. Briefly, trafficking towards the apical membrane was dependent on the F_{37}AFDNVGYE_{45} motif in the aminoterminus of ATP7B [140], and ATP7A and ATP7B contain a di/tri-leucine motif in the carboxyterminus involved in retrograde transport of both proteins [178].

P-type ATPase catalytic cycle

Copper export by ATP7A and ATP7B is essentially dependent on the cyclic ATP-hydrolysis activity, also known as the Post-Albers cycle [179, 180]. The overall structural elements of P-type ATPases are highly conserved (reviewed by [154]), and the high resolution structures of the sarcoplasmic calcium ATPase [181] have proved to form an excellent template for homology modeling (ATP7B homology model chapter 5). The high degree of sequence conservation in the P-type ATPase family enables extrapolation of the structural and functional characteristics of these proteins resulting in a model of the catalytic cycle of P-type ATPases in general. This model predicts that ATP7A- and ATP7B-dependent copper transport involves several discrete stages [154]. During the catalytic cycle, copper is translocated from the cytosol to the extracellular environment or to the lumen of the biosynthetic pathway, dependent on the localization of the protein. Subsequent translocation of another ion to the cytosol is common for many P-type ATPases, but this has not been observed for the copper-transporting P-type ATPases [52, 154]. The energy for copper translocation is generated by ATP hydrolysis. The ATP and Mg^{2+} dependency was demonstrated by copper translocation into ATP7B-containing membrane organelles isolated from rat liver, and by *in vitro* copper translocation experiments using ATP7A and ATP7B [151, 152, 175, 182, 183]. P-type ATPases undergo four conformational changes during their catalytic cycle [154, 175] (Figure 2). Briefly, the E1 state allows copper-binding and binding of ATP to the N-domain. The E1-P state is characterized by ATP hydrolysis and phosphorylation of the P-domain. Next, copper translocation across the membrane occurs and is named the E2-P state. Finally, dephosphorylation of the P-domain by the A-domain results in the E2 state.

The catalytic cycle is initiated by insertion of copper in the MBS in the M-domain when the copper-transporting P-type ATPase is in the E1-state [54], which promotes ATP binding to the N-domain. This results in conformational changes that bring the ATP-binding site within the N-domain in close proximity to the P-domain [154, 184]. Indeed, recombinant protein fragments of both the N- and P-domain of ATP7B could bind ATP [185-187]. Hydrolysis of ATP resulted in subsequent phosphorylation of the P-domain, which initiates the transition to the E1-P state [154, 184]. Molecular modeling predicts ATP binding in the P-domain in close proximity to the highly conserved invariant aspartic acid in the ^{1027}**D**KTGTLT^{1033} signature sequence [154, 184]. ATP hydrolysis generates the energy for ion transport, and the γ-phosphate is transferred to the invariant D1027. A Mg^{2+}-ion binds in the P-domain to compensate for the negative charge that is introduced by the reversible phosphorylation of this aspartic acid [154]. Mutation of the invariant aspartic acid D1027 abolished formation of this acylphospate intermediate [171, 173, 187] and resulted

in complete loss of copper translocation [173].

Actual copper translocation through the M-domain to the extracellular environment occurs during the E2-P state as a result of conformational changes in the M-domain. The N- and P-domain are attached to transmembrane helices 6 and 7, and rotation or movement of these two domains is transduced to the transmembrane helices. The A-domain is attached to transmembrane helices 4 and 5 and movement of the A-domain affects these membrane helices in a similar fashion. Hence, conformational transition from E1-P to E2-P by binding of the A-domain to the phosphorylated P-domain results in directional copper release from the copper-binding sites in the M-domain [154] (Figure 2). A conserved invariant TGEA motif in the A-domain mediates this interaction with the P-domain. The transition to the E2-state is accompanied by the dephosphorylation of the invariant aspartic acid in the P-domain. The A-domain contains intrinsic phosphatase activity and is therefore also known as the phosphatase domain. The exact mechanisms of dephosphorylation are currently unknown, but the TGEA motif is essential for ATP7B-dependent copper transport as ATP7B without this motif failed to complement the *ΔCcc2* yeast strain [166]. Interestingly, comparable mutations in ATP7A were associated with increased abundance of the phophorylated-intermediate (E1-P or E2-P state) of ATP7A [173]. The copper-transporting P-type ATPase returns from the E2 state into the E1 after release of the phosphate from D1027 and Mg^{2+}, and is ready for a new catalytic cycle.

Posttranslational regulation of cellular copper export by ATP7A and ATP7B

Regulation of ATP7A and ATP7B copper export activity by the copper chaperone ATOX1

Copper-binding to ATP7A and ATP7B forms a key event in the catalytic cycle. An essential step in ATP7B-dependent copper transport is copper delivery by the copper chaperone ATOX1 [72, 79, 80, 188]. The toxic potential of copper forces cells to maintain extremely low free copper concentrations, and it was estimated that less than one free copper ion per cell exists, due to the enormous cellular buffering capacity [68]. Copper chaperones have evolved to overcome this overwhelming non-specific sequestration of copper to make the metal bio-available in a safe and specific manner. Copper chaperones therefore transiently and specifically bind copper with remarkably high affinity and they utilize copper-dependent protein-protein interactions to ensure specific delivery of copper to its proper intracellular destination. In this way, they protect cells from adventitious redox chemistry and prevent binding of copper to a multitude of alternative binding sites [70]. The copper chaperone ATOX1 interacted with the aminotermini of ATP7A and ATP7B [72, 73, 75, 189-191]. The MBDs in the in the aminotermini of ATP7A and ATP7B are comparable to the MBDs in ATOX1. This enables a copper-dependent interaction between ATOX1 and ATP7A or ATP7B to exchange copper from ATOX1 to these P-type ATPases [71-77]. The importance of ATOX1 in mammalian biology is clearly illustrated by the *Atox1* knockout mice that displayed a copper deficiency phenotype similar to MD [79]. Furthermore, mouse embryonic fibroblasts from the *Atox1* knockout mice displayed defective copper transfer to ATP7A, thereby causing copper retention and abrogation of the copper-dependent relocalization of ATP7A [79, 80]. The necessity of ATOX1 for ATP7A-

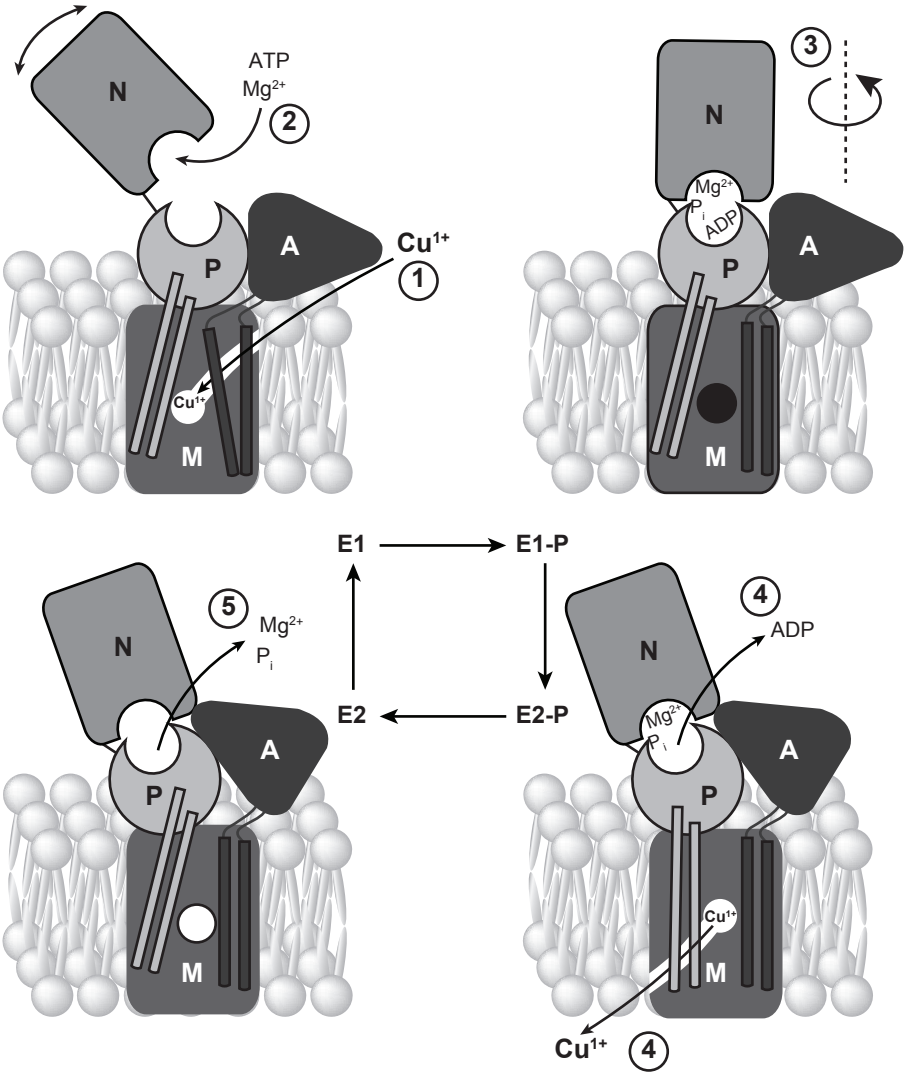

Figure 2. The catalytic cycle of copper-transporting P-type ATPases

The catalytic cycle of copper-transporting P-type ATPases starts in the E1 conformational state by copper-binding in the metal binding site (MBS) in the M domain (M) (1). This results in a conformational change of the P-domain (P) into the E1 conformational state. The N-domain (N) can bind ATP, and delivers ATP to the P-domain (2). Phosphorylation of the invariant aspartic acid in the P-domain, and subsequent binding of Mg^{2+} drives the copper-transporting P-type ATPase into the E1-P state (2). In the rate-limiting E1-P to E2-P transition, the P-domain reorients from the E1 to the E2 position. Subsequently, the N-domain rotates to bring its TGE loop into close contact with the phosphorylation site (3), which results in release of ADP (4). Rotation of the N-domain rotation might close the cytoplasmic ion-access channel by a scissor-like movement of the attached helices (light grey). The P-domain movement disrupts the high-affinity copper-binding site by its mechanical link to two membrane helices (dark grey), resulting in the release of copper into the extracellular/luminal side (4). Hydrolysis of the phosphorylated invariant aspartic acid results in the E2 state, and subsequent dissociation of Mg^{2+} and the inorganic phosphate forces the enzyme to the E1 state (5). This figure was modified from Kühlbrandt *et al.* [154].

and ATP7B-dependent copper transport is highly conserved in evolution. For instance, the ATP7A orthologue in *Archaeoglobus fulgidus*, CopA, was dependent on CopZ expression, the orthologue of ATOX1, for copper transport [54]. In conclusion, ATOX1 is required for copper transport under physiological conditions.

ATOX1-dependent copper delivery to the aminoterminal MBDs in ATP7A/ATP7B was long thought to be the mechanism of copper delivery into the copper-binding sites in the M-domain. Bacterial and yeast orthologues of ATP7A and ATP7B only contain one or two MBDs, indicating that the six MBDs in ATP7A and ATP7B are partially redundant [52, 78, 145]. Similarly, complementation of the *ΔCcc2* yeast strain was possible with ATP7B containing only the sixth MBD, suggesting that only on MBD is enough for copper transport [168]. Consistent with this observation is the unaffected copper-dependent trafficking of ATP7A in the absence of the first five MBDs [169]. Interestingly, copper transport by CopA in *A. fulgidus* was exclusively dependent on copper delivery by the copper chaperone CopZ to the copper-binding site in the M-domain of CopA, even when the aminoterminal MBDs were absent [54]. This suggests that the MBDs in the aminoterminus fulfill another function in ATP7A- and ATP7B-dependent copper transport. Arguello *et al.*, postulated a novel theory in which the aminoterminal MBDs regulate ATPase activity [78]. The aminoterminus of ATP7B interacted with the N-domain in the absence of copper [187]. This interaction inhibits ATP binding to the N-domain, thereby preventing copper transport by ATP7B [187]. Copper delivery to the aminoterminal MBDs by ATOX1 disrupts the interaction of the aminoterminus and the N-domain. This enables ATP binding to the N-domain and allows ATOX1 to deliver copper to the copper-binding sites in the M-domain, thereby stimulating copper translocation by these ATPases. Obviously, this proposed model that the aminoterminal domains of copper-transporting P-type ATPases perform a regulatory function needs further experimental validation.

ATOX1 was able to interact with all MBDs *in vitro* in a copper-dependent manner [192], but NMR data revealed that copper is preferentially transferred from Cu-ATOX1 to MBDs 2 and 4 in ATP7B [193], and to MBDs 2 and 5 in ATP7A [157]. Deletion of the first two MBDs in ATP7A did not affect copper transfer to ATP7A by ATOX1 [157], whereas ATP7B with only MBD 5 and 6 could no longer accept copper from ATOX1 [157, 193]. Furthermore, yeast two hybrid analysis revealed that ATOX1 binds preferentially to the aminoterminal MBDs 2 and 4 [77]. Interestingly, the ATOX1-dependent stimulation of the catalytic cycle was abolished only by mutation of the second aminoterminal MBD [194]. Together, these observations suggest that the different MBDs are not equally involved in the regulation of copper-transporting P-type ATPases.

Regulation of subcellular localization

Under basal (low copper) conditions, both ATP7A and ATP7B displayed a characteristic perinuclear localization [60, 62, 137], which has been identified as the TGN by immunogold electron microscopy [195]. Overexpression of ATP7B resulted in localization to the TGN in non-polarized cells including HepG2 cells and Huh7 cells [137, 167, 195, 196], Menkes patient fibroblasts [45], HeLa cells and CHO-K1 cells [167, 197]. Furthermore, endogenous ATP7B also localized to the TGN in polarized HepG2 cells and WIF-B cells [138, 140-142]. Similar localization under basal copper condition was observed for ATP7A in non-polarized

cells including Cos-7 cells, MRC5/V2 cells, human skin fibroblasts [169, 171, 198], CHO-K1 [60, 166, 174]. Furthermore, both ATP7A and ATP7B were localized to the TGN in the polarized mammary epithelial PMC42-LA and HCC1 cells [31, 58], and in placenta JEG-3 cells [29, 199, 200]. In contrast to the TGN localization, ATP7B localization in the endosomal compartment was observed [201-203]. Recent studies localized ATP7B to tight junctions in hepatocytes where it might be involved in paracellular copper transport [204]. The significance of this observation is currently under debate and awaits further verification [205]. Taken together, the general consensus is that ATP7B is localized in the TGN under basal copper conditions. Incorporation of copper into cuproenzymes like ceruloplasmin in the TGN is dependent on expression of ATP7A and ATP7B, which is consistent with the localization of ATP7A and ATP7B in the TGN.

In most of these studies, copper-dependent localization of ATP7A and ATP7B to peripheral organelles or to the plasmamembrane was observed. This copper-dependent relocalization of copper-transporting P-type ATPases is metal-specific, fast, does not require *de novo* protein synthesis and is reversible. Under high-copper conditions, ATP7B displayed overlap with the apical membrane in several polarized hepatic cell lines [138-141], whereas others observed that ATP7B did not traffic preferentially to the plasmamembrane but to peripheral organelles instead [142, 143]. Both *in vitro* and *in vivo* experiments have illustrated copper-dependent trafficking of ATP7B in hepatocytes [138, 140, 141, 206]. Comparable reversible copper-dependent trafficking of ATP7A was observed towards the basolateral membrane in polarized cells [29, 31, 58, 170, 199, 200] and to the plasma membrane or peripheral organelles in non-polarized cells [60, 166, 169, 171, 174, 198].

Although ATP7A and ATP7B both traffic in response to copper, their destination is clearly different. Specific targeting of ATP7B towards the apical membrane is dependent on an ATP7B-specific sequence, F_{37}AFDNVGYE_{45}, and disruption of this motif resulted in basolateral targeting [207] (Figure 1). This sequence motif is absent in ATP7A, and overexpression of ATP7A in hepatocytes results in basolateral localization [170], which is consistent with basolateral ATP7A localization in intestinal polarized cells [59, 65, 66, 170]. However, deletion of an ATP7A-specific PDZ-domain in the carboxyterminus of ATP7A resulted in apical localization of ATP7A in hepatocytes [170]. Apparently, these motifs target specific copper-dependent trafficking of ATP7A and ATP7B to distinct membranes in the cell. However, copper-dependent trafficking of both copper-transporting P-type ATPases is not dependent of these described motifs, suggesting that undiscovered other domains are involved in copper-dependent trafficking of ATP7A and ATP7B.

Copper-induced relocalization is reversed by retrograde transport of ATP7A and ATP7B to the TGN after returning copper concentrations to basal levels [143, 208]. In ATP7A, a putative TGN-targeting signal was identified within transmembrane helix 3 [198]. A certain degree of homology within this region is present between ATP7A and ATP7B, but it is currently unknown whether transmembrane helix 3 in ATP7B contains a similar TGN-targeting signal. A di-leucine sequence in the carboxyterminal tail of ATP7A is required for retrograde transport to the TGN, which was illustrated by the retention of ATP7A at the plasmamembrane when these leucines were mutated into alanines [63, 144, 209]. This di-leucine motif might therefore potentiate classical clathrin-dependent endocytosis [210], but contradictory observations showed that endocytosis of ATP7A is also clathrin-independent

[178, 210]. Apparently, other sequences contribute to the retrograde transport of ATP7A. ATP7B has a comparable tri-leucine motif in its carboxyterminal tail (Figure 1). Mutation of the tri-leucine in ATP7B does not result in retention at the plasmamembrane, but ATP7B was constitutively localized in peripheral organelles instead [178]. Thus, the di/tri-leucine clearly functions in retrograde transport of both ATP7A and ATP7B.

Copper transport activity strongly correlated with copper-induced trafficking of both ATP7A and ATP7B. Mutation of the CPC copper-binding site in the transmembrane region prevented copper-binding and copper-induced relocalization [170, 172, 173]. Furthermore, mutation of the invariant aspartic acid the in DKTG motif of the P-domain of ATP7B abolished copper induced trafficking from the TGN to the periphery of the cell [142]. In contrast, mutation of the TGEA motif in ATP7A completely abrogated ATP-dependent copper transport, and ATP7A was retained in peripheral organelles in a copper independent manner [173]. Mutation of the CPC motif in ATP7B resulted in a constitutive localization in cytosolic organelles, concomitant with increased phosphorylation of the invariant D1027 in ATP7B [166]. Such hyperphosphorylation of the invariant aspartic acid in the P-domain, secondary to a block in dephosphorylation was also observed in the sarcoplasmic calcium-ATPase after disruption of the TGEA motif [211]. More importantly, the peripheral localization could not be reversed by combining the TGEA mutation with deletion of the six aminoterminal MBDs and the CPC motif in ATP7B [142]. Apparently, copper-dependent localization is dependent on the progression through the different conformational stages of copper-transporting P-type ATPases (Figure 2).

Regulation by posttranslational modifications

The expression, localization, stability, and function of many proteins are dictated by signal transduction pathways that confer transient posttranslational protein modifications, such as phosphorylation, acetylation, and ubiquitination. Studies on protein modifications of ATP7A and ATP7B are limited, but these proteins undergo extensive posttranslational regulation, thus suggesting that these types of modifications exist. Phosphorylation of ATP7B, in a manner distinct from the transient phosphorylation of the invariant D1027 during the catalytic cycle, has been described and correlated with localization of ATP7B to the periphery of the cell [212]. This hyperphosphorylation of ATP7B appeared copper-dependent and dependent on the presence of an intact aminoterminus [212, 213]. In contrast, copper depletion resulted in dephosphorylation of ATP7B and concomitant retrograde trafficking of ATP7B to the TGN [212]. The responsible kinase for this phosphorylation event is currently unknown, but it is tempting to speculate that coupling of protein phosphorylation to copper binding at the aminoterminal domains of copper-transporting P-type ATPases comprises the mechanism by which the aminoterminus regulates protein function and localization in a copper-dependent way. Alternatively, it is also possible that copper-initiated signal transduction pathways exist and result in phosphorylation of ATP7A or ATP7B. Furthermore, a basal phosphorylation site that is independent of copper was characterized, which involves serine residues in the carboxyterminal Ser796-Tyr1384 region of ATP7B [212, 213]. The function of basal phosphorylation is currently unknown, but it might be involved in interactions with proteins either to retain ATP7B in the TGN or to modulate copper transport activity. In conclusion, identification of the exact phosphorylation sites,

the consequences of phosphorylation and the responsible kinases, will greatly enhance our understanding of regulation of ATP7B function. In addition, there is great demand for identification of other potential modifications of copper-transporting P-type ATPases.

Copper-independent regulation of ATP7A and ATP7B trafficking and activity

Other stimuli than copper can affect the regulation of copper transport in different tissues. Activation of the NMDA receptor by glutamate in hippocampal neurons resulted in copper-independent reversible trafficking of ATP7A from the TGN to neuronal processes [214]. This results in glutamate-dependent copper excretion, which prevents neuronal cell death due to NMDA-receptor activation [215]. Another tissue-specific copper-independent localization pathway is present in melanocytes. These cells require copper transport into specialized melanosomes where the cuproenzyme tyrosinase mediates maturation of the pro-melanin into melanin (pigment). After synthesis tyrosinase incorporates copper in the TGN, but unlike ceruloplasmin copper is loosely bound to tyrosinase and tyrosinase loses bound copper during progression to the endocytic compartments. Interestingly, ATP7A localized to melanosomes in a biogenesis of lysosome-related organelles complex-1 (BLOC-1)-dependent manner [61]. Hence, copper-independent localization of ATP7A to melanosomes ascertains organelle specific incorporation in tyrosinase, thereby regulating organelle-specific tyrosinase activity.

Mother-to-fetus transport of copper in the placenta is dependent on both ATP7A and ATP7B expression [29, 200, 216]. Interestingly, hormones markedly affected expression and localization of these proteins. Estrogen and insulin resulted in upregulation of ATP7A expression on both mRNA and protein levels [200]. Furthermore, these hormones resulted in copper-independent trafficking from the TGN to the basolateral membrane that corresponds to the fetal side of the cell. At the same time, stimulation with these hormones resulted in decreased ATP7B protein expression, and retention of ATP7B in the TGN to prevent copper excretion at the apical side of the membrane. In contrast, lactogenic hormones trigger ATP7B relocalization to the apical membrane in mammary tissue, which results in copper export back to the milk [31]. Furthermore, treatment with prolactin resulted in increased copper excretion in the milk by basolateral localization of CTR1 and ATP7A [58]. Apparently, signal transduction routes downstream of the described hormonal stimuli affect protein localization and expression, suggesting that posttranslational protein modifications and interacting proteins regulate cellular copper transport. For example, down regulation of ATP7B protein expression suggests that the cellular degradation machinery is involved, which implies that insulin and estrogen might induce poly-ubiquitination and subsequent proteasomal degradation of ATP7B. Consistent with this observation, degradation of ATP7B could be partly inhibited by inhibitors of proteasomal degradation [217]. Detailed analysis of the effects of these signal transduction cascades on ATP7A and ATP7B biology could dramatically increase our knowledge of protein modifications and protein interactions involved in regulation of ATP7A and ATP7B.

Regulation by interacting proteins

The necessity of interacting proteins for ATP7B was early recognized by the essential copper-dependent protein-protein interaction with the copper chaperone ATOX1 [72, 79, 80]. As

described above, ATOX1 is involved in copper transfer to the aminoterminal MBDs, copper transfer to the MBS in the M-domain, and regulation of copper-dependent trafficking. However, ATOX1 also interacted with the immunophillin FKBP52 [218]. This interaction was copper-dependent, and overexpression of FKBP52 increased cellular copper efflux similar to ATP7B overexpression [218]. Immunophilins are involved in protein trafficking, and interact with heat shock proteins (HSPs) involved in protein folding. Interestingly, another member of the immunophilin family stimulated HSP90 ATPase activity [219]. However, the exact mechanisms by which FKBP52 attenuates its role in the copper excretion pathway need to be further characterized.

Recently, two novel ATP7B-interacting proteins were identified by yeast-two-hybrid analysis [220-222]. First, glutaredoxin displayed a copper-dependent interaction with both ATP7A and ATP7B [221], and this interaction was dependent on the availability of the MBDs in the aminoterminus. Glutaredoxins are involved in keeping cysteine thiols in a reduced state. This might be a mechanism to keep the cysteines in the MXCXXC motifs available for copper-binding by preventing the formation of intramolecular disulfide bonds that are not accessible for copper coordination [221]. Second, the aminoterminus of ATP7B interacted with the dynactin subunit p62 in a copper dependent manner [220]. The dynactin complex is involved in mobilization of organelles along microtubules [223], suggesting that this interaction might be involved in copper-dependent relocalization of ATP7B.

One of the other ATP7B-interacting proteins that recently attracted attention is COMMD1. COMMD1 was characterized as the protein that was deleted in Bedlington terriers affected by hereditary copper toxicosis [224-226]. The exact function of COMMD1 in copper metabolism is currently unknown. *Commd1* knockout mice displayed an embryonic lethal phenotype as result of the absence of placental vascularisation, which was most likely caused by increased activity of the HIF1 signaling pathway [227]. Although it has been reported that COMMD1 binds Cu^{2+} [228], a direct and copper-independent interaction between the aminoterminus of ATP7B and COMMD1 has been characterized [217, 229]. Transient knockdown of COMMD1 by RNA interference resulted in increased cellular copper levels in HEK293T cells [230-232]. Together, these data suggest that ATP7B and COMMD1 cooperate in cellular copper export, which might be the underlying defect in Bedlington Terriers affected with copper toxicosis. Interestingly, the interaction between COMMD1 and ATP7B was markedly increased when WD disease-associated mutations in the aminoterminus of ATP7B were present (chapter 5 and [217]). These mutations were associated with mislocalization of ATP7B to the endoplasmic reticulum and decreased protein expression due to increased proteasomal degradation. COMMD1 has been implicated in regulation of protein stability of components of the NF-κB and HIF1 signaling pathways [227, 233-236]. Furthermore, COMMD1 also interacts with ATP7A, suggesting that COMMD1 affects cellular copper export in general (Vonk, W.I.M. *et al.* and de Bie, P. *et al.*, unpublished observations). These observations suggest that COMMD1 can affect copper homeostasis by regulating ATP7B stability, but detailed analysis is needed to unravel the regulatory role of COMMD1.

Conclusions

The regulation of ATP7A- and ATP7B-dependent copper translocation and the regulation of the spatial distribution in cells have been intensively studied during the past decades. The copper-dependent trafficking of ATP7A and ATP7B is correlated to their catalytic activity, but hardly any information is available on the mechanisms that facilitate this relocalization. The regulated trafficking to specific organelles and membranes in the cell requires posttranslational modifications and protein-protein interactions to direct these proteins to their specific destinations. The catalytic activity of ATP7A and ATP7B is regulated by inter- and intra-molecular interactions comprising the aminotermini and N-domains of ATP7A, ATP7B and ATOX1. However, the contribution of copper-dependent phosphorylation on catalytic activity remains elusive. Which interacting proteins target ATP7B to its destination in the cells, and which modifications are accompanied by this event? Furthermore, copper is not the only stimulus for relocalization, and identification of the cellular signaling pathways will improve our understanding of regulation of copper homeostasis greatly.

CHAPTER 3

Human Copper Transporter 2 is Localized in Late Endosomes and Lysosomes and Facilitates Cellular Copper Uptake

Peter V.E van den Berghe,
Dineke E. Folmer,
Helga E.M. Malingré,
Ellen van Beurden,
Adriana E.M. Klomp,
Bart van de Sluis,
Maarten Merkx,
Ruud Berger,
Leo W.J. Klomp

Biochemical Journal, 2007 Oct 1;407(1):49-59

Abstract

High-affinity cellular copper uptake is mediated by the CTR (copper transporter) 1 family of proteins. The highly homologous hCTR (human CTR) 2 protein has been identified, but its function in copper uptake is currently unknown. To characterize the role of hCTR2 in copper homoeostasis, epitope-tagged hCTR2 was transiently expressed in different cell lines. hCTR2-vsvG (vesicular-stomatitis-virus glycoprotein) predominantly migrated as a 17 kDa protein after immunoblot analysis, consistent with its predicted molecular mass. Chemical cross-linking resulted in the detection of higher-molecular-mass complexes containing hCTR2-vsvG. Furthermore, hCTR2-vsvG was co-immunoprecipitated with hCTR2-FLAG, suggesting that hCTR2 can form multimers, like hCTR1. Transiently transfected hCTR2-eGFP (enhanced green fluorescent protein) was localized exclusively to late endosomes and lysosomes, and was not detected at the plasma membrane. To functionally address the role of hCTR2 in copper metabolism, a novel transcription-based copper sensor was developed. This MRE (metal-responsive element)-luciferase reporter contained four MREs from the mouse metallothionein 1A promoter upstream of the firefly luciferase open reading frame. Thus the MRE-luciferase reporter measured bioavailable cytosolic copper. Expression of hCTR1 resulted in strong activation of the reporter, with maximal induction at 1 μM $CuCl_2$, consistent with the K_m of hCTR1. Interestingly, expression of hCTR2 significantly induced MRE-luciferase reporter activation in a copper-dependent manner at 40 and 100 μM $CuCl_2$. Taken together, these results identify hCTR2 as an oligomeric membrane protein localized in lysosomes, which stimulates copper delivery to the cytosol of human cells at relatively high copper concentrations. This work suggests a role for endosomal and lysosomal copper pools in the maintenance of cellular copper homoeostasis.

Introduction

Copper is a trace element which is essential for all organisms that utilize oxygen as an electron acceptor during respiration. As a transition metal, copper serves as a cofactor in a number of redox enzymes. The same redox-active properties also render the metal potentially toxic, as it can induce free radical formation and cause direct damage to proteins, lipids and DNA. To maintain copper homoeostasis, remarkably efficient mechanisms have evolved to regulate copper import and export and cellular distribution of the metal. The proteins involved in cellular copper homoeostasis are largely conserved in both prokaryotes and eukaryotes [234, 237, 238]. These proteins form intricate metabolic pathways aimed at maintaining an extremely low free copper concentration, while ensuring that sufficient copper is bioavailable to sustain essential copper-dependent cellular processes [68]. As one example, a significant proportion of cellular copper is bound to copper chaperones, which deliver copper to specific target enzymes or transporters via regulated protein-protein interactions [72, 239]. A second example, metallothioneins are small ubiquitously expressed proteins that scavenge cytosolic copper and other metals such as zinc and cadmium [133], and the expression of metallothionein genes is transcriptionally regulated in a copper-dependent fashion.

Severe disorders may arise as a result of disruption of copper homoeostasis. Recessive mutations in the gene encoding ATP7A (copper-transporting P_{1B}-type ATPase) result in Menkes disease, a fatal X-linked neurodevelopmental disorder [57, 240]. ATP7A deficiency results in a lack of copper transport through the placenta and the intestinal epithelium, leading to systemic copper deficiency and the failure to provide essential cuproenzymes with the metal. The *calamity* mutant of *Danio rerio*, the zebrafish, is a recently characterized animal model for Menkes disease [51], which displays a marked reduction in pigment formation and a strikingly altered notochord development in comparison with wild-type zebrafish. Interestingly, the *calamity* mutant is phenocopied by copper deficiency, thus illustrating further the essential role of copper in physiology and development.

Copper uptake is facilitated by the CTR (copper transporter) family of proteins, which are highly conserved [241]. In *Saccharomyces cerevisiae*, high-affinity uptake of copper is mediated by yCtr1p and yCtr3p [81, 83]. A third Ctr protein expressed in *S. cerevisiae*, yCtr2p, is thought to mediate low-affinity copper uptake. In mammals, a high-affinity copper permease, CTR1, facilitates copper import, with a K_m of approximately 1-5 μM (chapters 3 and 4) [85]. hCTR (human CTR) 1 is predominantly localized to intracellular vesicles which are in close apposition to the Golgi complex, but a fraction is also present at the plasma membrane [86, 105]. The proportion of cell-surface-exposed hCTR1 is dependent on the cell type [105], and elevated concentrations of copper have been shown to result in the internalization of cell-surface hCTR1, possibly as a rapid adaptive response to limit copper uptake [64]. hCTR1 contains three membrane-spanning regions and is thought to assemble into a trimer which forms an aqueous pore to enable copper transport (chapter 4) [67, 100].

The physiological role of the Ctr1 family of proteins has been addressed elegantly using knockout mouse models. *Ctr1*-knockout mice died during mid-gestation as a result of copper deficiency [89, 107]. Conditional knockout mice, lacking *Ctr1* specifically in the intestinal epithelium, were born healthy, but displayed markedly impaired dietary copper

uptake, resulting in a severe systemic copper deficiency comparable with Menkes disease patients [93]. This knockout mouse work established the essential role of Ctr1 in embryonic development and in dietary copper uptake. However, these animals display some residual cellular copper uptake, suggesting that additional pathways of copper import do exist. Furthermore, MEFs (mouse embryonic fibroblasts) obtained from *Ctr1*-knockout embryos survived in culture without the addition of extra copper to their medium, and were able to take up copper in a low-affinity manner [91]. The proteins mediating Ctr1-independent low-affinity copper import have currently not been characterized.

A candidate protein which may participate in such alternative copper import routes is hCTR2. Alignment of the primary amino acid sequences of hCTR1 and CTR2 from multiple species revealed marked homology in the transmembrane regions, suggesting that hCTR2 contains three putative transmembrane regions, similar to hCTR1 [85, 95] (Figure 1A). Extrapolating from hCTR1, the Aminoterminus of hCTR2 is probably located extracytoplasmically [85, 95]. The highly conserved MXXXM (Met-Xaa-Xaa-Xaa-Met) motif in the second transmembrane region of hCTR1, which has been shown to be critical for copper co-ordination during copper uptake [242], is also present in hCTR2. All amino acid residues that have been shown to be critical for oligomerization and copper transport activity of hCTR1 are conserved in hCTR2: the GXXXG (Gly-Xaa-Xaa-Xaa-Gly) motif in the third putative transmembrane region of hCTR1 [99], one methionine residue, approximately 20 residues upstream of the first transmembrane domain (Figure 1A, asterisks) and the MXXXM motif in the second transmembrane domain [96]. There are also notable differences between hCTR2 and hCTR1. hCTR2 lacks the MXXXM motif and histidine-rich regions that are important for high-affinity copper transport, and does not contain the appropriate consensus sites for N-glycosylation [96, 243, 244]. These observations support the hypothesis that hCTR2 does transport copper, but suggest that this occurs with a lower affinity than that of hCTR1. However, the function of hCTR2 has not been experimentally addressed and its annotation as a CTR has been based only on the alignment with other CTR sequences [84]. In the present study, we have characterized the role of hCTR2 in copper homoeostasis using a combination of biochemical analyses, cellular localization studies and a novel copper sensor. The results provide evidence that hCTR2 is an intracellular protein involved in copper uptake in human cells.

Experimental

Cell culture and MTT [3-(4,5-dimethylthiazol-2-yl)-2,5-diphenyl-2H-tetrazolium bromide] viability assay

The HEK-293T cell [human embryonic kidney cell expressing the large T-antigen of SV40 (simian virus 40)] line, HeLa cell line and U2OS cell line were purchased from the A.T.C.C. Cells were cultured at 37 °C under humidified air containing 5% CO_2, and were maintained in DMEM (Dulbecco's modified Eagle's medium) GlutaMAX™ (Invitrogen) containing 10% (v/v) FCS (fetal calf serum) (Invitrogen), 100 μg/ml penicillin (Invitrogen) and 100 μg/ml streptomycin (Invitrogen). For some experiments, cells were cultured in DMEM containing 10% FCS, 100 μg/ml penicillin and 100 μg/ml streptomycin in the presence of different concentrations of $CuCl_2$, $ZnCl_2$, $MgCl_2$, $FeCl_3$, $MnCl_2$ (Merck Chemicals) or a copper

Table 1. Primers

Name	**Sequence** (5′→3′)
FLAG–cullin1 rev	TCACTTGTCGTCATCGTCTTGTAGTCAGCCAAGTAACTGTAGGTGTC
FLAG–cullin1 fw	ATGGACTACAAAGACGATGACGACAAGTCGTCAACCCGGAGCCAG
hCTR2–vsvG fw	ATGGCGATGCATTTCATCTT
hCTR2–vsvG rev	TCACTTTCCTAGTCGGTTCATCTCGATGTCAGTGTAAGCTGTGCTGAGAAGTGG
hCTR1 fw	TGGATCATTCCCACCATATG
hCTR1 rev	ATGGGCAATGCTCTGTGATATC
hCTR2 fw	ATGGCGATGCATTTCATCTT
hCTR2 rev	AGCTGTGCTGAGAAGTGGGT
4MRE-F/HindIII	CCCAAGCTTGACTCGAGGAGCTCTGCAC
4MRE-R/PstI	CTGCAGTATGCCAAGGTCGACGGGC
hCTR2 BamHI fw	CTAGGATCCACCATGGCGATGCATTTCATCTTC
hCTR2 NotI rev	GTAAGCGGCCGCAGCTGTGCTGAGAAGTGGGTAAG
hCTR1 BamHI fw	GGATCCGCCACCATGGATCATTCCCACCATATG
hCTR1 NotI rev	GCGGCCGCATGGCAATGCTCTGTGATATC
hCTR1 IXXXI fw	CATAAGCTACTTCCTCATTCTCATCTTCATTACCTACAACGGGTAC
hCTR1 IXXXI rev	GTACCCGTTGTAGGTAATGAAGATGAGAATGAGGAAGTAGCTTATG
hCTR2 IXXXI fw	CATCGGCTACTTCATCATTCTGGCCGTAATTTCCTACAACACCTG
hCTR2 IXXXI fw	CAGGTGTTGTAGGAAATTACGGCCAGAATGATGAAGTAGCCGATG

fw, forward; rev, reverse.

chelator, BCS (bathocuproinedisulfonic acid) (Sigma). MTT viability assays [245] were performed after incubation of the cells with different concentrations of metals in 96-well microtitre plates (Corning). Cells were incubated with 0.4 mg/ml MTT (Sigma) in DMEM containing 10% (v/v) FCS, 100 µg/ml penicillin and 100 µg/ml streptomycin for 30 min at 37 °C. Prior to lysis, cells were rinsed twice with PBS (25 mM sodium phosphate buffer and 140 mM NaCl, pH 7.4) and lysed in 100 µl of 100% propan-2-ol containing 40 mM HCl. Conversion of MTT into formazan was measured at 595 nm using a multi-plate reader model 550 spectrophotometer (Bio-Rad), and the viability of the cells was calculated relative to untreated cells.

Plasmids

pCL-NEO RabIP4-vsvG (vesicular-stomatitis-virus glycoprotein) was kindly provided by Dr P. J. van de Sluijs (Department of Cell Biology, University Medical Center Utrecht, Utrecht, The Netherlands). pcDNA3.1-cullin1-FLAG was amplified from liver cDNA using FLAG-cullin forward and reverse primers (Table 1). The PCR fragment was cloned into pCRII (Invitrogen) and subsequently cloned into pcDNA3.1/ZEO. hCTR2-vsvG cDNA was amplified from cDNA by PCR using hCTR2-vsvG forward and hCTR2-vsvG reverse primers, and subsequently subcloned into pZeoSV2. The reverse primer contained a sequence to add the vsvG tag at the Carboxyterminus of hCTR2 as described previously for hCTR1-vsvG [105]. To construct pcDNA3.1/Zeo-hCTR1-vsvG (hCTR1-vsvG) and pcDNA3.1/Zeo-hCTR2-vsvG (hCTR2-vsvG), hCTR1-vsvG and hCTR2-vsvG fragments were isolated from pZeoV2-hCTR1-vsvG [105] or pZeoV2-hCTR2-vsvG after digestion with BamHI

and XbaI. The fragments were ligated into the BamHI and XbaI sites of pcDNA3.1/Zeo (Invitrogen). To generate Carboxyterminal eGFP (enhanced green fluorescent protein)-tagged hCTR1 and hCTR2, hCTR1 and hCTR2 fragments were amplified from cDNA by PCR using the Advantage cDNA polymerase mix (Clontech), with hCTR1 and hCTR2 forward and reverse primers respectively (Table 1). The fragments were ligated into the pCRII vector using the TA-cloning kit (Invitrogen). hCTR1 and hCTR2 fragments were isolated from pCRII after EcoRI digestion and subsequently cloned into the EcoRI site of pEGFP-N3 (Clontech), resulting in peGFP-N3-hCTR1 (hCTR1-eGFP) and peGFP-N3-hCTR2 (hCTR2-eGFP). To generate the pGL3-E1b-TATA-4MRE construct [MRE (metal-responsive element)-luciferase reporter], four MREs were amplified by PCR from the 4×MRE(d) construct [133, 246] using 4MRE-F/HindIII and 4MRE-R/PstI primers (Table 1). The fragment was digested by HindIII and PstI, and subsequently subcloned into the E1b-TATA pGL3 vector (kindly provided by Dr Eric Kalkhoven, University Medical Centre Utrecht, Utrecht, The Netherlands). hCTR1 and hCTR2 constructs with a Carboxyterminal FLAG tag were generated by PCR of hCTR1-vsvG and hCTR2-vsvG template constructs using Pfu Turbo polymerase (Stratagene) and the corresponding BamHI forward and NotI reverse primers for hCTR1 and hCTR2 respectively. These PCR fragments were digested with BamHI and NotI, and the fragments were ligated into the BamHI and NotI sites in pEBB-FLAG (kindly provided by Dr C.S. Duckett, University of Michigan Medical School, Ann Arbor, MI, U.S.A.), resulting in pEBB-hCTR1-FLAG and pEBB-hCTR2-FLAG constructs. pEBB-hCTR1-FLAG IXXXI (Ile-Xaa-Xaa-Xaa-Ile) and pEBB-hCTR2-FLAG IXXXI were generated by QuikChange® site-directed mutagenesis (Stratagene), using the hCTR1 IXXXI forward and reverse primers and the hCTR2 IXXXI forward and reverse primers. All constructs were verified by sequence analysis.

Transfection, chemical cross-linking, immunoprecipitation, and immunoblot analysis

HEK-293T cells were transiently transfected with either hCTR1-vsvG or hCTR2-vsvG using the calcium phosphate precipitation protocol [247]. DNA was diluted to a maximum concentration of 10 µg/ml in 244 mM $CaCl_2$ solution. The DNA mixture was then diluted with an equal volume of 2×HBSS (to a final concentration of 6.275 mM Hepes, 190 µM Na_2HPO_4, 68.5 mM NaCl and 122 mM $CaCl_2$, pH 7.5). After incubating for 20 min at 20 °C, the transfection mixture was added to the cells in 10 ml DMEM, and the cells were harvested after 2 days. Chemical cross-linking was performed by incubation of transfected HEK-293T cells for 30 min at room temperature (20 °C) with PBS containing 1% DMSO in 0 mM, 0.5 mM or 1 mM EGS [ethylene glycolbis(succinimidylsuccinate)] (Pierce). For cross-linking experiments and immunoprecipitation, HEK-293T cells were lysed in RIPA buffer [50 mM Tris/HCl, pH 7.4, 0.1% (v/v) SDS, 1% (v/v) Nonidet P40, 150 mM NaCl, 10 mg/ml sodiumdeoxychalate, 2 mM EDTA and 1 mM $NaVO_3$] supplemented with Complete™ protease inhibitor cocktail (Roche), and lysates were solubilized by passage seven times through a needle (23 gauge). For immunoprecipitation, 1 mg of total protein, 20 µl of Protein A-agarose beads (Sigma) and 0.6 µg of rabbit anti-vsvG antibody (Abcam) were incubated overnight at 4 °C in a volume of 500 µl while rotating. For co-immunoprecipitation experiments, 1 ml of the cell lysate was divided into two precipitation reaction mixtures with either 20 µl of Protein A-agarose beads and 0.6 µg of rabbit anti-vsvG antibody or 20 µl

of anti-FLAG M2-agarose (Sigma), which were incubated for 4 h at 4 °C with rotation. Immunocomplexes were precipitated by microcentrifugation at 2000 ***g*** for 3 min at 4 °C and washed four times in RIPA buffer. Immunoprecipitates were resuspended in SDS/PAGE sample buffer [62.5 mM Tris/HCl, 4% (v/v) SDS, 5% (v/v) glycerol, 0.01% (w/v) Bromophenol Blue and 2% (v/v) 2-mercaptoethanol, pH 6.8] and heated at 95 °C for 5 min prior to resolution by SDS/PAGE (12% gels). Proteins were transferred on to Hybond-P PVDF membranes (Amersham Biosciences) by standard immunoblot procedures. The membranes were blocked in Tris-buffered saline (25 mM Tris/HCl, pH 7.4, 137 mM NaCl and 2.7 mM KCl) containing 5% (w/v) non-fat dried milk (Sigma) and 0.1% (v/v) Tween 20. Immunoblots were probed with rabbit anti-vsvG antibody (0.6 μg/ml) (Abcam), mouse anti-(vsvG hybridoma) supernatant from clone P5D4 (1:250 dilution) [95] or horseradish-peroxidase-conjugated mouse anti-FLAG M2 antibody (Sigma) for 1 h. Reactivity was detected using horseradish-peroxidase-conjugated secondary antibodies (1 ng/ml; Pierce) and ECL® (enhanced chemiluminescence) (Amersham Biosciences), according to the manufacturer's instructions.

Indirect immunofluorescence and confocal laser-scanning microscopy

HEK-293T cells, U2OS cells and HeLa cells were transiently transfected with hCTR1-eGFP, hCTR2-eGFP or hCTR2-vsvG, using Lipofectamine™ 2000 (Invitrogen) according to the manufacturer's protocol. At 1 day after transfection, cells were treated with trypsin and seeded on to coverslips (Paul Marienfeld, GmbH & Co.). After 24 h, cells were rinsed with ice-cold PBS and fixed in 3.7% (w/v) paraformaldehyde in PBS for 20 min at 4 °C. Cells were rinsed three times with 0.02% (v/v) Triton X-100 in PBS, and non-specific binding was blocked with blocking buffer [5% (w/v) BSA in PBS and 0.02% (v/v) Triton X-100] for 30 min at room temperature. Immunolabelling was performed in blocking buffer for 1 h with the antibodies indicated below. Cells were rinsed three times with 0.02% (v/v) Triton X-100 in PBS, and secondary labeling was performed with affinipure Alexa Fluor® 568-conjugated goat anti-(mouse IgG) or goat anti-(rabbit IgG) antibodies (10 μg/ml; Molecular Probes). Coverslips were mounted in Fluorsave (VWR International), and confocal laser-scanning microscopy was performed using a Leica TCS 4D microscope equipped with a Plan APO ×63 oil immersion objective (numerical aperture 1.4) and dedicated imaging software (Leica TCSNT version 1.6.587). hCTR1-vsvG and hCTR2-vsvG were labeled with rabbit anti-vsvG antibodies (0.6 μg/ml) (Abcam). For double-labeling experiments, monoclonal antibodies against p230 (230 kDa protein) [a TGN (*trans*-Golgi network) marker] (1.25 μg/ml; BD Biosciences), human TfR (transferrin receptor) (1 μg/ml; Molecular Probes), CD63 (a late endosomal marker) (75 ng/ml; Zymed Laboratories) and the lysosomal markers CD107a [LAMP (lysosome-associated membrane protein)-1] and CD107b (LAMP-2) (5 μg/ml; BD Biosciences) were used.

Luciferase reporter assays

For luciferase reporter assays, HEK-293T cells were seeded in 96-well plates and transiently transfected using the calcium phosphate transfection protocol. Each well was co-transfected with 35 ng of the MRE-luciferase reporter, 0.25 ng of pRL-TK vector (Promega Benelux BV) and 3.5 ng of hCTR1-vsvG, 3.5 ng of hCTR2-vsvG, 0.35 ng of pEBB-hCTR1-FLAG

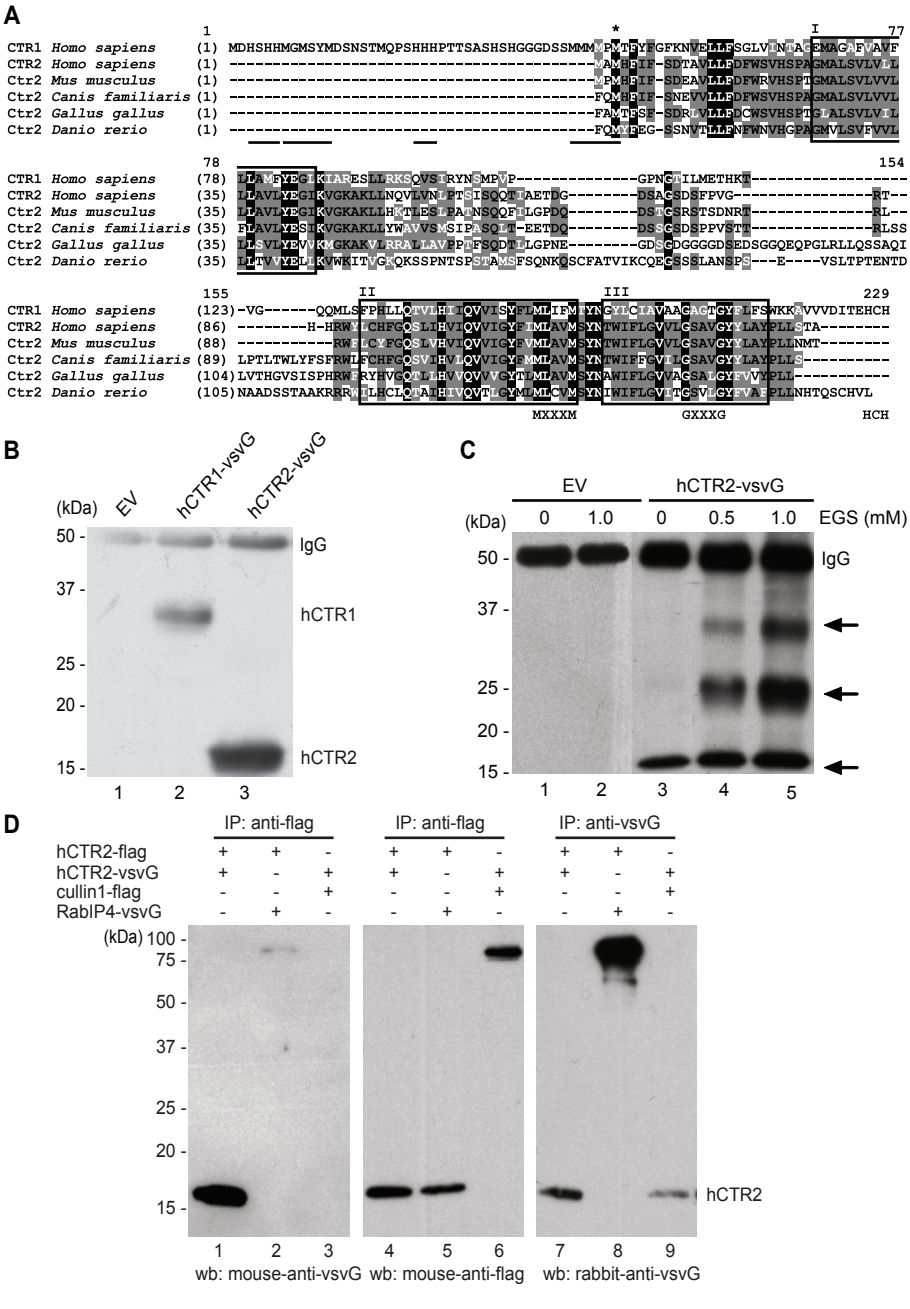
A
CTR1 Homo sapiens
CTR2 Homo sapiens
Ctr2 Mus musculus
Ctr2 Canis familiaris
Ctr2 Gallus gallus
Ctr2 Danio rerio
MXXXM
GXXXG
HCH
B
(kDa)
EV
hCTR1-vsvG
hCTR2-vsvG
50
37
25
20
15
IgG
hCTR1
hCTR2
1 2 3
C
EV
hCTR2-vsvG
(kDa)
0 1.0 0 0.5 1.0 EGS (mM)
50
37
25
20
15
IgG
1 2 3 4 5
D
IP: anti-flag
IP: anti-flag
IP: anti-vsvG
hCTR2-flag
hCTR2-vsvG
cullin1-flag
RabIP4-vsvG
(kDa)
100
75
50
37
25
20
15
hCTR2
1 2 3 4 5 6 7 8 9
wb: mouse-anti-vsvG
wb: mouse-anti-flag
wb: rabbit-anti-vsvG

Figure 1. Biochemical characterization of hCTR2
(A) Sequence alignment between hCTR1 and CTR2 from different species using the AlignX module from Vector NTI (Invitrogen). Identical regions (white text on black background), conserved regions (black text on grey background) and similar regions (white text on grey background) of amino acids are indicated. The transmembrane regions (boxed regions) are indicated by roman numerals. The MXXXM motif, the GXXXG motif involved in intrahelical interactions and the C-terminal His-Cys-His (HCH) motif are indicated. The methionine motifs and histidine-rich regions involved in high-affinity copper transport are underlined, and one conserved methionine residue is indicated by an asterisk. (B) Empty vector (EV), hCTR1–vsvG or hCTR2–vsvG constructs (lanes 1–3) were transiently transfected into HEK-293T cells prior to lysis. Immunoblot analysis was performed on proteins immunoprecipitated by anti-vsvG antibodies. (C) HEK-293T cells were transiently transfected with EV (lanes 1 and 2) or hCTR2–vsvG (lanes 3–5) constructs. Cells were incubated for 30 min at room temperature with increasing concentrations of the chemical cross-linker EGS (lanes 2–5). Immunoprecipitation and subsequent immunoblot analysis was performed to detect hCTR2–vsvG-containing complexes (arrows). The heavy chain of the antibodies is indicated (IgG). (D) HEK-293T cells were transiently co-transfected with hCTR2–FLAG (flag), hCTR2–vsvG, cullin1–FLAG or RABIP4–vsvG. Immunoprecipitation (IP) was performed with either mouse anti-FLAG M2–agarose beads or rabbit anti-vsvG attached to Protein A–agarose beads. Precipitates were washed and resolved by SDS/PAGE (12% gels), and immunoblot (wb) analysis was performed with antibodies as indicated. Molecular masses in kDa are shown on the left-hand side of the immunoblots.

or 0.35 ng of pEBB-hCTR2-FLAG constructs as indicated. After incubation for 24 h, the cells were rinsed with PBS and subsequently maintained for 24 h in DMEM in the presence or absence of different metals. To investigate the response to hypoxia, cells were transiently transfected with 10 ng of the hypoxia-responsive reporter vector with 5×HRE [248] and 0.25 ng of pRL-TK vector. After 24 h, cells were incubated for a further 24 h with 100 μM DFO (desferrioxamine), an iron chelator. After incubation, the cells were rinsed in PBS, harvested in passive lysis buffer (Promega) according to the manufacturer's protocol and assayed by luminometry (Berthold Technologies) using the Dual-Luciferase® reporter assay system (Promega) for firefly luciferase activity and *Renilla* luciferase activity, according to the manufacturer's protocol. The RLU (relative light units) were calculated by dividing firefly luciferase measurements by *Renilla* luciferase measurements. All values were expressed as fold inductions relative to empty vector control incubations (set at 1). Statistical analysis was performed on RLU data for the different incubations. A two-tailed Student's *t* test was used to analyze the statistical differences between different data points.

Results

Biochemical characterization of hCTR2

To characterize hCTR2, hCTR1-vsvG and hCTR2-vsvG were expressed in HEK-293T cells, immunoprecipitated and subjected to immunoblot analysis. No precipitated proteins were detected in cells transfected with the empty vector, whereas hCTR1-vsvG was observed to migrate on SDS/PAGE at approximately 35 kDa (Figure 1B). This was consistent with previous studies [105], which indicated that the fully glycosylated mature hCTR1 was expressed. hCTR2-vsvG was detected to migrate with an apparent molecular mass of approx. 17 kDa (Figure 1B), in agreement with its size as predicted from amino acid sequence analysis (17000 Da). Crude cell fractionation studies indicated that hCTR2 was associated with cellular membranes (results not shown). This biochemical analysis indicated that hCTR2-vsvG was expressed as a stable membrane-associated protein and was most probably not glycosylated.

Chemical cross-linking and two-dimensional crystallography experiments conducted previously revealed that hCTR1 assembles as a trimer [86, 100]. Thus we considered the

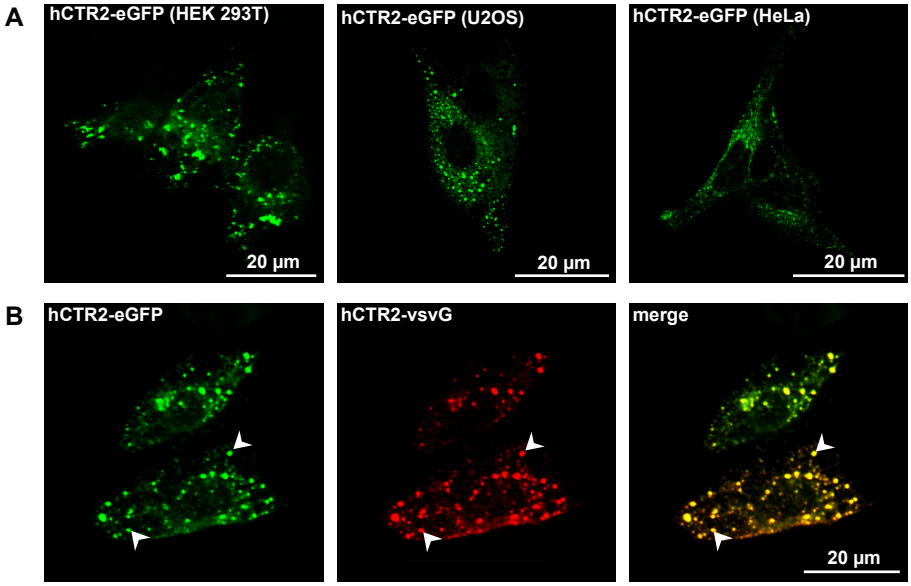

Figure 2. hCTR2 is localized in intracellular vesicles
(A) Localization of hCTR2 was assessed by direct confocal laser-scanning microscopy in HEK-293T, U2OS and HeLa cells after transient transfection with hCTR2–eGFP. (B) HeLa cells were transiently co-transfected with both hCTR2–vsvG and hCTR2–eGFP constructs. hCTR2–vsvG was immunolabelled with rabbit anti-vsvG antibodies, and secondary labelling was performed with Alexa Fluor® 568 conjugated-goat anti-rabbit and goat anti-mouse antibodies. hCTR2–eGFP was visualized by direct confocal microscopy. Co-localization is indicated by arrowheads.

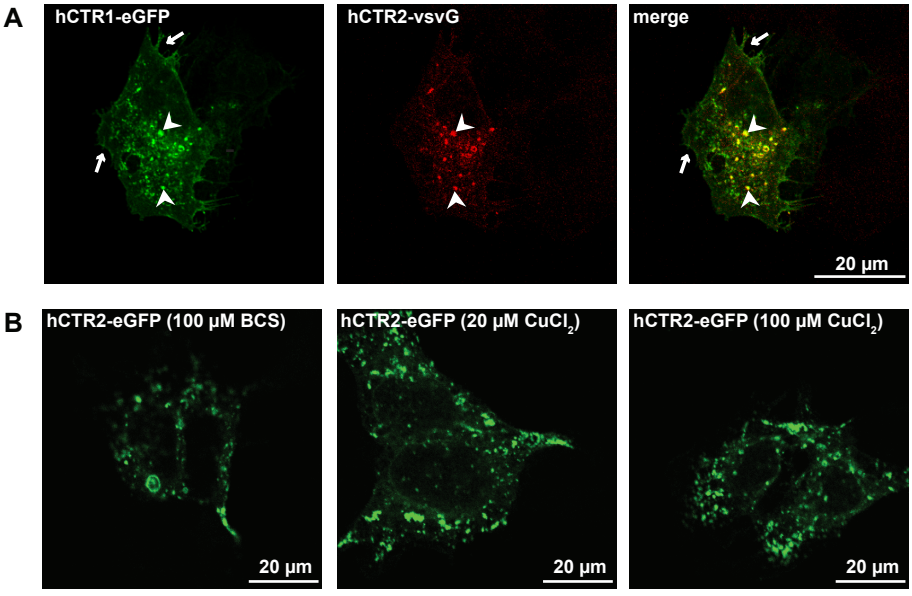

Figure 3. hCTR2 is partially co-localized with hCTR1
(A) Confocal laser-scanning microscopy was performed on HeLa cells which were transiently transfected with hCTR1–eGFP and hCTR2–vsvG constructs. hCTR2–vsvG was immunolabelled with rabbit anti-vsvG antibodies, and secondary labelling was performed using Alexa Fluor® 568-conjugated antibodies. hCTR1–eGFP was visualized by direct confocal microscopy. Plasma membrane localization of hCTR1–eGFP is indicated with arrows, and co-localization with arrowheads. (B) HEK-293T cells were transiently transfected with the hCTR2–eGFP construct. Prior to analysis, cells were incubated for 1 h with either BCS or $CuCl_2$ at the concentrations indicated.

possibility that hCTR2 also exists as an oligomeric complex. The amine-reactive chemical cross-linker EGS was used to covalently link cellular interacting proteins. Chemical cross-linking with EGS in HEK-293T cells transiently transfected with hCTR2-vsvG resulted in the detection of discrete vsvG immunopositive bands which migrated at apparent molecular masses of approx. 24 and 35 kDa. The intensity of these putative hCTR2-vsvG oligomers increased in an EGS concentration-dependent manner (Figure 1C; arrows). At high EGS concentrations (1 mM), additional complexes of even higher molecular mass (>200 kDa) were also observed (results not shown). These results suggested that hCTR2 may be capable of forming oligomeric complexes, similar to those observed for hCTR1 (chapter 4) [86].

To investigate further this possibility, hCTR2 constructs were generated with a FLAG tag present at the Carboxyterminus. These constructs were co-expressed with hCTR2-vsvG in HEK-293T cells, and cell lysates were subjected to co-immunoprecipitation with either anti-FLAG M2-agarose beads or Protein A-agarose beads coupled to rabbit anti-vsvG antibodies. Immunoprecipitation of both vsvG-tagged proteins (Figure 1D, lanes 7-9) and FLAG-tagged proteins (Figure 1D, lanes 4-6) was observed. Co-immunoprecipitation of hCTR2-vsvG with hCTR2-FLAG was observed (Figure 1D, lane 1), but no interaction was noted with RabIP4-vsvG (Figure 1D, lane 2), and with Cullin1-FLAG (Figure 1D, lane 3), which were used as negative controls. Taken together, these experiments suggest that hCTR2 monomers mutually interact, and support the hypothesis that CTR proteins form trimeric complexes to enable copper transport.

Intracellular localization of hCTR2

To investigate the cellular localization of hCTR2, we generated constructs encoding hCTR2 with a Carboxyterminal eGFP tag. Similarly to hCTR2-vsvG, hCTR2-eGFP expressed in HEK-293T cells also migrated at its expected molecular mass of 40 kDa and could be detected in higher-molecular-mass oligomers (results not shown). The cellular localization of hCTR2 was determined after transient transfection of hCTR2-eGFP into HEK-293T cells, U2OS cells and HeLa cells (Figure 2A). hCTR2-eGFP was not detected at the plasma membrane, but was primarily localized in relatively large vesicles in all three cell types (Figure 2A). We set out to exclude the possibility that the inserted tag could have interfered with the localization of transiently expressed hCTR2. Independently transfected hCTR2-vsvG and hCTR2-FLAG were also detected in large vesicular compartments in multiple cell types (results not shown), and co-expression of hCTR2-vsvG with hCTR2-eGFP resulted in strong co-localization between the two constructs (Figure 2B). The latter result indicates that the cellular localization of hCTR2 was independent of the tag added to the protein.

Consistent with previous results, hCTR1-eGFP was detectable in HeLa cells at the plasma membrane, but was primarily localized in intracellular vesicles, and hCTR1-eGFP also partly co-localized with hCTR2 (Figure 3A) [86, 105]. Cell-surface hCTR1 is known to

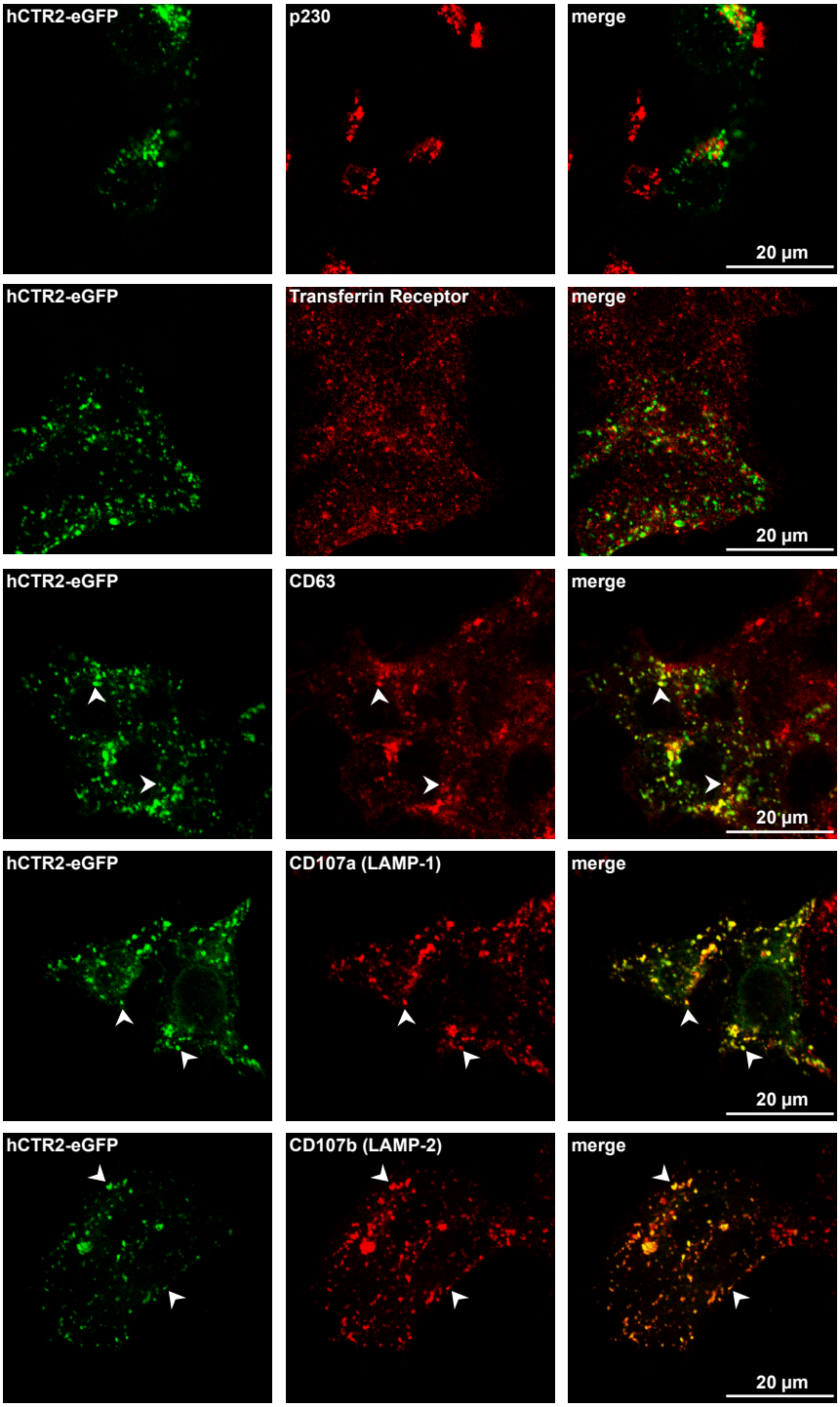
hCTR2-eGFP
p230
merge
20 µm
hCTR2-eGFP
Transferrin Receptor
merge
20 µm
hCTR2-eGFP
CD63
merge
20 µm
hCTR2-eGFP
CD107a (LAMP-1)
merge
20 µm
hCTR2-eGFP
CD107b (LAMP-2)
merge
20 µm

Figure 4. hCTR2 co-localized with late endosomal and lysosomal vesicles
HEK-293T cells were transiently transfected with hCTR2–eGFP prior to labelling with antibodies against different vesicular markers: the TGN marker p230, TfR (early endosomal marker), CD63 (late endosomal marker) and the lysosomal markers LAMP-1 and LAMP-2. Secondary labelling was performed using Alexa Fluor® 568-conjugated antibodies before being visualized by direct confocal microscopy. Green and red channels were merged to determine the co-localization of hCTR2–eGFP with the different compartmental markers (arrowheads).

be rapidly and specifically internalized upon incubation of HEK-293T cells with increasing concentrations of copper [64]. To determine whether copper affects hCTR2 localization, HEK-293T cells were transiently transfected with hCTR2-eGFP. Cells were incubated with different copper concentrations or with the copper-chelating agent, BCS, for 1 h. No apparent copper-dependent relocalization of hCTR2 was observed (Figure 3B), which is in accordance with previous results suggesting that the intracellular fraction of hCTR1 does not undergo copper-dependent relocalization [105].

The nature of the vesicular localization of hCTR2 in HEK-293T cells was investigated further. HEK-293T cells were transiently transfected with hCTR2-eGFP, and immunofluorescence labeling of different cellular marker proteins was performed. No significant co-localization was observed between hCTR2-eGFP and TfR, an early endosomal marker, or between hCTR2-eGFP and p230, a TGN-resident protein (Figure 4). However, hCTR2 was partly co-localized with late endosomes, identified by labeling with an anti-CD63 antibody, and marked co-localization was observed with the lysosomal markers LAMP-1 and LAMP-2 (Figure 4, arrowheads). Similar results were observed in HeLa cells (results not shown), indicating that the localization of hCTR2 in late endosomes and lysosomes was not cell-type-specific.

A novel transcription-based copper sensor to measure cytosolic bioavailable copper pools

To address whether hCTR2 could facilitate copper uptake, a novel transcription-based copper biosensor was designed. The design of this sensor was based on the endogenous capacity of cells to transactivate metallothionein genes in response to elevated cytosolic copper availability. An increase in the concentration of copper in the cytosol results in the displacement of zinc from metallothioneins. The released zinc binds to and activates MTF (metal responsive transcription factor)-1, which subsequently induces gene expression by binding to MREs in the promoter region of specific genes [133, 249]. Four MREs from the murine metallothionein 1A promoter [133, 246] were cloned upstream of the firefly luciferase open reading frame in the pGL3-E1b-TATA vector (Figure 5A), and this resulted in the formation of the MRE-luciferase reporter. A construct encoding the metal-insensitive TK (thymidine kinase)-*Renilla* luciferase was used to correct for differences in transfection efficiencies. Similarly to the endogenous metallothionein 1A promoter, the MRE-luciferase reporter was predicted to be transactivated in a metal-concentration-dependent fashion by MTF-1 [133]. In this way, the MRE-luciferase reporter measured bioavailable cytosolic copper. To test the validity of this approach, the MRE-luciferase reporter was transiently transfected into HEK-293T cells (Figure 5C) and U2OS cells (results not shown), and cells were incubated with different copper concentrations for 24 h. At the concentration of copper normally present in the medium, reporter activity was slightly increased compared with cells transfected with a control vector containing no MREs. A linear concentration-

dependent induction of the activity of the MRE-luciferase reporter was noted when cells were incubated with 20-100 µM $CuCl_2$, an effect that was not observed in cells transfected with the empty vector only (Figure 5C). The induction of the MRE-luciferase reporter activity was approx. 5-fold increased at a concentration of 100 µM $CuCl_2$, in comparison with the activity observed at the concentration of basal copper present in the medium. Higher concentrations of copper did not result in further induction of MRE-luciferase reporter activity. A more detailed examination of MRE-luciferase reporter activities at low copper concentrations revealed that the sensor was not effectively induced by copper concentrations below 20 µM in these cells (results not shown). Since the reporter is responsive to cytosolic copper, an increase in reporter activity was interpreted as an indication that copper import and transport across a cellular membrane had occurred. Quantitative RT (reverse transcription)-PCR experiments revealed that induction of the endogenous metallothionein 1A promoter also occurred at the same copper concentrations as the MRE-luciferase reporter activity was induced (results not shown). As different metals are known to induce MTF-1-mediated transcription [133], the specificity of the MRE-luciferase reporter for several other biologically important metals was tested. Zinc is especially relevant in this respect, since activation of MTF-1 is caused by incorporation of cellular zinc into MTF-1 after displacement of zinc from metallothioneins by other metals, such as copper [133]. Initially, metal toxicity was determined by MTT viability assays to calculate LD_{50} values in our cells (Figure 5B). Subsequently, HEK-293T cells were transiently transfected with the MRE-luciferase reporter, and, 24 h after transfection, cells were incubated with either a low or a high metal concentration that was still below the lethal concentration (Figure 5D). $CuCl_2$ and $ZnCl_2$ resulted in the induction of reporter activities in a concentration-dependent manner, whereas $MgCl_2$, $FeCl_3$ and $MnCl_2$ failed to activate the MRE-luciferase reporter. MTF-1-mediated transcription may also be induced by other factors, such as oxidative stress and hypoxia [133, 250]. However, no MRE-luciferase reporter induction was observed as a result of oxidative stress. This was examined by incubation of transfected cells with 100 µM hydrogen peroxide or 100 µM paraquat for 24 h (results not shown) [251]. To mimic hypoxia, cells were treated with DFO [252], which resulted in induction of the hypoxia-responsive 5x HRE reporter (Figure 5E). The MRE-luciferase reporter activity was only slightly induced upon DFO treatment, whereas $CuCl_2$ strongly induced the MRE reporter, but not the 5× HRE reporter (Figure 5D). Considered together with the idea that all experiments in the present study were performed under normoxic conditions, we concluded that the MRE-luciferase reporter specifically detects elevated copper and zinc concentrations under these defined experimental conditions.

hCTR1 and hCTR2 facilitate copper uptake

Next, we tested whether this approach could be used to effectively assess perturbations in the known copper import pathway. To investigate this, hCTR1-FLAG was co-transfected into HEK-293T cells together with the MRE-luciferase reporter. Without supplementing the medium with additional $CuCl_2$, this resulted in a significant increase (approx. 3-fold) in reporter activity when compared with cells transfected with the empty vector (Figure 6A and 6B). This increase in reporter activity could be prevented completely by incubation with the copper chelator, BCS (results not shown), indicating that exogenous expression

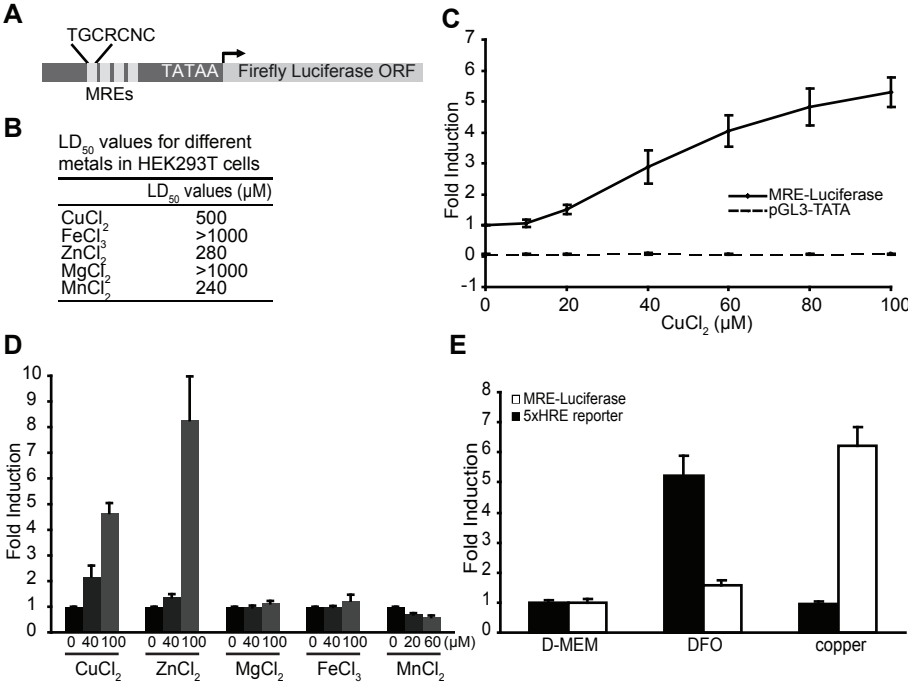

Figure 5. Characterization of a novel MRE-Luciferase reporter assay

(A) The MRE–luciferase reporter was constructed by cloning four MREs upstream of the firefly luciferase open reading frame of the pGL3-TATA construct as indicated. (B) HEK-293T cells were transiently transfected with the MRE–luciferase reporter or the control vector, pGL3-TATA. After transfection, cells were incubated for 24 h with different concentrations of CuCl2. (C) Metal toxicity was measured using MTT viability assays after incubation for 24 h with different metal concentrations, and LD_{50} values were also determined. (D) HEK-293T cells were transiently transfected with the MRE–luciferase reporter, and, 24 h after transfection, cells were incubated with a low or a high sub-lethal metal concentration. (E) HEK-293T cells were transiently transfected with either the MRE–luciferase reporter or a HRE–luciferase reporter. After transfection, cells were incubated with 100 μM $CuCl_2$ or 100 μM of DFO (to mimic hypoxia). Luciferase reporter activities were measured and normalized for Renilla luciferase activities. Values are expressed as fold induction relative to control incubations ±S.E.M. (see the Experimental section) (n≥3).

of hCTR1-FLAG resulted in a significant increase in the cytosolic copper concentration in the presence of cell culture medium containing a low concentration of copper. Addition of $CuCl_2$ (up to 2.5 μM) resulted in a marked and significant increase in the reporter activity, with a maximal 10-fold induction observed at 2.5 μM $CuCl_2$ (Figure 6A). Since the MRE-luciferase reporter was activated by zinc as well as by copper, one possible explanation for the reporter induction is that exogenous expression of hCTR1-FLAG resulted in the mobilization of sequestered vesicular zinc pools under conditions of excess cytosolic copper. To address this possibility, the effects of transient transfection of hCTR1-FLAG on zinc-induced reporter activity were assessed. In transfected cells containing the empty vector, no induction of the MRE-luciferase reporter activity was observed when incubated with $ZnCl_2$ at the same concentrations as used in the copper experiments. In cells expressing exogenous hCTR1-FLAG, the basal reporter activity was raised approx. 3-fold as shown above (Figure 6A and 6B), but the MRE-luciferase reporter activity was not induced further as a result of additional $ZnCl_2$ (Figure 6B). These results strongly indicate that expression of hCTR1-FLAG resulted in an increase in the bioavailability of copper, but not zinc. As a

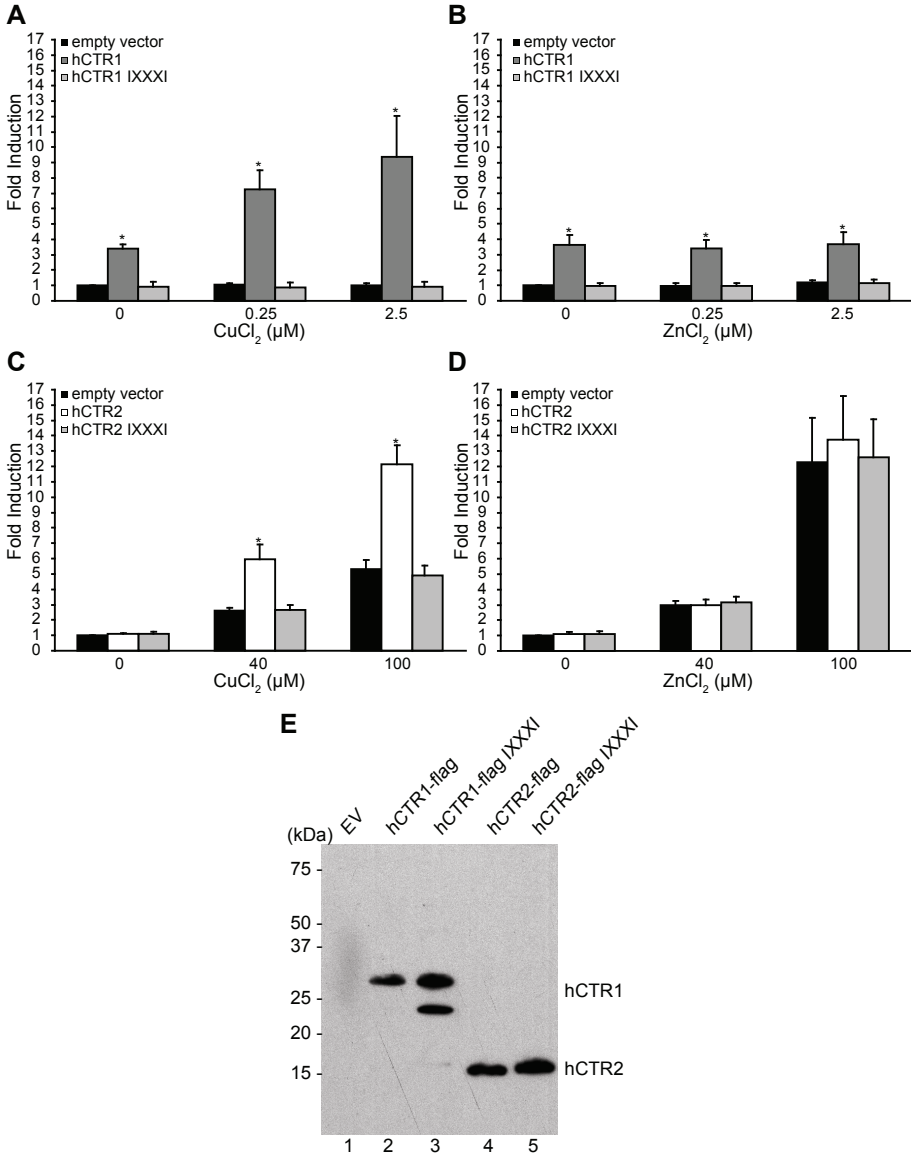

Figure 6. Cellular copper uptake is facilitated by hCTR2 and is dependent on the CTR-specific MXXXM motif
The MXXXM motifs were mutated to form IXXXI in pEBB-hCTR1-FLAG and pEBB-hCTR2-FLAG. HEK-293T cells were transiently transfected with the MRE–luciferase reporter in combination with wild-type pEBB-hCTR1-FLAG (A,B), pEBB-hCTR2-FLAG (C,D) or the IXXXI mutant motif constructs. After transfection, cells were incubated for 24 h with increasing amounts of $CuCl_2$ (A,C) or $ZnCl_2$ (B,D). MRE–luciferase reporter activities were measured and RLU were calculated after normalization for Renilla luciferase activity. Values are expressed as fold induction relative to control incubations (see the Experimental section)±S.E.M. (n=3). Statistical differences between empty vector (EV)- and hCTR1- or hCTR2-transfected cells are indicated (*P<0.01). (E) Lysates from the MRE–luciferase assay were resuspended in SDS/PAGE sample buffer, resolved by SDS/PAGE and subjected to immunoblot analysis using the mouse anti-FLAG antibody. Molecular masses are indicated in kDa.

control, immunoblot analysis of hCTR1-FLAG was used to determine protein expression under these conditions (Figure 6E). Together, these data indicated the feasibility of using the MRE-luciferase reporter to specifically assess changes in the expression of copper import proteins on copper uptake. Furthermore, these results confirmed previous observations that the expression of hCTR1 was a limiting factor in copper import, at least at relatively low copper concentrations [85].

Next, the potential role of hCTR2 in copper import was studied in a similar manner to that of hCTR1 by co-transfection of hCTR2-FLAG and MRE-luciferase reporter in HEK-293T cells. Expression of hCTR2-FLAG was verified by immunoblot analysis (Figure 6E). In cells transfected with the empty vector, reporter activity was induced in the presence of 10-20 μM $CuCl_2$ (results not shown). However, hCTR2-FLAG expression resulted in a significantly higher reporter induction compared with cells transfected with the empty vector. At concentrations of 40 and 100 μM $CuCl_2$, expression of hCTR2-FLAG resulted in a >2-fold increase (Figure 6C). The increased hCTR2-FLAG-dependent MRE-luciferase reporter activation was copper-specific, as no differences were observed on incubation with $ZnCl_2$ (Figure 6D). To demonstrate further that the function of hCTR2 was copper-specific, we mutated the methionine residues in the MXXXM motif to isoleucine. Previous findings by Eisses and Kaplan [242] revealed a marked reduction in hCTR1-mediated copper uptake after disruption of the analogous methionine residues present in the MXXXM motif of hCTR1. Whereas expression of wild-type hCTR1-FLAG or hCTR2-FLAG resulted in a significant copper-dependent induction of the MRE-luciferase reporter, substitution of the MXXXM motif to IXXXI completely abolished the induction of the reporter by hCTR1-FLAG and by hCTR2-FLAG (Figures 6A and 6C). The lack of induction was a result of the amino acid substitution, as all the constructs were shown to be expressed successfully (Figure 6E). No differences were observed after incubation with $ZnCl_2$ (Figures 6B and 6D). Taken together, expression of hCTR2 facilitates cellular copper uptake with a lower affinity compared with hCTR1.

Discussion

Since the initial characterization of hCTR1 almost a decade ago [84], elegant studies have addressed the structure and localization of mammalian Ctr1, its transport kinetics, regulation by copper and the role in embryonic development and dietary copper uptake in mice [64, 85, 86, 88, 89, 91, 93, 95, 96, 98-100, 105, 107, 242, 244]. Although these studies have greatly increased our knowledge of the mechanisms of cellular copper uptake, they also established that Ctr1-independent copper import pathways exist. MEFs obtained from *Ctr1*-knockout embryos displayed low-affinity copper uptake [91]. On the basis of the evidence of the present study, we propose that hCTR2, a protein with structural similarity to hCTR1, but with a previously unknown function, mediates an alternative low-affinity copper import pathway in human cells.

To be able to characterize the function of hCTR2, we constructed a novel metal sensor. This sensor allowed sensitive and high-throughput assessment of copper homoeostasis. It is important to note that the MRE-luciferase reporter measures cytosolic bioavailable copper and was based on a cell-intrinsic copper-sensing mechanism, removing the need

to add exogenous compounds that bind copper directly and might potentially interfere with the copper homoeostatic mechanisms present in the cell [253]. By performing control experiments using zinc, the sensor allowed determination of the specific effects of exogenously expressed proteins on copper metabolism. Our data strongly indicated that hCTR2 facilitates cellular copper import with a lower affinity than that mediated by hCTR1. At copper concentrations below 10 μM, at which hCTR1-dependent MRE-luciferase reporter activity was maximally induced, no effect of hCTR2 expression on reporter activity could be detected. In contrast, exogenous expression of hCTR2 resulted in significantly higher copper-dependent MRE-luciferase activity compared with empty vector controls. This effect was copper-specific, since mutation of conserved methionine residues known to be essential for copper transport in CTR proteins completely abolished the activation of the reporter. Therefore hCTR2 expression resulted in a specific increase in cytosolic copper availability at high concentrations of copper in the extracellular medium. Since the copper sensor does not measure the transport of copper directly, further studies are necessary to address the kinetics of hCTR2-mediated copper import in more detail.

The apparent steady-state localization of this protein in the endosomal and lysosomal compartments is notable. Lysosomes in mammalian cells and vacuoles in yeast have equivalent functions. In *Saccharomyces cerevisiae*, the hCTR2 orthologue, yCtr2p, is localized to the vacuolar membrane and can mobilize vacuolar copper pools [254]. A similar vacuolar membrane localization was observed for Ctr6, the hCTR2 orthologue in the fission yeast, *Schizosaccharomyces pombe* [255]. Combined with our data, we suggest that the endosomal and lysosomal localization and mobilization of intracellular copper stores are common properties of yeast and mammalian CTR2/Ctr6 proteins. Our data suggest that the observed intracellular localization of hCTR2 is correct, since it was observed in multiple cell types and appeared to occur independently of the tags present. Moreover, expressed proteins were demonstrated to stimulate functional copper uptake activity. A similar localization of endogenous CTR2 in large vesicular compartments, reminiscent of late endosomes and lysosomes, was observed in human and monkey cells in other independent studies (J. Bertinato, personal communication). There is ample precedence for the localization of CTRs in intracellular compartments. Under basal copper levels, ATP7A resides in the Golgi-network and is only distributed towards peripheral vesicles and the plasma membrane in response to an increase in cytosolic copper concentrations [60, 62]. In addition, hCTR1 also resides predominantly in intracellular vesicles, but has been shown to recycle constitutively between this vesicular compartment and the plasma membrane [64, 95]. In fact, part of the intracellular pool of hCTR2 resided in vesicular compartments that also contained hCTR1, but further studies are required to clarify the implications of this intriguing observation.

Our results suggest that hCTR2 is an intracellular oligomeric membrane protein which is rate-limiting for the delivery of copper into the cytosol at high copper concentrations. We have proposed a model of cellular copper uptake by hCTR2. In mammalian cells, extracellular copper and cuproenzymes destined for lysosomal degradation may be endocytosed or pinocytosed by CTR-dependent or -independent mechanisms. Copper may subsequently be concentrated into lysosomes, prior to mobilization by hCTR2. This process may require high extracellular concentrations of copper or prolonged concentration of copper in lysosomal vesicles, consistent with our observation that hCTR2 stimulates copper

uptake at relatively high copper concentrations. This model fits with the current knowledge of the biology of dietary copper import and intracellular copper sequestration. Intestinal epithelium of gut-specific *Ctr1*-null mice unexpectedly accumulated dietary copper [93]. The failure to express Ctr1 did not lead to reduced cellular copper uptake, but rather caused an increase in the intracellular sequestration of copper, presumably in lysosomal vesicles. If mouse Ctr2 could function to mobilize copper from intracellular pools in gut epithelium, this activity is clearly not sufficient to prevent the severe systemic copper deficiency present in intestine-specific *Ctr1*-null mice [93]. Although the existence of vesicular copper stores in mammalian cells remains speculative, extensive copper accumulation has indeed been observed in lysosomes of Wilson disease patients [256], in LEC (Long-Evans Cinnamon) rats (a model for Wilson disease) [257] and in the liver cells of Bedlington terriers affected with copper toxicosis [258]. Finally, several other metal transport systems utilize the endocytic machinery to import metals into the cytosol. In yeast, zinc transporters regulate vacuolar zinc stores to modulate zinc homeostasis [259]. Mouse zinc transporter ZIP1, ZIP3, and ZIP4 are localized in intracellular vesicles, and may translocate to the plasma membrane for zinc uptake [260, 261]. Furthermore, the DMT (divalent metal transporter) 1 protein is involved in the transfer of endocytosed iron into the cytosol [116, 262]. Therefore cellular copper uptake may require a combination of transport across the plasma membrane, endocytosis of the metal and mobilization from intracellular pools, as observed for the uptake of other transition metals.

In summary, these results suggest that hCTR2 is predominantly localized in the endosomal system and stimulates copper uptake with a relatively low affinity to make it bioavailable in the cytosol, and suggest that hCTR2 may be responsible for the residual copper uptake activity observed in cells obtained from *Ctr1*-null embryos. Since this work is the first study on the function and localization of hCTR2, many questions remain unanswered. It will be important to examine further the nature and function of vesicular copper sequestration in copper homoeostasis, and to identify the mechanisms that are responsible for import of copper into endosomes and lysosomes. Ultimately, studying the impact on copper homoeostasis of knocking out *Ctr2* from the mouse genome at the level of the entire organism will be required to obtain a complete understanding of the regulation of copper uptake under different conditions and cellular demands

Acknowledgements

We thank Dr Walter Schaffner for providing the 4×MRE(d) construct, and Dr P. J. van de Sluijs for providing the pCL-NEO RabIP4-vsvG construct. We are grateful to Dr Eric Kalkhoven and Professor Dr Cisca Wijmenga for critical evaluation of the manuscript, and the members the Klomp-Wijmenga group for valuable discussions and assistance. This work was supported by a grant from the Netherlands Organization for Scientific Research (NWO: 912-04-106).

CHAPTER 4

Cellular Copper Uptake Requires Oligomerization of the Human High Affinity Copper Transporter 1

Peter V.E. van den Berghe
Margriet Hendriks
Ruud Berger
Leo W.J. Klomp

Submitted

Abstract

The transition metal copper is an essential trace element for all organisms that utilize oxygen. Cellular copper uptake is critically dependent on the high-affinity copper transporter 1 (CTR1). Biochemical and structural analyses indicated that human CTR1 (hCTR1) forms oligomeric complexes. This study aimed to characterize these hCTR1 oligomers and to assess the role of hCTR1 oligomerization in functional copper uptake. Co-immunoprecipitation of wild type (WT) hCTR1 with different epitope tags indicated that hCTR1 subunits interact and confirmed that oligomerization of hCTR1 is copper-independent. Next, we utilized a transcription-based copper sensor to determine the importance of hCTR1 oligomerization. Expression of hCTR1 WT in HEK 293T cells resulted in strong reporter activation, with maximal induction at 1 μM $CuCl_2$, consistent with the K_m of hCTR1. Conversion of two highly conserved methionine residues in the second transmembrane region of hCTR1 into isoleucines (hCTR1 M150I-M154I) completely abolished hCTR1-dependent copper uptake. Interestingly, hCTR1-dependent copper uptake was inhibited in a dominant-negative manner when hCTR1 WT and hCTR1 M150I-M154I were coexpressed, suggesting a direct functional interaction between the wild type protein and the mutant. In concordance with this observation, hCTR1 M150I-M154I subunit interacted with hCTR1 WT and these proteins colocalized at the plasma membrane and in intracellular vesicles. Statistical modeling of functional copper uptake after coexpression of hCTR1 WT and hCTR1 M150I-M154I mutant revealed that at least four methionine residues are required in the aqueous pore of the hCTR1 complex. Taken together, these data provide biochemical and functional evidence that oligomerization of hCTR1 is required for functional high-affinity copper transport activity by permitting the formation of a permeable channel necessary for copper uptake.

Introduction

The transition metal copper is essential for all organisms that use oxygen for respiration. Copper is a cofactor in several enzymatic processes that require redox-activity, such as the respiratory chain in the mitochondria, neurotransmitter synthesis and iron metabolism. Paradoxically, this same redox-activity can also catalyze the generation of toxic free hydroxyl radicals [1]. The existence of two genetic disorders of copper homeostasis, Wilson disease (WD) (OMIM 277900) and Menkes disease (MD) (OMIM 309400), clearly illustrate why copper homeostasis is maintained within narrow boundaries. To maintain copper homeostasis, cells have intricate mechanisms to control copper uptake, intracellular distribution and copper export. Cellular copper uptake is mediated by copper transporters (CTR) of the SLC31 superfamily that is highly conserved in eukaryotes. CTR proteins enable copper uptake in an energy-independent manner. Based on complementation assays in yeast, the yCtr1p and yCtr3p were characterized as high-affinity copper uptake proteins in *Saccharomyces cerevisiae* [83, 263]. Two homologous CTR genes, *CTR1* and *CTR2*, have been annotated in the genomes of humans and other mammals [84]. hCTR1 (human CTR1; SLC3131A) was identified as the orthologue of yCtr1p by complementation of the *ΔCtr1ΔCtr3* yeast strain [84], and subsequently shown to mediate copper uptake with a K_m of approximately 1-5 μM (chapter 3) [85-87]. The importance of Ctr1 readily appeared from studies with Ctr1 knockout mice, which displayed an embryonic lethal phenotype [88, 89]. Mouse embryonic fibroblasts (MEFs) isolated from these mice displayed a substantial defect in copper uptake and copper incorporation into cuproenzymes [91]. Finally, conditional knockout mice that lack intestinal Ctr1 expression displayed a copper deficiency phenotype similar to MD due to abrogated intestinal copper uptake [93]. Hence, Ctr1 is an essential protein for dietary copper absorption and for cellular copper uptake in mice.

hCTR1 is an integral membrane protein, containing three transmembrane helices [95]. Since it is unlikely that three transmembrane helices could form an aqueous pore that is large enough to permit transport of copper ions [264], considerable attention has focused on understanding hCTR1 quaternary structure in relation to its copper transport function. Biochemical crosslinking experiments revealed that hCTR1 forms oligomeric complexes of different apparent molecular masses [86]. A Cysteine residue in the carboxyterminus [98] and a Gly-Xaa-Xaa-Xaa-Gly (GXXXG) sequence in the second transmembrane helix [99, 100] have been implicated in hCTR1 oligomerization. The latter sequence stabilizes helix-helix interactions in several other proteins [101, 102]. In addition, yeast-two-hybrid experiments [95] provided evidence that aminotermini of CTR proteins could interact. Reconstitution of recombinant hCTR1 in native phospholipid bilayers permitted determination of the structure of the hCTR1 oligomer at approximately 6-Å resolution by electron microscopic crystallography [99, 100]. These studies suggested that hCTR1 formed compact trimeric complexes containing nine transmembrane helices in total [99, 100]. Nevertheless, it is currently unknown whether oligomerization of hCTR1 is in fact required for functional cellular copper uptake. The aim of this study was therefore to characterize whether hCTR1-mediated copper uptake was indeed dependent on hCTR1 oligomerization, using a series of mutant hCTR1 proteins that either prohibited oligomerization or functional copper uptake.

Experimental Procedures

Antibodies

Rabbit-anti FLAG (Sigma, Zwijndrecht, The Netherlands), rabbit-anti-HA (Sigma), mouse-anti-beta-Tubulin (Sigma) and horseradish-peroxidase-conjugated secondary antibodies (Pierce Biotechnology Inc, Rockford, IL, USA) were used for immunoblot analysis. For immunofluoresescence, FLAG epitopes were visualized by fluorescein isothiocyanate (FITC)-conjugated mouse-anti-FLAG (Sigma). HA-epitopes were labeled with mouse-anti-HA antibodies (Sigma), and secondary labeling was performed using Alexa Fluor® 568-conjugated antibodies (Molecular Probes, Eugene, OR, U.S.A.). Rabbit anti-Na/K ATPase was a generous gift from Dr. J. Koenderink (Nijmegen Centre for Molecular Life Sciences, Nijmegen, The Netherlands).

Cell culture and transfections

The HEK-293T cell line and the U2OS cell line were purchased from the A.T.C.C. (Rockville, MD, U.S.A.). Cells were cultured at 37°C under humidified air containing 5% CO_2, and were maintained in DMEM (Dulbecco's modified Eagle's medium) GlutaMAX™ (Invitrogen, Breda, The Netherlands) containing 10% (v/v) FCS (fetal calf serum) (Invitrogen), 100 µg/ml penicillin (Invitrogen) and 100 µg/ml streptomycin (Invitrogen). For some experiments, cells were cultured in the presence of different concentrations of $CuCl_2$, $AgNO_3$, $ZnCl_2$, $MgCl_2$, $FeCl_3$, $MnCl_2$ (Merck Chemicals, Amsterdam, The Netherlands) or a copper chelator, bathocuproinedisulfonic acid (BCS) (Sigma, Zwijndrecht, The Netherlands) as indicated. HEK-293T cells were transiently transfected with hCTR1 constructs using the calcium phosphate precipitation protocol as described elsewhere (chapter 3) [87]. For immunofluoresence, U2OS cells and HEK-293T cells were transiently transfected using linear polyethylenimine (PEI) (Polysciences) at a 1:5 DNA:PEI ratio in serum free DMEM.

Plasmids

The pGL3-E1b-TATA-4MRE construct [MRE (metal-responsive element)-luciferase reporter], pEBB-hCTR2-FLAG, pEBB-hCTR1-FLAG and M150I-M154I CTR mutants were previously generated (chapter 3) [87]. Mutations of conserved residues were generated in the pEBB-hCTR1-FLAG and pEBB-hCTR1-HA constructs by QuikChange® site-directed mutagenesis (Stratagene, La Jolla, CA, USA). All constructs were verified by sequence analysis.

Immunoprecipitation and immunoblot analysis

Cells were lysed in lysis buffer [25 mM HEPES, 1% (v/v) Triton-X100, 100 mM NaCl, 1 mM Na-EDTA, 10% (v/v) glycerol; pH 7.9] supplemented with complete protease inhibitor cocktail (Roche, Woerden, The Netherlands). Immunoprecipitation was performed with either anti-FLAG M2-agarose (Sigma) or anti-HA agarose (Sigma). Immunoprecipitates were eluted in SDS-PAGE sample buffer [62.5 mM Tris/HCl, 4% (v/v) SDS, 5% (v/v) glycerol, 0.01% (w/v) Bromophenol Blue and 2% (v/v) 2-mercaptoethanol; pH 6.8] and heated at 95 °C for 5 min prior to resolution by SDS-PAGE (12% gels). Proteins were transferred onto

Hybond-P PVDF membranes (Amersham Biosciences, Buckinghamshire, UK) by standard immunoblot procedures. The membranes were blocked in Tris-buffered saline (25 mM Tris/HCl, 137 mM NaCl and 2.7 mM KCl; pH 7.4) containing 5% (w/v) non-fat dried milk (Sigma) and 0.1% (v/v) Tween-20. Immunoblots were probed with antibodies as indicated. Reactivity was detected using horseradish-peroxidase-conjugated secondary antibodies (Pierce Biotechnology Inc, Rockford, IL, USA) and ECL® (enhanced chemiluminescence) (Amersham Biosciences), according to the manufacturer's instructions.

Indirect immunofluorescence and confocal laser-scanning microscopy

HEK-293T cells or U2OS cells were seeded onto coverslips (Marienfeld, Paul GmbH & Co.KG, Bad Bergentheim, Germany) at a confluency of 20%, and the cells were transiently transfected one day after seeding. Two days after transfection, cells were rinsed with ice-cold PBS and fixed in 4% (w/v) paraformaldehyde in PBS for 20 min at 4 °C. Cells were quenched with 50 mM NH_4Cl for 5 minutes at room temperature, and cells were washed with PBS. Next, cells were blocked and permeabilized using blocking buffer [0.2% (w/v) BSA, 0.1% (w/v) saponin (Sigma) in PBS] for 30 minutes at room temperature. Immunolabeling was performed in blocking buffer for 1 h with primary antibodies as indicated. Cells were rinsed three times with blocking buffer, and secondary labeling was performed with affinipure Alexa Fluor® 568-conjugated goat anti-(mouse IgG) or goat anti-(rabbit IgG) antibodies (10 µg/ml; Molecular Probes, Eugene, OR, U.S.A.). Coverslips were mounted in Fluorsave (VWR International Ltd, Leicestershire, UK), and confocal laser-scanning microscopy was performed using a Zeiss laser-scanning microscope 510 Meta equipped with a Plan APO ×63 oil immersion objective (numerical aperture 1.4) and dedicated imaging software (Zeiss AIM4.2).

Cell surface biotinylation

Two days after transfection, HEK-293T cells were washed with PBS supplemented with 0.5 mM $CaCl_2$ and 1.0 mM $MgCl_2$ (PBS-CM), and proteins present at the cell surface were biotinylated at 4°C using sulfo-NHS-SS-biotin (0.5 mg/ml, Pierce, Etten-Leur, The Netherlands) in PBS-CM for 30 min. Unreacted biotin was quenched using 0.1 % (w/v) BSA in PBS-CM. Subsequently, cells were washed with PBS-CM and lysed in 25 mM HEPES, 1% (v/v) Triton-X100, 100 mM NaCl, 1 mM Na-EDTA, 10% (v/v) glycerol; pH 7.9 supplemented with complete protease inhibitor cocktail (Complete, Roche) at 4°C. The lysate was centrifuged for 10 min at 16,000 x g and biotinylated proteins were precipitated for 2h using neutravidin-coupled beads (Pierce) and analyzed by immunoblot analyses. Cytosolic proteins were undetectable in the precipitated fraction and no precipitated proteins were detected when sulfo-NHS-SS-biotin was omitted, demonstrating the specificity of the procedure.

Luciferase reporter assays

MRE-Luciferase reporter assays were performed as described before on HEK293T cells seeded in 96-wells microtiterplates (chapter 3) [87]. Each well was co-transfected with 35 ng of the MRE-luciferase reporter, 0.25 ng of pRL-TK vector (Promega Benelux BV, Leiden, the Netherlands) and 0.35 ng of pEBB-hCTR1-FLAG or hCTR1 mutants as indicated. In

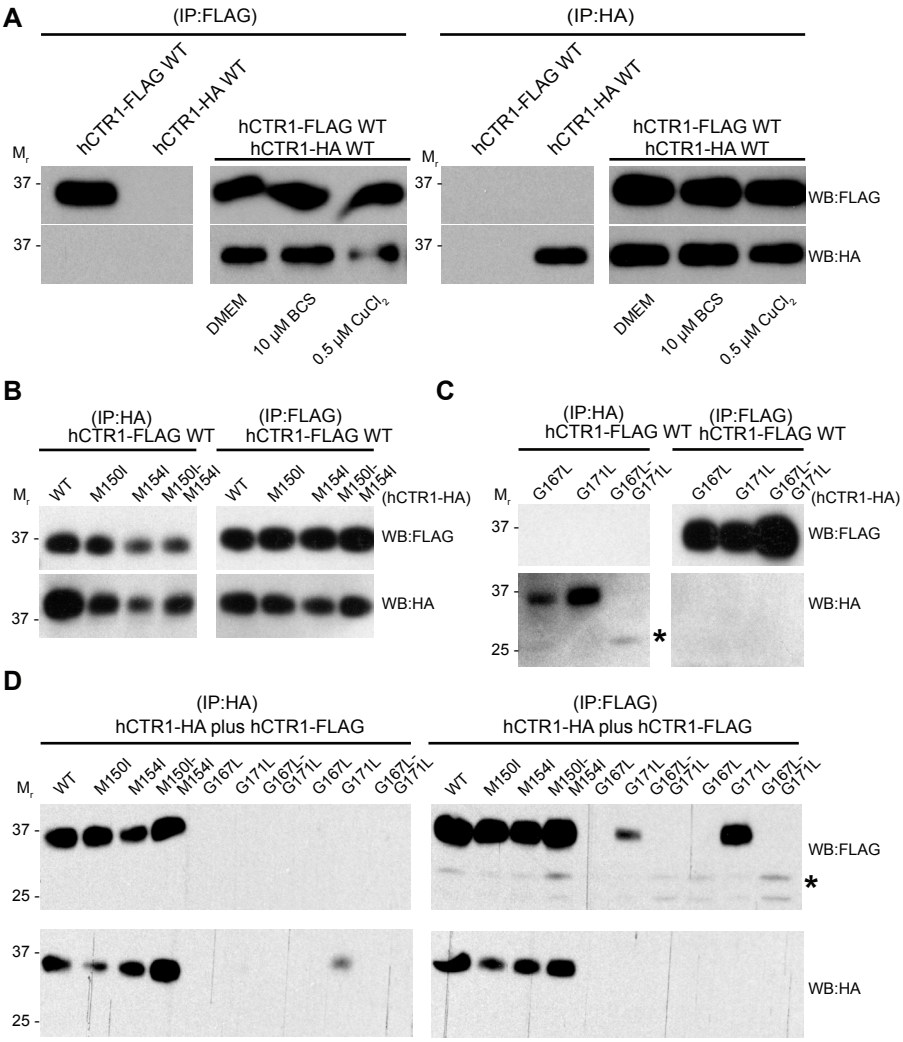

Figure 1. Interaction of hCTR1 subunits is independent of copper

HEK293T cells were transiently transfected with WT hCTR1-FLAG, WT hCTR1-HA or hCTR1-FLAG and hCTR1-HA containing the indicated mutations. Proteins were precipitated using anti-FLAG and anti-HA antibodies and precipitates were subjected to immunoblot analysis. Molecular masses in kDa are shown on the left-hand side of the immunoblots. (A) HEK293T cells expressing hCTR1 were incubated with DMEM, 10 µM BCS, or 0.5 µM $CuCl_2$ prior to immunoprecipitation. (B, C) HEK293T cells coexpressing wild-type hCTR1 and mutant hCTR1 were immunoprecipitated as indicated. Asterisks indicate the 28-kDa immature core-glycosylated hCTR1. (D) HEK293T cells expressing HA and FLAG tagged WT or mutant hCTR1 were subjected to immunoprecipitation and immunoblotting.

some cases, hCTR1 WT and M150I-M154I mutant were co-transfected in different ratios. After incubation for 24 h, the cells were rinsed with PBS and subsequently maintained for 24 h in DMEM in the presence or absence of different metals. The ratios between firefly luciferase and renilla luciferase values were calculated as relative light units (RLUs) and all RLU values were normalized relative to empty vector control incubations (empty vector set at 1; all experimental conditions expressed as fold inductions relative to empty

vector control). Statistical analysis was performed on RLU data for the different incubations by students' T-test. In co-transfection experiments, the relative contribution to hCTR1-dependent copper uptake was calculated in a matrix for each of the possible complexes (Figure 6A). The measured values were expressed as fold induction and were logarithmical transformed. These data were statistically analyzed on this predicted matrix (Figure 6A) by Restricted Maximum Likelihood (REML) analysis [265].

Results

Copper-independent interaction of hCTR1 subunits

To directly test the ability of full-length hCTR1 to assemble in an oligomeric complex *in vivo*, we performed co-immunoprecipitation analysis of wild type (WT) hCTR1-FLAG and hCTR1-HA (Figure 1A). Expression of hCTR1-FLAG or hCTR1-HA in HEK293T cells resulted in a single immunopositive band of approximately 35 kDa after immunoprecipitation with FLAG or HA antibodies, respectively (Figure 1A). This size is in accordance with the molecular mass of the mature complex glycosylated hCTR1 protein [105]. After co-expression of hCTR1-FLAG and hCTR1-HA and co-immunoprecipitation, we observed a direct interaction between hCTR1 subunits. This interaction was not affected by copper supplementation or depletion in the culture medium of hCTR1 expressing cells, indicating that this interaction was independent of copper (Figure 1A). Overexposure of these immunoblots revealed that not only the 35-kDa mature polypeptide was co-precipitated, but also the 28-kDa core glycosylated hCTR1 precursor (data not shown), indicating that hCTR1 self-interaction occurred early during hCTR1 biosynthesis.

Two highly conserved motifs in hCTR1 were mutated to study the contribution of these motifs to hCTR1 oligomerization and function. Methionine residues at positions 150 and 154 (MXXXM motif) in the second transmembrane region of hCTR1 are essential for hCTR1-dependent copper uptake [96, 98, 244]. The putative thioether copper ligands were removed, either individually or together, by converting these methionines into isoleucines to create hCTR1 M150I, hCTR1 M154I, and hCTR1 M150I-M154I. Furthermore, two glycine residues at positions 167 and 171 are likely involved in intra-helical interactions in hCTR1 [99, 266]. As this glycine zipper motif is involved in stabilizing oligomeric complexes in multiple proteins [101, 102], we converted these residues, either individually or together, into leucines , which resulted in hCTR1 G167L, hCTR1 G171L, and hCTR1 G167L-G171L. Mutation of the conserved M150 and M154 did not affect protein expression (Figure 1B), whereas hCTR1 expression was impaired by mutation of G167 and G171 (Figure 1C). However, when more DNA was transfected to increase expression, hCTR1 G167L, and hCTR1 G171L were more readily detectable. hCTR1 G167L-G171L was still poorly expressed and was visible as a protein of approximately 28 kDa, which presumably represents the immature core-glycosylated form of hCTR1 (Figure 1C, asterisk) [105]. Next, we investigated the ability of these mutants to interact with hCTR1 WT by co-immunoprecipitation of the mutant hCTR1-HA and the WT hCTR1-FLAG. Mutation of M150, M154 or both did not affect the interaction with hCTR1 WT (Figure 1B), whereas the mutations at position G167 and G171 completely abolished the interaction with hCTR1 WT (Figure 1C). Finally, we addressed whether hCTR1 mutant subunits could interact. To

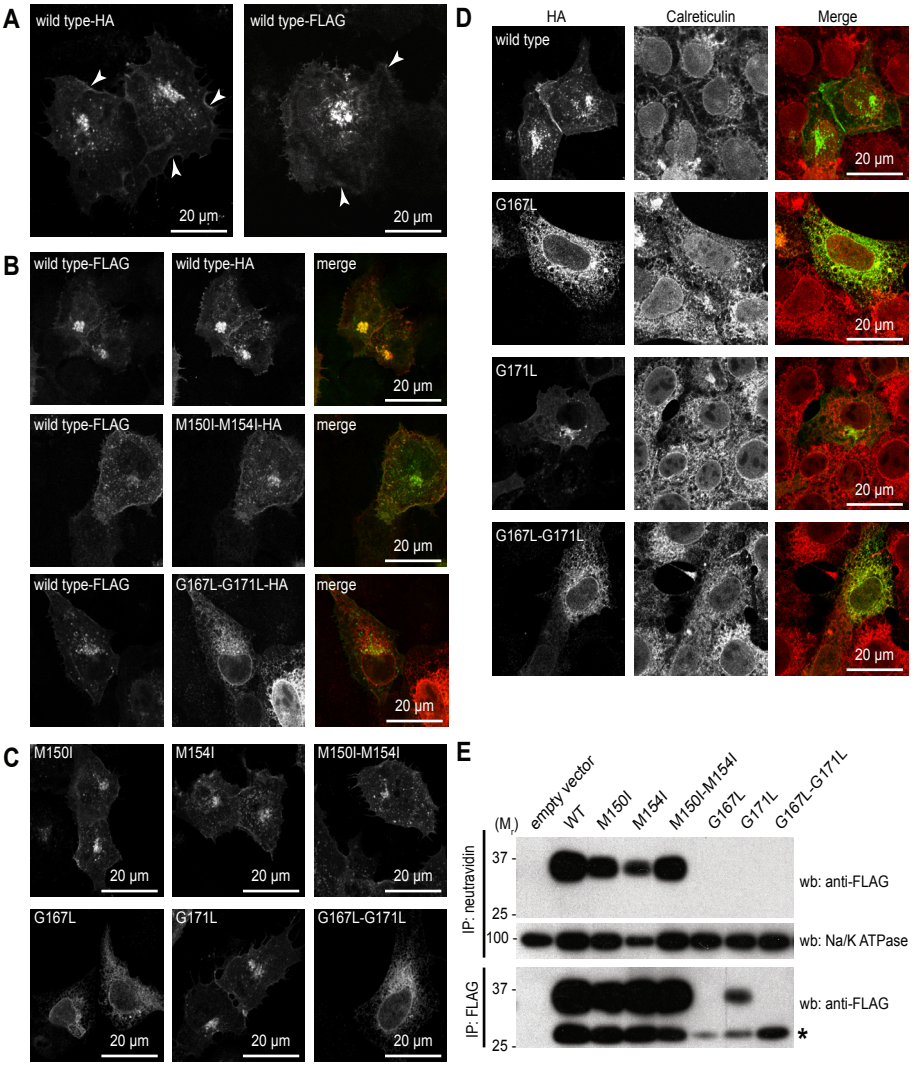

Figure 2. subcellular localization of wild type and mutant hCTR1
(A - C) Localization of hCTR1 was assessed by indirect confocal laser-scanning microscopy in U2OS cells after transient transfection with WT or mutant hCTR1-FLAG and hCTR1-HA. FLAG tagged proteins were labeled with FITC-conjugated mouse-anti-FLAG antibodies, HA-tagged antibodies were labeled with mouse-anti-HA, and secondary labeling was performed with Alexa Fluor® 568 conjugated goat anti-mouse antibodies. Green and red channels were merged to determine co-localization. Plasma membrane localization is marked by arrows. (D) Co-localization analysis of hCTR1 was performed in U2OS cells using the ER-marker Calreticulin. (E) Surface abundance of WT and mutant hCTR1-FLAG was assessed by cell surface biotinylation. Biotinylated proteins were precipitated by Neutravidin Agarose beads and precipitates were analyzed by immunoblot using indicated antibodies. The plasma membrane Na/K-ATPase was used as a positive loading control. Molecular masses in kDa are shown on the left-hand side of the immunoblots.

this end, we co-expressed each mutant hCTR1 with a FLAG or HA epitope tag prior to co-immunoprecipitation. hCTR1 subunits with mutated M150 and M154 residues self-interacted as strongly as the interaction with WT hCTR1 (Figure 1D). In contrast, hCTR1 with mutated G167 or G171 residues were not able to self-interact.

Subcellular localization of hCTR1

To compare the subcellular localization of hCTR1 WT with mutant hCTR1, U2OS cells (Figure 2A) and HEK293T cells (data not shown) were co-transfected with hCTR1 FLAG or hCTR1 HA as indicated. Expression of hCTR1 WT resulted in localization at intracellular vesicles and at the plasma membrane of U2OS cells (Figure 2A), which is in concordance with previous observations that hCTR1 constitutively recycles between intracellular vesicles and the plasma membrane [64, 86, 94, 105]. This localization was independent of the epitope tag used (Figure 2A, B). hCTR1 M150I-M154I displayed a similar localization pattern as hCTR1 WT, and both proteins showed considerable colocalization (Figure 2B). Similar results were observed for both hCTR1 M150I and hCTR1 M154I (Figure 2C), and to some extent also for hCTR1 G171L. However, hCTR1 G167L and hCTR1 G167L-G171L localized in a reticular pattern that was reminiscent of the endoplasmic reticulum (ER) (Figure 2B and 2C). Indeed, extensive colocalization was observed with the ER-marker calreticulin (Figure 2C), and no colocalization was observed with hCTR1 WT (Figure 2B). Noticeably, co-expression of mutant hCTR1 in all cases did not induce changes in localization of the WT hCTR1 (Figure 2B). A fraction of hCTR1 WT appeared at the surface of the cell (Figure 2A, B), and therefore we tested the surface abundance of hCTR1 WT and different hCTR1 mutants by cell surface biotinylation. hCTR1 WT was clearly expressed at the cell surface, which was confirmed by the specific precipitation of the plasma membrane-resident Na^+/K^+-ATPase (Figure 2D). hCTR1 cell surface abundance was not affected by disruption of the MXXXM motif, whereas mutation of the GXXXG motif completely abolished hCTR1 cell surface localization (Figure 2E). In summary, subcellular localization of hCTR1 is not dependent on the MXXXM motif. However, disruption of the GXXXG motif, which is involved in stabilization of helix-helix interactions, resulted in a drastic decrease in protein expression, hCTR1 subunit interaction, oligosaccharide maturation, and resulted in retention in the ER.

Copper uptake by hCTR1 is copper- and hCTR1-concentration dependent

hCTR1-dependent copper uptake was investigated using the MRE-Luciferase reporter that monitors bio-available cytoplasmic copper (chapter 3) [87]. Expression of this reporter together with hCTR1 resulted in a copper-concentration-dependent and saturable increase in the range of 1 - 5 μM $CuCl_2$ (Figure 3A). Incubation in DMEM without supplemented $CuCl_2$ induced the reporter when hCTR1 was expressed, and the copper chelator BCS abrogated this induction (Figure 3A, B), indicating hCTR1-dependent reporter induction by copper present in basal medium. HEK293T cells were transfected with increasing amounts of hCTR1 to determine the hCTR1-concentration dependence of reporter induction. Indeed, this experiment revealed a linear correlation between hCTR1 expression and the increase in reporter activity (Figure 3C). The reporter was induced by copper, but not by other metals (Figure 3D). Interestingly, incubation with silver resulted in a reduction of

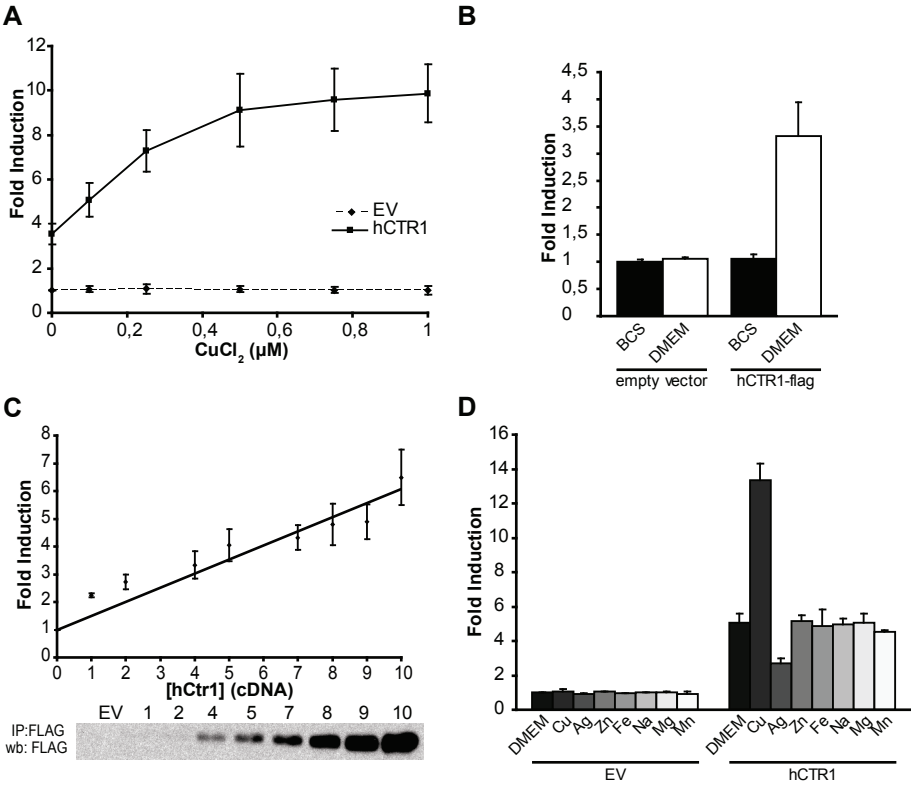

Figure 3. copper uptake by hCTR1 WT is copper- and hCTR1-concentration dependent
HEK293T cells were transiently cotransfected with the MRE-Luciferase reporter together with pEBB or pEBB-WT hCTR1-FLAG or pEBB-mutant hCTR1-FLAG. (A) Cells were treated for 24 hrs with different concentrations of $CuCl_2$ (B) or with 10 μM BCS. (C) HEK293T cells were transiently cotransfected with the MRE-Luciferase reporter together with increasing DNA concentrations of pEBB-hCTR1-FLAG (1 to 10 on the x-axis). After transfection, cells were incubated with 0.5 μM $CuCl_2$ for 24 hrs. Immunoprecipitation and subsequent immunoblot analysis was performed to detect hCTR1-FLAG. (D) HEK293T cells transfected with pEBB or pEBB-hCTR1-FLAG were incubated for 24 hrs with DMEM or 0.1 μM of the different metals. Luciferase reporter activities were measured and normalized for Renilla luciferase activities. Values were expressed as fold induction relative to control incubations ± S.E. (n≥3).

reporter activity, consistent with previous observations that silver competes with copper for hCTR1 [86]. Together, these observations indicate that hCTR1 specifically mediates high-affinity copper uptake in a copper- and hCTR1-concentration dependent manner, and qualify the MRE-luciferase reporter as a *bona fide* quantitative tool to analyze copper import capacity of hCTR1 under the described conditions.

Oligomerization of hCTR1 is essential for copper uptake

This reporter assay was therefore used to determine the functionality of the hCTR1 MXXXM and GXXXG mutants. Incubation with 0.5 μM $CuCl_2$ resulted in a strong reporter induction when hCTR1 WT was expressed compared to EV (Figure 4A). However, no reporter induction was observed when hCTR1 M150I, hCTR1 M154I, hCTR1 M150I-M154I, or hCTR1 G167L-G171L were expressed. In contrast to this observation, the hCTR1 G167L and hCTR1 G171L mutants displayed residual reporter induction

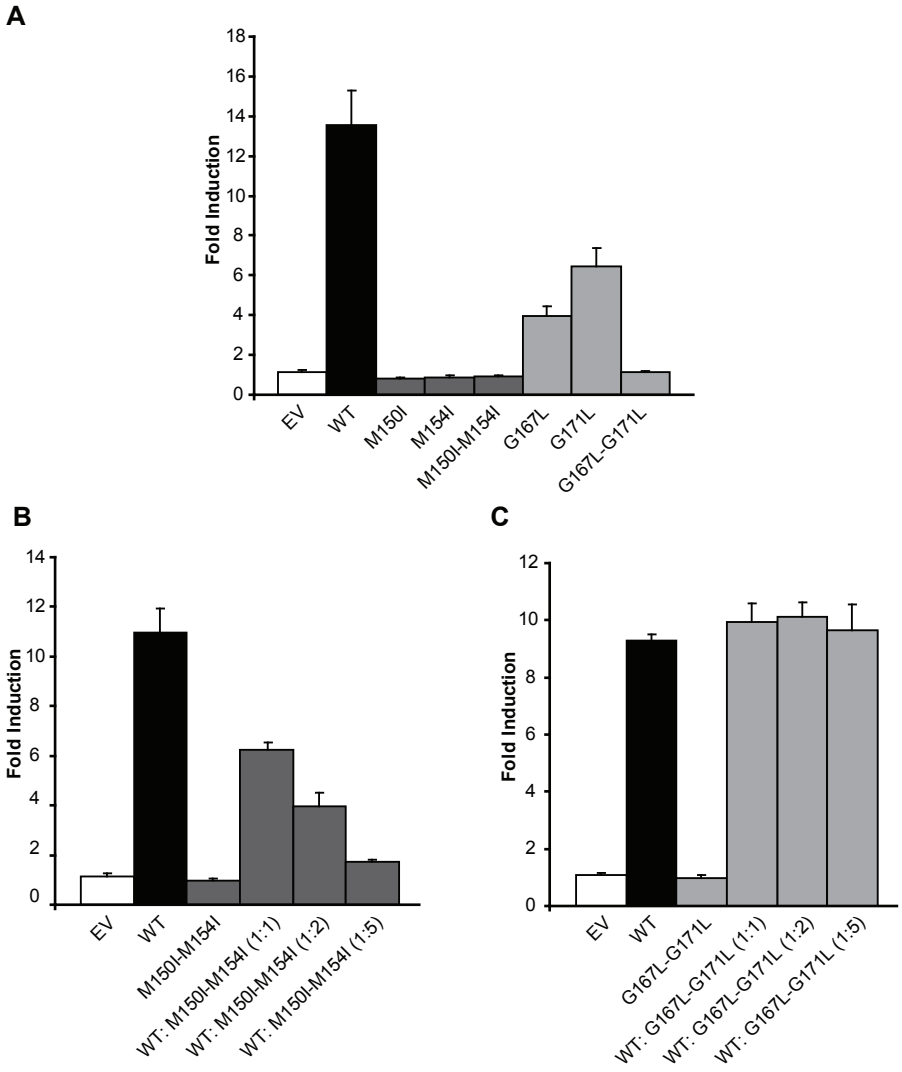

Figure 4. Cellular copper uptake by hCTR1 is dependent on the CTR-specific M150-M154 motif
(A) HEK293T cells were transiently cotransfected with the MRE-Luciferase reporter together with EV or hCTR1 WT-FLAG, or mutant hCTR1-FLAG as indicated. (B) HEK293T cells were cotransfected as above with hCTR1 WT and mutant hCTR1 in a ratio of 1:1. Cells were cotransfected as in (A) together with hCTR1 and increasing amounts of M150I-M154I hCTR1-HA (C) or G167L-G171L hCTR1-HA (D). After transfection, cells were incubated with 0.5 μM $CuCl_2$ for 24 hrs, and Luciferase reporter activities were measured and normalized for Renilla luciferase activities. Values were expressed as fold induction relative to control incubations ± S.E. (n≥3; each experiment performed in triplicate).

compared to hCTR1 WT. hCTR1 M150I-M154I did not induce copper uptake, while its interaction with hCTR1 WT was not impaired. Hence, co-expression of hCTR1 M150I-M154I together with hCTR1 WT proteins would result in formation of mixed oligomeric complexes that would lack copper uptake activity. We directly tested this prediction by co-expression of hCTR1 WT and hCTR1 M150I-M154I. In these experiments, the total

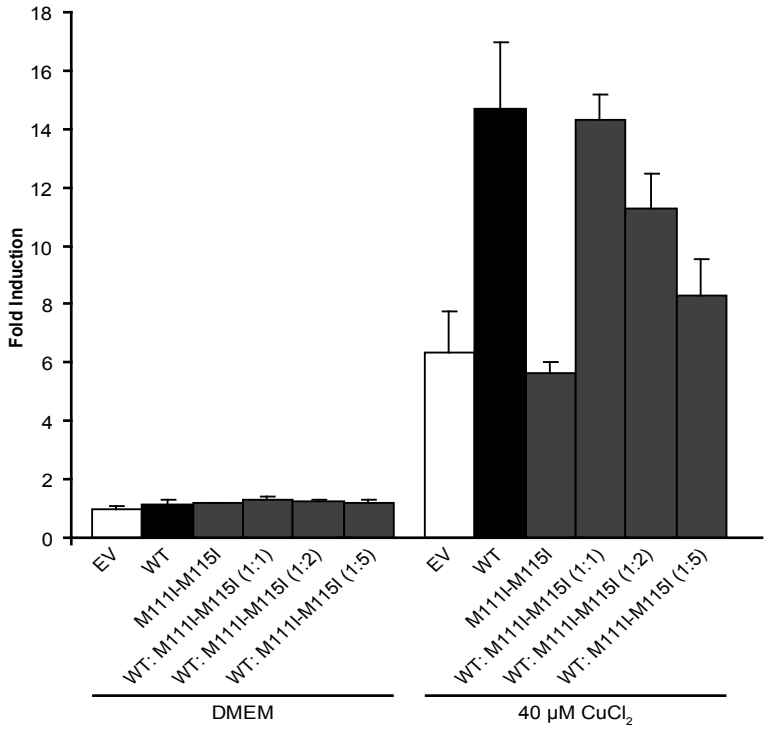

Figure 5. Cellular copper uptake by hCTR2 is dependent on the M111-M115 motif
HEK293T cells were transiently co-transfected with the MRE-Luciferase reporter together with EV, hCTR2-FLAG WT, hCTR2-HA M111I-M115I or with both hCTR2-FLAG WT and increasing amounts of hCTR2-HA M111I-M115I. After transfection, cells were incubated with 0 or 40 µM $CuCl_2$ for 24 hrs, and Luciferase reporter activities were measured and normalized for Renilla luciferase activities. Values were expressed as fold induction relative to control incubations ± S.E. (n≥3; each experiment performed in triplicate).

amount of transfected hCTR1 WT cDNA was kept constant. Indeed, reporter activation was reduced by co-expression of hCTR1 WT with hCTR1 M150I and hCTR1 M154I (data not shown). In addition, reporter activity was attenuated in a dose-dependent manner by coexpression of hCTR1 WT with increasing amounts hCTR1 M150I-M154I (Figure 4B). Addition of an equal amount of hCTR1 M150I-M154I to hCTR1 WT resulted in almost 50% reduction in copper uptake capacity, while reporter induction was reduced to basal levels when hCTR1 M150I-M154I was overexpressed 5-fold compared to WT protein (Figure 4B). We concluded that hCTR1 M150I-M154I is a dominant-negative mutant of hCTR1 copper import function. We then co-expressed constant levels of hCTR1 WT with increasing amounts of hCTR1 G167L-G171L, a non-interacting, non-functional mutant. Reporter induction was not affected by the addition of hCTR1 G167L-G171L, even when this mutant was transfected in 5-fold excess. Taken together, these experiments indicated that non-functional hCTR1 mutants could only dominantly inhibit hCTR1 WT function, when the WT and mutant proteins formed mixed oligomers, thus providing strong evidence that hCTR1 requires oligomerization for functional copper uptake.

Next, we determined whether this observation was applicable to human CTR-proteins in general, and therefore we performed similar experiments using hCTR2. The function of

hCTR2 was recently characterized (chapter 3) [87, 109]; hCTR2 mediates copper uptake with lower affinity compared to hCTR1, and therefore reporter induction was monitored at 40 μM $CuCl_2$ (Figure 5) [87]. Again, expression of hCTR2 M111I-M115I mutant resulted in negligible reporter induction compared to hCTR2 WT. Indeed, co-expressing constant amounts of hCTR2 WT with increasing amounts of hCTR2 M111I-M115I reduced hCTR2-dependent low-affinity copper uptake in a concentration-dependent fashion. Similar to the results obtained using hCTR1, 5-fold overexpression of the mutant relative to WT completely abrogated hCTR2-dependent reporter induction. Thus, oligomerization is essential for copper uptake mediated by human CTR proteins in general.

Functional modeling of the hCTR1 trimer

Next, we set out to model the functional contribution of the three individual intrahelical MXXXM motifs, contributed by each subunit, to hCTR1-dependent copper uptake. A theoretical mixture of four distinct homotrimeric or heterotrimeric complexes is formed when hCTR1 WT and hCTR1 M150I-M154I are coexpressed. These are designated here as complex 1 (three WT subunits), complex 2 (two WT subunits plus one M150I-M154I subunit), complex 3 (one WT subunit plus two M150I-M154I subunits), and complex 4 (three M150I-M154I subunits). The propensity to form each of these different complexes was calculated for different ratios between hCTR1 WT and hCTR1 M150I-M154I (Figure 6A). We then compared these calculated values with the copper uptake activity measured after expression of WT and mutant hCTR1 in the same ratio, while keeping the total expression of hCTR1 constant. The activity of hCTR1 WT alone (representing complex 1) was set at 1 (Figure 6B). After co-expression of hCTR1 WT and hCTR1 M150I-M154I in different ratios, measured values were substantially higher than would be predicted based on activity of complex 1 alone, but substantially lower than would be predicted when complex 2 and / or 3 would have equal activity as complex 1 (Figure 6B). This indicated that complex 2 and/or complex 3 also displayed copper uptake activity, but apparently to a reduced extent compared to complex 1.

To quantitate the contribution of each complex total copper uptake activity, all measured values were expressed as fold induction and data were logarithmically transformed to enable REML analysis using the theoretical values depicted in Figure 6A as our predictor matrix, where the relative abundance of the four different complexes were used as predictor variables. This statistical modeling revealed that complex 3 had no significant contribution to copper uptake, but we cannot exclude that it is remotely functional. In contrast, complex 2 had a residual contribution of copper uptake of 47 ± 5 % compared to complex 1. In conclusion, full copper transport activity of the hCTR1 trimer requires all six intramembraneous methionine residues. The presence of four methionine residues in the aqueous pore of the hCTR1 complex permits copper import, but to a reduced extent. Two methionines or less likely result in a non-functional trimer.

A

WT	M150I-M154I	complex 1	complex 2	complex 3	complex 4
1	0	100,0%	0%	0%	0%
0,80	0,20	51,2%	38,4%	9,6%	0,8%
0,67	0,33	29,6%	44,4%	22,2%	3,7%
0,50	0,50	12,5%	37,5%	37,5%	12,5%
0,33	0,67	3,7%	22,2%	44,4%	29,6%
0,25	0,75	1,6%	14,1%	42,2%	42,2%
0,17	0,83	0,5%	6,9%	34,7%	57,9%
0	1	0%	0%	0%	100,0%

B

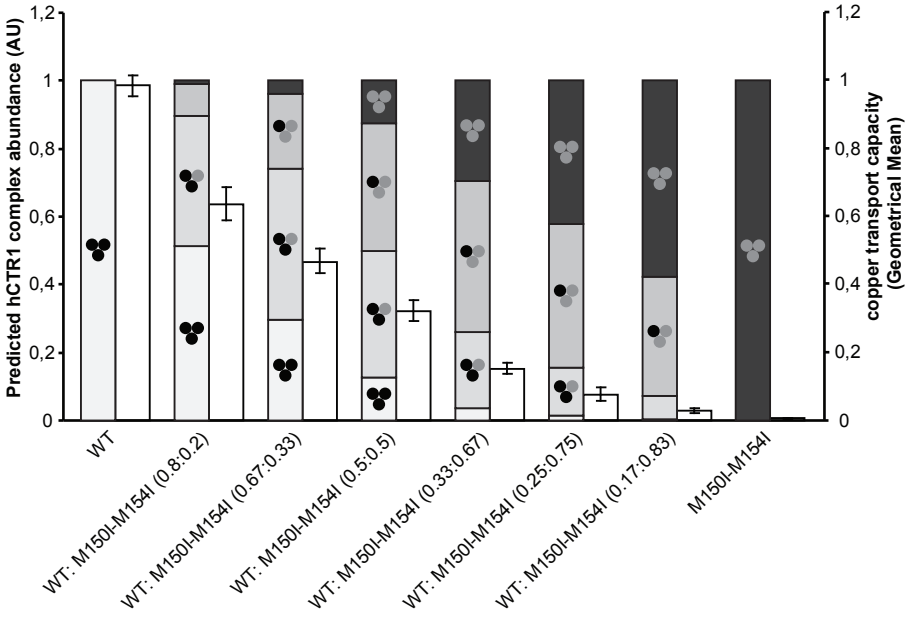

Figure 6. hCTR1-dependent copper transport requires at least two intact MXXXM motif in a trimeric hCTR1 complex

(A) hCTR1 assembles as homotrimeric complexes comprising three hCTR1 subunits per functional complex. Four different complexes can be formed when both hCTR1 WT and hCTR1 M150I-M154I are expressed while keeping the total amount of transfected hCTR1 (hCTR1 WT plus hCTR1 M150I-M154I) constant. These complexes are numbered complex 1-complex 4 and are schematically indicated at the top. Black subunits represent hCTR1 WT and grey subunits represent hCTR1 M150I-M154I. Shown is the calculated abundance of the four different complexes as a result of different ratios between hCTR1 WT and hCTR1 M150I-M154I. (B) The cumulative predicted abundance of each complex (calculated data from Figure 6A) is depicted in the grey bars. Black subunits represent hCTR1 WT and grey subunits represent CTR1 M150I-M154I. HEK293T cells were transiently cotransfected with the MRE-Luciferase reporter together hCTR1 WT and mutant hCTR1 in different ratios. Cells were incubated with 0.5 μM $CuCl_2$ for 24 hrs after transfection. Luciferase reporter activities were measured and normalized for Renilla Luciferase activities. The calculated relative abundance of the four different complexes (A) was used as predictor variables to perform REML analysis to model the contribution of the four predicted complexes to functional copper uptake, using the theoretical values depicted in (A) as our predictor matrix. The measured values were presented as geometrical means normalized for hCTR1 WT ± S.E.M. (n≥3; each experiment performed in triplicate) (white bars).

Discussion

Structural analysis of recombinant hCTR1, reconstituted in phospholipid membranes, suggested that hCTR1 is assembled as homotrimers *in vitro* [86 , 95, 98-100], but several important questions regarding the oligomeric structure of hCTR1 in relation to its copper transport activity remained unanswered. Here we show that hCTR1 oligomerization is required for functional copper uptake. Essentially, this conclusion is based on systematic analysis of two mutant hCTR1 proteins; hCTR1 G167L-G171L that fails to form stable oligomers, and hCTR1 M150I-M154I that undergoes normal oligomerization but inhibits protein function in a *trans*-dominant fashion.

The glycine zipper (Glycophorin A motif or GXXXG motif) has been detected in a large number of membrane channels and was shown to be necessary for helix packing, formation of stable oligomers and transport to the cell surface [101, 102, 267-269]. The GXXXG motif in the third transmembrane domain of hCTR1 performs a similar function in the assembly of hCTR1 trimers. This conclusion is supported by several observations. First, co-immunoprecipitation experiments demonstrated a direct and specific interaction of hCTR1 WT subunits *in vivo* (Figure 1). Second, the core-glycosylated, ER-resident hCTR1 subunit was also coprecipitated (data not shown). Third, conversion of the glycine residues at positions 167 and 171 abrogated the self-interaction of hCTR1 subunits (Figure 1) and prevented the detection of hCTR1 trimers after chemical crosslinking [99]. Fourth, hCTR1 G167L-G171L was localized in the ER (Figure 2), failed to undergo oligosaccharide maturation (Figure 1), was undetectable at the plasma membrane by cell surface biotinylation (Figure 2), and lacked functional copper uptake capacity (Figure 4 [99]), suggesting that hCTR1 oligomerization is a default and essentially irreversible process. Together, these data are most consistent with our working model that assembly of a functional hCTR1 trimer requires an intact GXXXG motif. In addition, trimerization is a highly-regulated process initiated in the ER, and incorrectly or incompletely assembled subunits are not transported to the plasma membrane. Based on these observations, we consider it unlikely that cellular copper import is modulated by regulated assembly or disassembly of hCTR1 trimers in analogy with formation of functional STIM1 oligomers after Ca^{2+}-depletion to activate Ca^{2+}-uptake [270] or with the disassembly of the gamma-aminobutyric acid (GABA)-B receptor upon capsaicin stimulation to reduce signaling by the neurotransmitter GABA [104].

Until now it was unclear if oligomerization was essential for hCTR1 function. We reasoned that if hCTR1 subunits were functionally interacting in a trimeric complex, the addition of a non-functional subunit would exert a dominant-negative effect on copper uptake activity by the formation of mixed oligomers. Such an approach has been successfully utilized to analyze functional assembly of a variety of oligomeric channels and transporters [271-279]. This approach necessitated a number of prerequisites that were all met by the hCTR1 M150I-M154I subunit in the case of hCTR1. For instance, it required the demonstration that the hCTR1 M150I-M154I subunit was truly non-functional in our MRE-Luciferase reporter assay (Figure 4). In addition, we demonstrated that this non-functional hCTR1 M150I-M154I subunit was abundantly expressed and properly localized and did not interfere with the expression and localization of the wildtype hCTR1. This is not trivial, since dominant interference of a mutant subunit with the localization of

wildtype transporter has been demonstrated in the case of FXYD2 FXYD2 [271], hIK1 [274], KCNJ2 [272], hRFC [273], NCLX [277] and the alpha1b-adrenoreceptor [275], but apparently did not seem to be a relevant mechanism in the case of hCTR1 (Figures 1 and 2). This dominant-negative approach further necessitated that the non-functional hCTR1 M150I-M154I subunit would retain its ability to interact with the wildtype hCTR1, which indeed appeared the case. Finally, we ascertained that the hCTR1-dependent induction of the MRE luciferase reporter linearly correlated with hCTR1 expression, thus allowing quantitative assessment of hCTR1 function. Our data clearly show that, despite the normal interaction of hCTR1 M150I-M154I, co-expression with hCTR1 WT disrupted hCTR1-dependent cellular copper uptake in a dominant-negative manner, indicating that oligomerization is essential for the activity of hCTR1. Oligomerization is likely essential for CTR protein function in general, since similar dominant-negative interference of mutating the homologous MXXXM motif in hCTR2 with hCTR2 function was also demonstrated, and Puig *et al*. previously presented genetic evidence of cooperativity between yeast Ctr1 subunits [96].

In our experiments, increasing the amount of dominant-negative hCTR1 M150I-M154I resulted in a dose-dependent decrease in copper uptake, thus permitting quantitative analysis of the inhibitory effect. A similar strategy has been successfully applied to calculate the number of transporter subunits present in active oligomers [276, 279]. Since the subunit stoichiometry of hCTR1 is already known [100], we used this approach to calculate the functional contribution of the three individual intrahelical MXXXM motifs, contributed by each subunit, to hCTR1-dependent copper uptake. Our data and statistical modeling indicated that optimal activity required all six methionine residues within the aqueous channel. The methionine thioethers at position 150 and 154 are located at the same side of the transmembrane helix, enabling trigonal or tetragonal copper (I) coordination within the transmembrane region, which is common for methionine thioether copper (I) coordination [280]. Surprisingly, hCTR1 trimers containing four intrahelical methionine residues (two MXXXM motifs contributed by two subunits), displayed reduced, but significant transport capacity (47% of normal). In contrast, trimers with no intrahelical methionines were unable to mediate copper transport, and statistical analysis indicated that trimers with only two intrahelical methionines (one MXXXM motif contributed by one subunit) were unlikely to contribute to copper uptake. These findings underscore the importance of the MXXXM residues to the copper transport process, but at the same time indicate that there is some flexibility with respect to the copper coordination chemistry within the copper permeable pore. This notion is consistent with the hypothesis that the thermodynamic energy that drives copper transport and confers inward directionality is mainly provided by the difference in copper affinity between the intracellular trimeric His-Cys-His motif and the extracellular methionine-rich motifs, but less by the trimeric MXXXM motif within the transmembrane copper permeable pore. Further structure-function studies of hCTR1 are required to elucidate the exact contribution of each of the MXXXM motifs to the copper import process.

In conclusion, these data suggest that default oligomerization of CTR proteins into homotrimers takes place in the ER and is a prerequisite for their function. Furthermore, the proposed flexibility of the number of sulfur ligands within the aqueous transmembrane

copper channel provides important novel insight into the hCTR1-mediated copper transport process and in the function of thioether copper coordination chemistry, which represents an important new paradigm in inorganic chemistry [280]. Finally, we predict that hereditary missense mutations in the human *CTR* genes could manifest both as recessive as well as dominant traits, depending on the affected amino acid residue.

Acknowledgements

This study was supported by NWO-grant (NWO: 912-04-106). We gratefully acknowledge the contributions of Dineke Folmer in the initial phases of this study. We thank Dr. Stan van de Graaf for helpful discussions and critical reading of the manuscript.

CHAPTER 5

Reduced expression of ATP7B affected by Wilson disease-causing mutations is rescued by pharmacological folding chaperones 4-phenylbutyrate and curcumin

Peter V.E. van den Berghe
Janneke M. Stapelbroek
Elmar Krieger
Prim de Bie
Stan F.J. van de Graaf
Reinoud E.A. de Groot
Ellen van Beurden
Ellen Spijker
Roderick H.J. Houwen
Ruud Berger
Leo W.J. Klomp

Submitted

Abstract

Wilson disease (WD) is an autosomal recessive copper overload disorder of the liver and basal ganglia. WD is caused by mutations in the gene encoding ATP7B, a protein localized to the *trans*-Golgi network that primarily facilitates hepatic copper excretion. Current treatment comprises reduction of circulating copper by zinc supplementation or copper chelation. Despite treatment, 5% of all patients develop fulminant liver failure, and a significant number of patients have neurological deterioration. The aim of this study was to investigate the possibility that defects arising from some WD mutations are ameliorated by drug treatment aimed at improvement of protein folding and restoration of protein function. This necessitated systematic characterization of the molecular consequences of distinct *ATP7B* missense mutations associated with WD. With the exception of p.S1363F, all mutations tested (p.G85V, p.R778L, p.H1069Q, p.C1104F, p.V1262F, p.G1343V, and p.S1363F) resulted in reduced ATP7B protein expression, whereas mRNA abundance was unaffected. Retention of mutant ATP7B in the endoplasmic reticulum, increased expression and normalization of localization after culturing cells at 30°C, and homology modeling suggested that these proteins were misfolded. Four distinct mutations exhibited residual copper export capacity, whereas other mutations resulted in complete disruption of copper export by ATP7B. Treatment with pharmacological chaperones curcumin and 4-phenylbutyrate (4-PBA), a clinically approved compound, partially restored expression and localization of most ATP7B mutants. These findings enable novel treatment strategies in Wilson disease, by directly enhancing the expression of mutant ATP7B with residual copper export activity.

Introduction

Wilson disease (WD) is an autosomal recessive disorder of copper homeostasis with an incidence of approximately 1:50,000 [27]. WD is caused by mutations in the gene encoding the copper-transporting P_{1B}-type ATPase ATP7B, and currently over 300 different mutations have been described [28]. ATP7B expression is restricted to the liver and to some regions of the brain, placenta, kidney, and mammary tissue [29-31]. Mutations in *ATP7B* result in toxic copper accumulation in these tissues, and patients may present with predominant hepatic abnormalities, neurological manifestations or a combination of both. Hepatic symptoms comprise liver cirrhosis, chronic liver inflammation and fulminant liver failure, whereas neurological manifestations include Parkinsonian movement disorders, seizures, personality changes, depression and psychosis (reviewed in [27]).

Approximately 5% of WD patients require liver transplantation [27]. Less-severely affected patients may benefit from treatment with copper-chelating agents like penicillamine [32], trientine [32] and ammonium tetramolybdate [33, 34]. Approximately 30% of patients have hypersensitive reactions to penicillamine after initial treatment [281, 282] and neurological symptoms may worsen in a substantial proportion of cases [283]. Trientine treatment, which is currently mostly used as second-line therapy, also has substantial risk of neurological deterioration [284]. Treatment with zinc, resulting in decreased intestinal copper absorption and a negative copper balance, is an alternative strategy [35, 285]. In contrast to copper chelation therapy, zinc treatment rarely leads to worsening of neurological symptoms [286], but its effect is contested especially in patients with liver disease [287]. Apparently, not all patients benefit sufficiently from the reduction of circulating copper, as illustrated by the notion that mortality rates exceed 10% in the first few years after diagnosis [288]. Taken together, there is a clear demand for novel treatment strategies in addition to conventional therapy in WD.

Most WD mutations are missense mutations that do not necessarily completely disrupt protein function. These mutated proteins might be susceptible to pharmacological treatment to restore their function. Indeed, pharmacological folding chaperones like 4-phenylbutyrate (4-PBA) and curcumin have been successfully used *in vitro* to ameliorate protein folding in lysosomal storage disorders [289], and functional recovery of the misfolded CFTR protein involved in cystic fibrosis [290-292]. However, the contribution of protein misfolding in the pathogenesis of WD is poorly understood, and therefore thorough characterization of the molecular consequences of mutations in ATP7B is pivotal. We selected seven distinct WD-associated missense mutations distributed throughout the entire open reading frame of ATP7B, together representing a significant proportion of all WD-patients. The cellular mechanisms that affect ATP7B function were systematically analyzed and compared to the effects caused by four mutations in functional domains of ATP7B (Figure 1A). The potential to rescue ATP7B protein-folding defects was subsequently investigated using treatment with 4-PBA and curcumin.

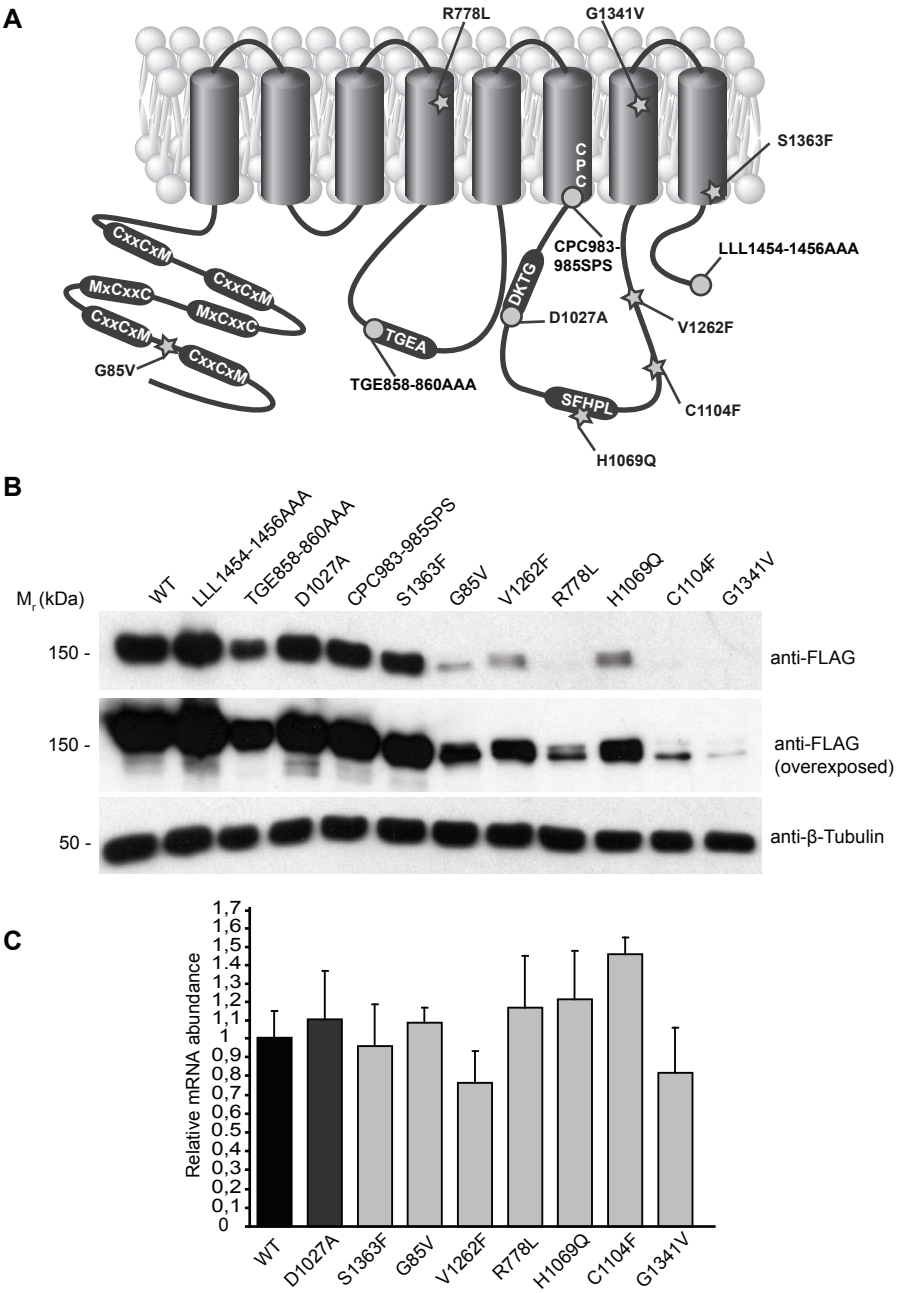

Figure 1. Reduced protein expression of Wilson disease-associated mutations in ATP7B
(A) See text for explanation of the structural and functional characteristics of ATP7B. Mutations that were generated by site-directed mutagenesis are depicted by grey circles for mutations in functional domains and grey stars for Wilson disease associated mutations. (B) HEK293T cells, transfected with WT or mutant ATP7B-FLAG were lysed and protein expression determined by western blot analysis using anti-FLAG, and anti-ß-tubulin. (C) mRNA abundance of WT or mutant ATP7B-FLAG was analyzed by qRT-PCR and mean ± SD. of quadruplicate measurements is indicated for each condition. Data were normalized to average of the WT.

Experimental Procedures

Antibodies and plasmids

Antibodies used were rabbit-anti-FLAG (Sigma, Zwijndrecht, The Netherlands), rabbit-anti-Glutathione S transferase (GST; Santa Cruz, CA, USA), mouse-anti-beta-Tubulin (Sigma), mouse anti-p230 (BD transduction Laboratories, Franklin Lakes, NJ) and rabbit anti-Calreticulin (Alexis Biochemicals, San Diego, CA), FITC-conjugated mouse-anti-FLAG (Sigma), HRP-conjugated secondary antibodies (Pierce Biotechnology Inc, Rockford, IL, USA), and Alexa Fluor® 568-conjugated antibodies (Molecular Probes, Breda, The Netherlands). Mutations in pEBB-ATP7B-FLAG [217] were generated by QuickChange® site-directed mutagenesis (see Table 1 for primer sequences) according to the manufacturer's instructions (Stratagene, La Jolla, CA, USA).

Table 1. Primers

Name	**Sequence** (5′→3′)
ATP7B LLL1454-1456AAA forward	GACAAGTGGTCTGCGGCCGCGAATGGCAGGGATG
ATP7B LLL1454-1456AAA reverse	CATCCCTGCCATTCGCGGCCGCAGACCACTTGTC
ATP7B D1027A forward	GACTGTGATGTTTGCCAAGACTGGCACC
ATP7B D1027A reverse	GGTGCCAGTCTTGGCAAACATCACAGTC
ATP7B CPC983-985SPS forward	GTGCTGTGCATTGCCAGCCCCAGCTCCCTGGGGCTGGCC
ATP7B CPC983-985SPS reverse	GGCCAGCCCCAGGGAGCTGGGGCTGGCAATGCACAGCAC
ATP7B TGE858-860-AAA forward	GATGAGTCCCTCATCGCAGCGGCGGCCATGCCAGTCAC
ATP7B TGE858-860AAA reverse	GTGACTGGCATGGCCGCCGCTGCGATGAGGGACTCATC
ATP7B S1363F forward	GCCATGGCAGCCTCCTTTGTGTCTGTGGTGCTC
ATP7B S1363F reverse	GAGCACCACAGACACAAAGGAGGCTGCCATGGC
ATP7B V1262F forward	GAAGAAAGTCGCCATGTTCGGGGATGGGGTCAATG
ATP7B V1262F reverse	CATTGACCCCATCCCCGAACATGGCGACTTTCTTC
ATP7B R778L forward	GTTCATTGCCCTGGGCCTGTGGCTGGAACACTTG
ATP7B R778L reverse	CAAGTGTTCCAGCCACAGGCCCAGGGCAATGAAC
ATP7B H1069Q forward	GAGGCCAGCAGTGAACAACCCTTGGGCGTGGCAG
ATP7B H1069Q reverse	CTGCCACGCCCAAGGGTTGTTCACTGCTGGCCTC
ATP7B C1104F forward	GCTGTGGAATTGGGTTCAAAGTCAGCAACGTG
ATP7B C1104F reverse	CACGTTGCTGACTTTGAACCCAATTCCACAGC
ATP7B G1341V forward	GATACCCATTGCAGCAGTTGTCTTCATGCCCATC
ATP7B G1341V reverse	GATGGGCATGAAGACAACTGCTGCAATGGGTATC
hypoxanthine-guanine phosphoribosyltransferase forward	TGACCTTGATTTATTTTGCATACC
hypoxanthine-guanine phosphoribosyltransferase reverse	CGAGCAAGACGTTCAGTCCT
hygromycin phosphotransferase forward	AGGCCGTGGTTGGCTTGTAT
hygromycin phosphotransferase reverse	GACCAATGCGGAGCATATACG
ATP7B-FLAG forward	TGTCCTCCCTGACGTCCGACAA
ATP7B-FLAG reverse	ATCGTCTTTGTAGTCGGCGGCC

Cell culture, transient transfections, and drug treatment

U2OS and HEK293T cells were cultured in Dulbecco's Modified Eagle medium (DMEM) supplemented with 10% fetal calf serum and antibiotics. Transient transfections were

performed using calcium phosphate or polyethylenimine (PEI) using standard procedures and cells were harvested after 1-3 days. Cells were incubated with 0-100 µM $CuCl_2$ (Merck Pharmacologicals, Amsterdam, The Netherlands) or 50 µM BCS (bathocuproinedisulfonic acid) (Sigma) for 24 hours, or at 30°C, with 5 mM 4-phenyl butyric acid (4-PBA; Sigma) or with 5 µM curcumin (Sigma) for 48 hours as indicated.

Metal-responsive element (MRE)-luciferase reporter assays

MRE-Luciferase reporter assays using the pGL3-E1b-TATA-4MRE construct were performed as described before on HEK293T cells seeded in 96-wells microtiterplates (chapter 3) [87]. Briefly, cells were incubated with 0-100 µM $CuCl_2$ for 24 hours. Relative light units (RLU) were calculated by normalizing Firefly luciferase activities for *Renilla* luciferase activity. To calculate copper export capacity, RLU values were corrected for EV controls, and the extent of the reduction in reporter activity mediated by WT ATP7B after incubation with 50 µM

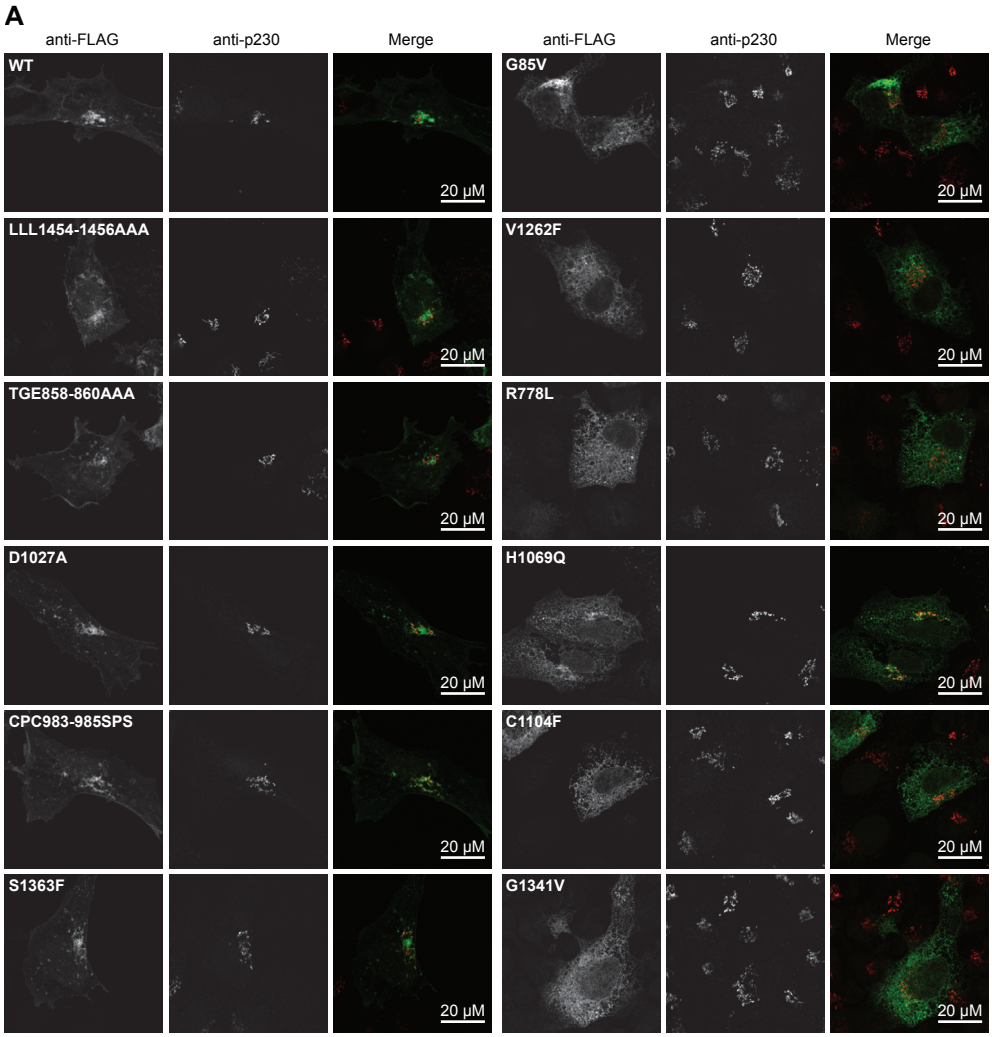

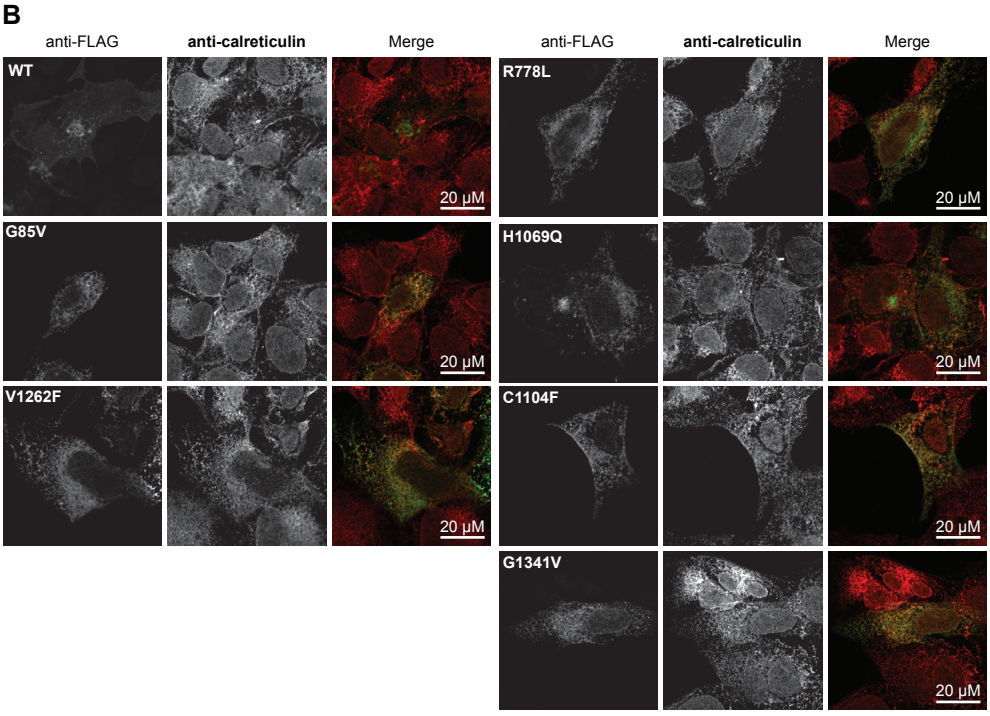

Figure 2. mislocalization of ATP7B to the endoplasminc reticulum
Localization of ATP7B WT and mutants was determined in transiently transfected U2OS cells. ATP7B-FLAG was labeled with FITC-conjugated anti-FLAG antibodies. Colocalization analysis was performed with the TGN marker p230 (A), and the ER marker calreticulin (B). Green and red channels were merged to determine co-localization.

$CuCl_2$ was set at 1. Mutants were expressed relative to WT ATP7B. A two-tailed Student's *t* test was used to analyze the statistical differences between different data points.

GST-precipitations and westernblot analysis

Cells were lysed in lysisbuffer supplemented with 1 mM $CuCl_2$ or with 1 mM BCS as described [217]. Precipitations with Glutathione (GSH)-sepharose were performed and analyzed as described previously.

Fluorescence microscopy

U2OS cells were grown on coverslips and transfected with pEBB-ATP7B-FLAG using PEI. After 2 days, cells were washed once with PBS, fixed using 4% paraformaldehyde and ATP7B was visualized with FITC-conjugated mouse-anti-FLAG antibodies, followed by staining colocalization markers. Images were acquired using a LSM510 Meta confocal microscope (Carl Zeiss, Jena, Germany).

Quantitative reverse transcriptase polymerase chain reaction (qRT-PCR)

HEK293T cells were transiently co-transfected with pEBB-ATP7B-FLAG and pCB7-hygro. After two days, RNA was isolated using TRIZOL (Invitrogen), and residual DNA in the samples was degraded by DNase I treatment according to the manufacturer's protocol

(Invitrogen). After reverse transcription using oligo (dT) primers (Roche) and Superscript II reverse transcriptase (Invitrogen), quantitative PCR (qPCR) was performed using a MyIQ real time PCR cycler (BioRad). Results were presented as fold induction, normalized to expression of hypoxanthine-guanine phosphoribosyltransferase (*HPRT*), which was selected as the most stable reference gene as described previously [293]. Hygromycin phosphotransferase was used as a transfection marker.

Molecular modelling of ATP7B

To build the homology model of ATP7B, four different templates were combined using the YASARA molecular modeling program [294]. The aminoterminus of ATP7B contains six metal binding domains (MBDs), four of which have already been solved by NMR spectroscopy (PDB file 2ROP [295] contains domains 3 and 4, while 2EW9 [193] contains domains 5 and 6). The high sequence homology between the MBDs was used to build a homology model for MBD 1 and 2 for which the template 2ROP yielded a slightly better [296] model than 2EW9. The six MBDs were then manually arranged around the ATPase and joined by unstructured random loops.

The homology model of the remainder of ATP7B was built using the crystal structure of the sarco/endoplasmic reticulum calcium ATPase from Oryctolagus cuniculus as a template; PDB file 2ZBD [181], the one with the best WHAT_CHECK scores [296] was used. After a structural alignment with YASARA's MUSTANG module [297], a hybrid template was built by replacing the N-domain of 2ZBD with the known NMR structure of the ATP7B N-domain (PDB file 2ARF [185]. The alignment between ATP7B and the hybrid template was created with T-Coffee [298] as described previously [299]. Due to the very low sequence identity in some parts of the protein, the critical parts of the alignment around the mutations described here were additionally verified using Phyre [300] and mGenThreader [301]. As noted previously [302], the first two transmembrane helices of ATP7B do not have a match in the template and were therefore included at a plausible, but unreliable position for visualization purposes only. The actual model was built with YASARA as described [299], including the SCWRL side-chain prediction algorithm [303] and high-resolution refinement [304]. The coordinates are available from the authors upon request.

Results

Effects of WD-associated mutations in ATP7B on protein expression and localization

ATP7B contains the nucleotide binding domain (N) with the SEHPL motif, the phosphorylation domain (P) with the invariant aspartic acid in the DKTG motif, and the actuator domain (A) with the TGEA motif, which are all required for catalytic activity (chapter 2). The CPC motif in the 6th transmembrane helix coordinates copper during export. The aminoterminus contains six highly conserved metal binding domains (MBDs) containing MXCXXC motifs. Four artificial mutations in these known functional domains and seven distinct WD-associated missense mutations were introduced in the ATP7B cDNA construct (Figure 1A). To study the effects of these mutations, HEK293T cells were transiently transfected with wild type (WT) and mutant ATP7B cDNA. The amount of WT ATP7B, immunodetectable at approximately 150 kDa, was linearly dependent on

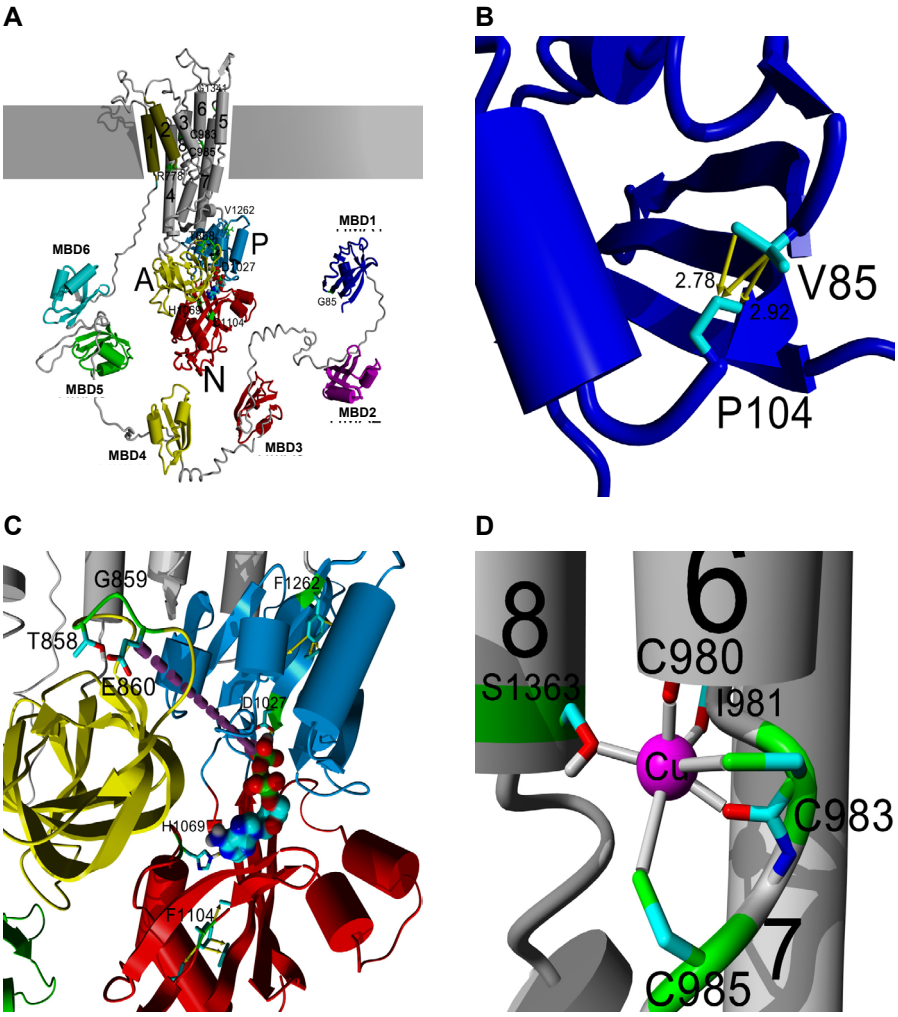

Figure 3. Homology modeling of Wilson disease-associated mutations in ATP7B

A homology model of ATP7B with bound ATP was constructed based on sequence alignment with other P-type ATPases and available structural data. (A) The six aminoterminal MBDs are colored from blue to cyan. The transmembrane helices are sequentially numbered, and the first two helices are colored differently as their position can hardly be predicted reliably. Conserved structural domains generally identified in P-type ATPases (A; actuator domain; P; phosphorylation domain; N; nucleotide binding domain) are indicated and the location of the various mutations in the protein is highlighted in green. (B) G85 is part of a beta hairpin in the MBD. This residue is tightly packed against P104 in the neighboring beta-strand, and therefore introduction of the bulky less flexible valine causes a distortion of the structure (yellow arrows). (C) The highly conserved TGE triplet starting at T858 is part of a surface loop in the N-domain. This loop is moved into the phosphorylation site (dotted magenta arrow), where T858 and G860 position a water molecule to perform the hydrolysis [181] of the phosphorylated D1027 during the catalytic cycle. This explains the functional consequences of the TGE858-860AAA and D1027A mutants. H1069 is predicted to be involved in ATP binding via a hydrogen bond to the N1 atom, and the p.H1069Q mutation abolishes this interaction. V1262 is tightly packed in the hydrophobic core of the P-domain, and introduction of the larger phenylalanine causes strong clashes with the neighboring residues M1025, L1255 and M1264 (yellow arrows) and thus a disturbance of the P-domain. p.C1104F disrupts the N-domain as the phenylalanine side-chain bumps into the side-chains of V1106, V1146 and I1148. (D) In addition to the backbone carbonyl groups of C980, I981 and C983, the side-chains of C983, C985 and S1363 coordinate copper in the transmembrane metal binding site. CPC983-985SPS removes the negatively charged thiolates, thereby disrupting copper binding. A phenylalanine side-chain in the p.S1363F mutant would completely disrupt the binding site. Molecular graphics were created with www.YASARA.org.

the amount of ATP7B cDNA (Figure 1B, data not shown). Whereas the expression of ATP7B with mutations in functional domains was comparable to WT ATP7B expression, all selected WD mutants, with the exception of ATP7B S1363F, displayed a significantly reduced protein expression. The mRNA abundance of these mutants with reduced protein expression was not affected (Figure 1C). The localization of all ATP7B mutants was determined by indirect immunofluorescence microscopy in U2OS cells, which have high spatial resolution in immunocytochemistry. In accordance with literature [62], WT ATP7B was localized in a perinuclear area, which colocalized with the *trans*-Golgi network (TGN) marker p230 (Figure 2A), but some WT ATP7B localized at the cell periphery. Mutations in functional domains and the patient mutation p.S1363F did not affect this localization pattern. In contrast, all other patient mutations resulted in predominant localization in the endoplasmic reticulum (ER) as was visualized by colocalization with the ER marker calreticulin (Figure 2B). However, both ATP7B G85V and H1069Q exhibited some co-localization with p230.

Homology modeling reveals conformational changes in ATP7B

A structural model of WT ATP7B was constructed based on the crystal structure of the related Ca^{2+} P-type ATPase, and the selected patient-associated WD mutations were modeled to get further insights into the molecular consequences of these mutations on the protein structure (Figure 3 and supplemental information). G85 is part of a beta hairpin in the first MBD, and the p.G85V mutation distorts the structure due to the bulky valine side-chain (Figure 3B). The highly conserved TGE triplet starting at T858 in the N-domain is required for hydrolysis of the phosphorylated D1027 in the P-domain (Figure 3C), and therefore TGE858-860AAA and D1027A are predicted to disrupt the catalytic cycle of P-type ATPases. H1069 is predicted to be involved in ATP binding and p.H1069Q abolishes this interaction. Substitutions p.V1262F and p.C1104F are predicted to result in conformational changes that disturb the N-domain and P-domain (Figure 3C) close to the phosporylation site, respectively. The CPC983-985SPS mutant and the phenylalanine side-chain from the S1363F mutant disrupt the copper-binding site within the intramembranous channel (Figure 3D). The effects of substitutions p.R778L, p.G1341V, and LLL1454-1456AAA could not be predicted reliably. Together, significant conformational changes in the ATP7B protein structure, combined with the reduction of protein expression, and protein retention in the ER, strongly suggested that the majority of the patient-associated ATP7B mutations lead to impaired folding, mislocalization and subsequent degradation. In contrast, mutations in functional ATPase domains were not associated with folding defects.

ATP7B protein-protein interactions with the copper chaperone ATOX1 and COMMD1

The copper-dependent interaction between the copper chaperone ATOX1 and ATP7B is essential for efficient copper export by ATP7B [72], and therefore we investigated this interaction by GST-pulldown analysis. ATOX1-GST was co-expressed with ATP7B in HEK293T cells. Since some of the mutants were expressed at low levels (Figure 1), we tuned the amounts of ATP7B cDNA to obtain approximately similar ATP7B protein levels. Cells were incubated in the presence of 50 μM of the copper chelator BCS or 100 μM $CuCl_2$. None of the introduced mutations in ATP7B resulted in abrogation of the copper-dependent

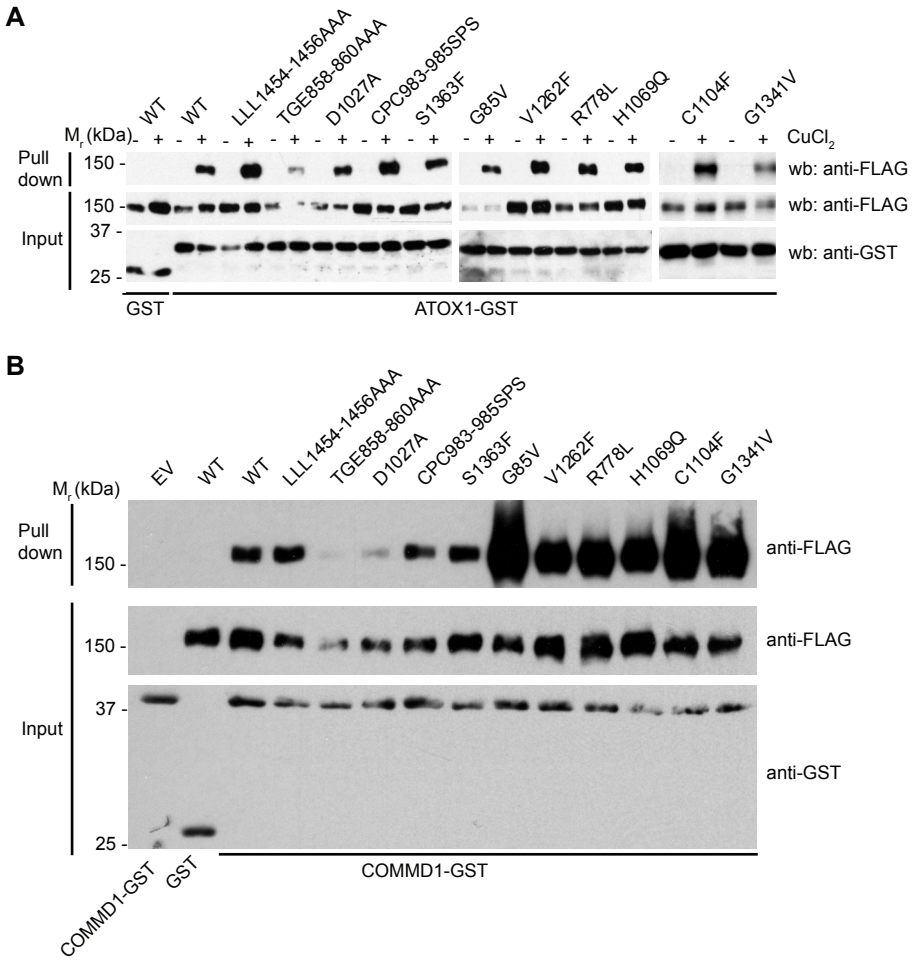

Figure 4. ATP7B protein-protein interactions with the copper chaperone ATOX1 and COMMD1
(A) HEK293T cells expressing WT or mutant ATP7B-FLAG together with GST or ATOX1-GST were incubated overnight with 50 µM BCS or 100 µM $CuCl_2$, and lysates were precipitated by GSH-sepharose. Precipitates were analyzed by western blots as indicated. Input indicates direct analysis of cell lysates. (B) GSH-sepharose precipitation was performed as described above using cell lysates of HEK293T cells expressing ATP7B-FLAG together with GST or COMMD1-GST.

interaction between ATOX1 and ATP7B (Figure 4A). Previous studies established that the aminoterminal domain of ATP7B interacts with COMMD1, encoded by the gene deleted in Bedlington terriers affected with hepatic copper toxicosis [145, 225, 229]. All ATP7B proteins with mutations that do not impair the protein expression (see Figure 1B) displayed unaffected interaction with COMMD1 (Figure 4B). In contrast, all ATP7B mutants with reduced protein expression and mislocalization to the ER had a markedly increased interaction with COMMD1.

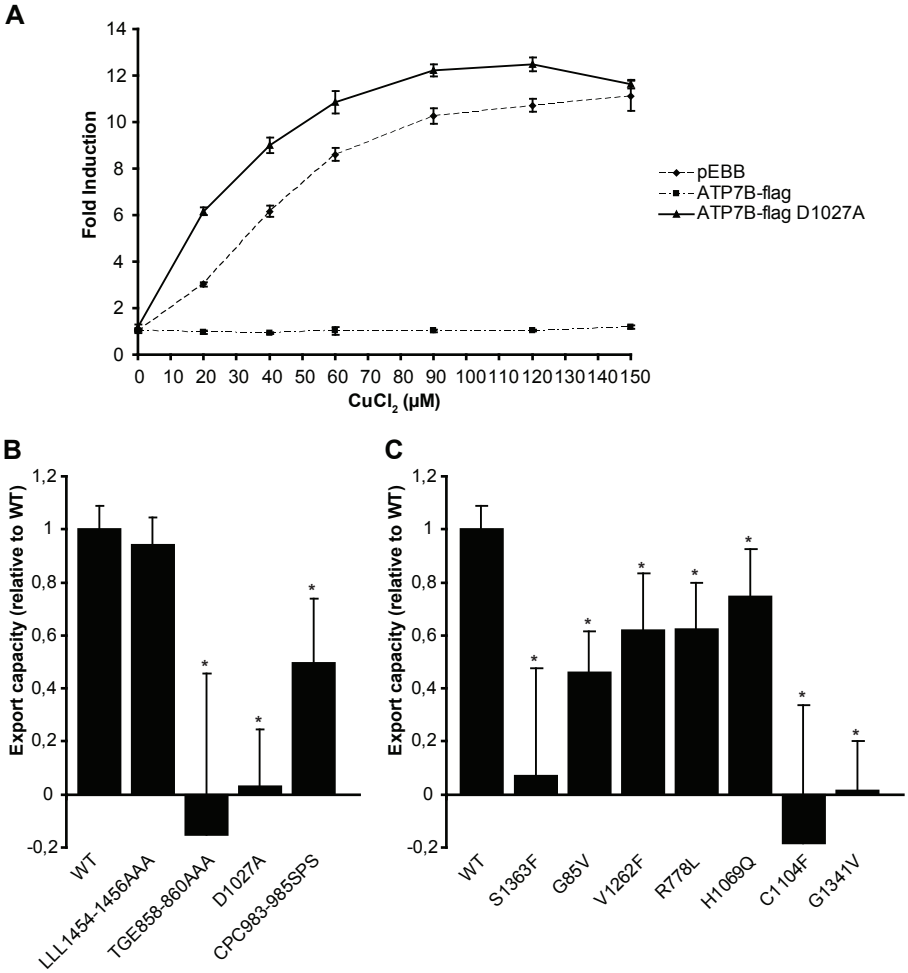

Figure 5. Reduced copper export capacity of ATP7B
(A-C) HEK-293T cells were transiently transfected with the MRE–luciferase reporter together with pEBB, WT pEBB-ATP7B-FLAG or mutant pEBB-ATP7B-FLAG. After transfection, cells were incubated for 24 hours with different concentrations of $CuCl_2$ (A) or 50 µM $CuCl_2$ (B, C). (A) MRE–luciferase reporter activities were measured and expressed as fold induction relative to EV. (B, C) Copper export capacity was calculated as described in the methods section. Values are expressed ±S.E.M. (*, p≤0.05; n=3).

Reduced copper export capacity of ATP7B

To address functional copper export capacity of ATP7B, we transiently transfected HEK293T cells with the MRE-Luciferase reporter, a copper sensor based on the metallothionein-1 promoter that responds to bioavailable cytosolic copper, and which was previously used to characterize cellular copper import [87]. Incubation with different $CuCl_2$ concentrations resulted in a copper concentration-dependent and saturable induction of Firefly Luciferase activity (Figure 5A). When we overexpressed ATP7B, this copper-dependent reporter induction was completely abrogated (Figure 5A), and this effect was linearly dependent on the amount of ATP7B expressed (data not shown). Mutation of the invariant aspartic acid residue essential for the catalytic cycle of all P-type ATPases (ATP7B D1027A) resulted in

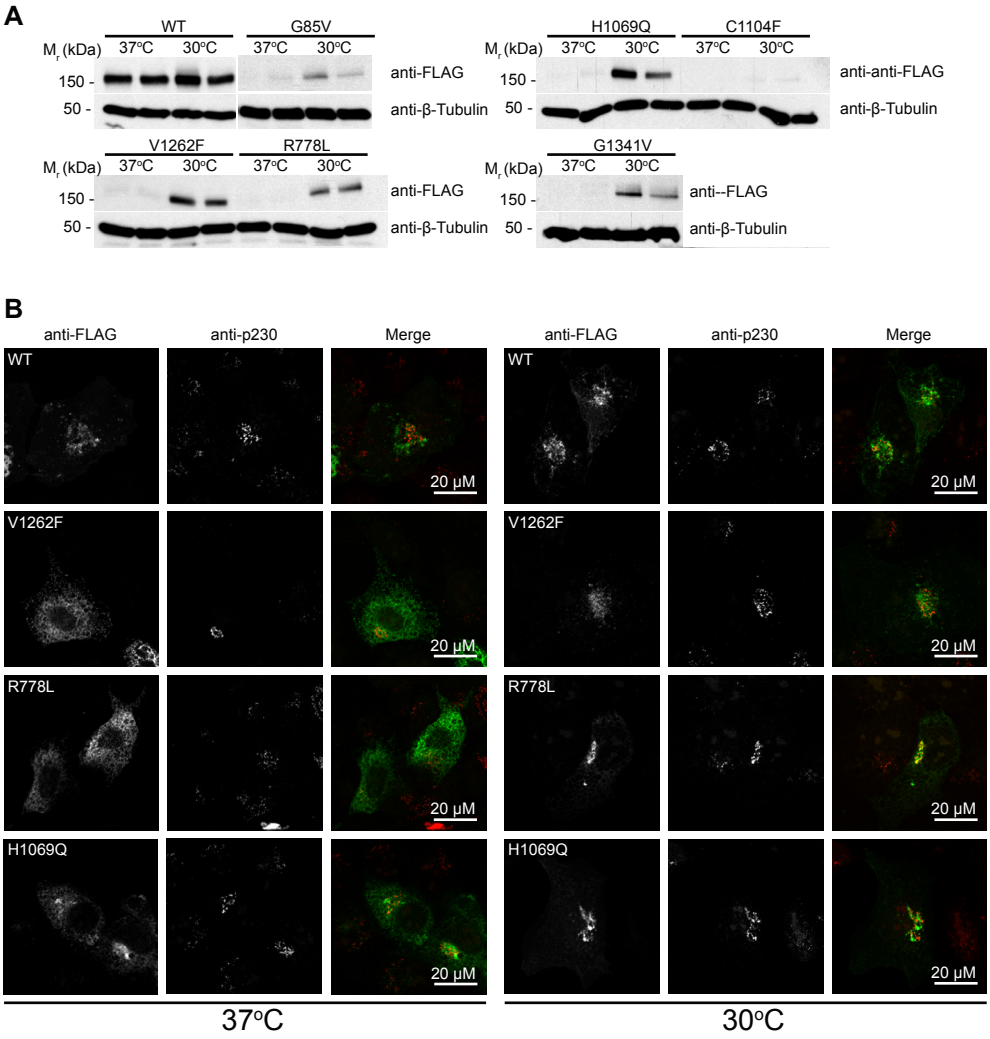

Figure 6. Recovery of ATP7B expression and localization by low temperature
HEK293T cells were transiently transfected with WT or mutant ATP7B-FLAG, and cells were cultured for 48 hours at 30°C or 37°C. (A) Protein lysates were subjected to western blot analysis with anti-FLAG and anti-β-tubulin. (B) Localization of ATP7B WT and mutants was determined as described in Figure 2 after incubation for 48 hours at 30°C and 37°C.

restoration of reporter induction to levels comparable to empty vector-transfected cells. This observation indicated that expression of ATP7B reduced cytosolic copper concentrations, which required catalytically active ATP7B. Next, all different ATP7B mutants were systematically cotransfected with the MRE-Luciferase reporter and cells were incubated at 50 μM $CuCl_2$ (Figure 5B, 5C). Copper export capacity of ATP7B D1027A, TGE858-860AAA, S1363F, C1104F, and G1341V mutants was drastically reduced, whereas significant residual copper export capacity was observed when ATP7B LLL1454-1456AAA, CPC983-985SPS, G85V, R778L, H1069Q and V1262F mutants were overexpressed (Figure 5B, 5C).

Recovery of ATP7B expression by low temperature and pharmacological folding chaperone treatment

As some of the ATP7B mutants displayed residual copper export capacity, recovery of protein expression and normalization of intracellular localization might be of clinical significance. First, we investigated whether the effects of the mutations on expression were ameliorated by culturing the cells at low temperature (30°C), as this can stimulate expression of otherwise misfolded proteins [292]. Expression of mutant ATP7B proteins that were expressed at low levels at 37°C (Figure 1B) was analyzed. Expression of all tested mutant ATP7B proteins, with the exception of ATP7B C1104F, was profoundly increased at 30°C (cf. Figure 1B, Figure 6A). WT ATP7B and all mutant ATP7B proteins that were localized in the TGN at 37°C were also localized in the TGN after incubation at 30°C (Figure 6B, data not shown; summarized in Table 2). Of all ER-resident ATP7B mutants at 37°C, TGN localization of ATP7B V1262F, R778L, and H1069Q was completely normalized after incubation at 30°C (Figure 6B). These results prompted us to investigate the influence of treatment with the pharmacological chaperones 4-PBA and curcumin on protein expression of ATP7B. Indeed, expression of several ATP7B mutants was improved by treatment with both 4-PBA and curcumin (Figure 7). A marked increase in expression was observed for ATP7B G85V, R778L, H1069Q, C1104F, V1262F, and G1341V. The extent of induction depended on the specific mutation, and 4-PBA generally appeared somewhat more effective in inducing mutant ATP7B expression than curcumin.

Discussion

Since the hallmark cloning of the gene mutated in Wilson disease, over 300 distinct patient-associated mutations have been documented [28]. Most of these are missense mutations [28]. Here, we have performed an extensive and systematic analysis of cell-biological and functional consequences of a selection of mutations distributed across the open reading frame of *ATP7B* [28]. Our results taken together with previous reports on individual WD-associated mutations [186, 305] indicate that whereas mutations in functional ATPase domains were not associated with folding defects, a surprisingly large number of patient-derived mutations (six out of seven) resulted in protein misfolding (summarized in Table 2; misfolding mutations are depicted in the grey box). These mutant proteins clearly exhibit characteristic properties of misfolded proteins; decreased protein expression, and retention in the ER. Furthermore, protein expression was restored when cells were cultured at 30°C, which is well-known to improve protein folding [292] (Table 2). Incubation at 30°C completely restored localization to the TGN for some, but not all mutants. Misfolding was further supported by homology modeling of the effects of these mutations on the ATP7B structure. In addition, at least one of these mutations, p.G85V, leads to enhanced proteasomal degradation, yet another hallmark of misfolded proteins and the most likely overall explanation for the observed reduced mutant ATP7B protein expression [217]. Previous studies have shown that COMMD1 interacts with the aminoterminal peptide of ATP7B [217, 229]. We now present evidence that COMMD1 interacts more avidly with mutant ATP7B even when the mutated residue is outside the N-terminal interaction domain. This observation was strictly correlated to those mutations that were associated

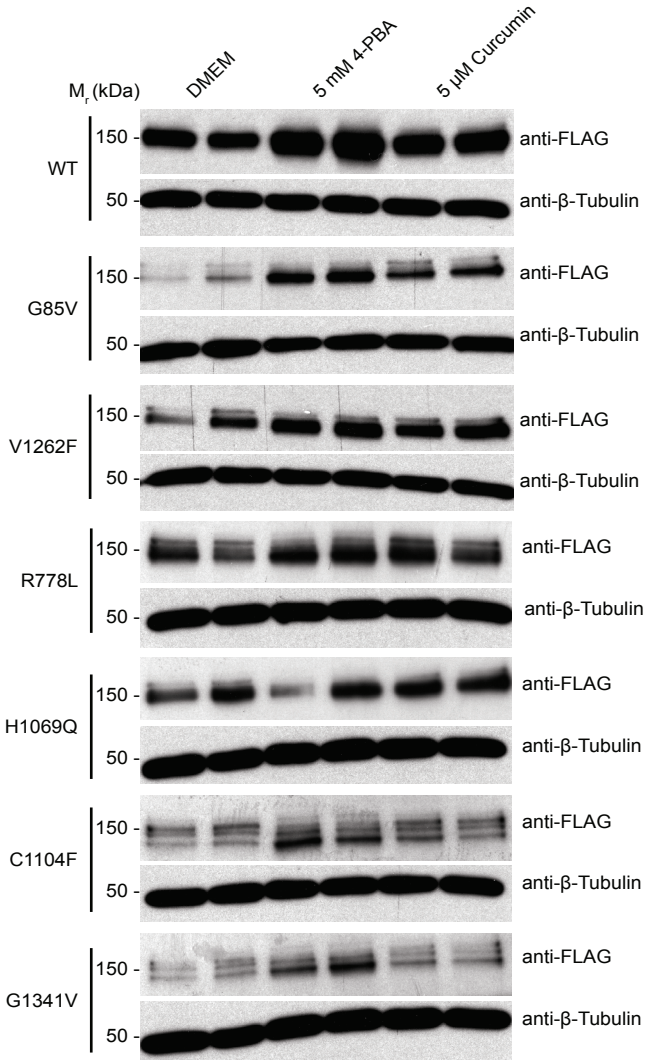

Figure 7. Recovery of ATP7B expression by pharmacological folding chaperone treatment
HEK293T cells were transiently transfected with WT or mutant ATP7B-FLAG, and cells were cultured for 48 hours with either 5 mM 4-PBA or 5 µM curcumin. ATP7B expression was quantified by western blot analysis. Experiments are depicted in duplicate.

with protein misfolding (Table 2). We thus propose that ATP7B protein misfolding leads to a general effect on ATP7B structure, secondarily inducing increased COMMD1 binding. In conclusion, protein folding and quality control of nascent ATP7B are pivotal for efficient hepatic copper export.

The current work has clear implications for the development of novel therapeutic strategies to improve clinical management of WD. Importantly, the mutations that were shown here to result in misfolding, actually represent a significant proportion of the WD patient population. Amongst them are two of the most frequent mutations: p.H1069Q (30

Table 2. Summary of systematic analysis of cell-biological and functional consequences of mutations in ATP7B

Mutation	Expression[a]				Localization[b]		Export capacity[c]	Interacting proteins[d]	
	37°C	**30°C**	**4-PBA**	**Curcumin**	**37°C**	**30°C**		**ATOX1**	**COMMD1**
LLL1454-1456AAA	+	n.d	n.d	n.d	TGN	TGN	+	+	+
D1027A	+	n.d	n.d	n.d	TGN	TGN	-	+	+
CPC983-985SPS	+	n.d	n.d	n.d	TGN	TGN	-	+	+
TGE858-860AAA	+	n.d	n.d	n.d	TGN	TGN	-	+	+
S1363F	+	n.d	n.d	n.d	TGN	TGN	-	+	+
G85V	-	++	++	++	TGN/ER	TGN/ER	-/+	+	++
V1262F	-	++	++	++	ER	TGN	-/+	+	++
R778L	-	++	++	++	ER	TGN	-/+	+	++
H1069Q	-	++	++	++	TGN/ER	TGN	-/+	+	++
C1104F	-	-	++	++	ER	ER	-	+	++
G1341V	-	++	++	++	ER	ER	-	+	++

[a]ATP7B protein expression at 37°C was comparable to WT (+), decreased compared to WT (-). ++ indicates increased expression as a result of incubation at 30°C, with 4-PBA, or with curcumin compared to incubation at 37°C. n.d.: not determined. [b]Subcellular localization in the trans-Golgi Network (TGN) or the endoplasmic reticulum (ER). [c]Export capacity by ATP7B was comparable to WT (+), residual (-/+) or absent (-). [d]Protein-protein interactions between ATP7B and ATOX1 or COMMD1 were comparable to wild type (+) or were increased (++). The grey box represents misfolding mutations in ATP7B.

to 75% of the Caucasian population) and p.R778L (10 to 40% of the Asian population) [306]. We attempted rescue of mutant ATP7B expression using curcumin and 4-PBA, because these pharmacological chaperones have been shown to restore *in vitro* expression of other membrane proteins mutated in liver disease (CFTR, BESP) [291, 292, 307, 308]. Each of these chaperones display different mechanisms of action, thus providing independent verification of their effects on ATP7B expression and underscoring the general applicability of this approach. More importantly, 4-PBA is clinically approved and its administration resulted in increased chloride conductance in cystic fibrosis patients [290, 309-311]. Consistent with our expectations, expression of most mutant ATP7B proteins was significantly induced by both curcumin and 4-PBA. Direct assessment of functional recovery of ATP7B activity using the MRE-Luciferase reporter appeared inconclusive, since expression of the reporter itself was also induced by pharmacological chaperones (data not shown).However, the residual copper uptake capacity when several of these ATP7B mutants were overexpressed suggests that recovery of expression and localization might restore functional copper export.

In conclusion, current treatment of WD patients with copper chelators and zinc is mostly efficient, but neurological deterioration is still a major complication [283, 284, 286]. Such neurological complications may be overcome or prevented by additional treatment with pharmacological chaperones, since both 4-PBA and curcumin can cross the blood-brain-barrier [312, 313]. It remains to be established to what extent ATP7B expression and function needs to be restored to relieve toxic copper accumulation in such patients. The current strategy to rescue expression of selected misfolded mutant proteins based on detailed systematic *in vitro* analysis of the cell biological consequences of patient-associated mutations may serve as a paradigm for other genetic liver diseases potentially associated with protein misfolding.

Financial support

Dutch Digestive Disease foundation WS 02-34 to LWJK), NWO Program grant 912.04.106 to LWJK, NWO VENI grant 016.096.108 to SFJvdG and Stichting BRIC, de leverziekte (to RHJH)

CHAPTER 6

General Discussion

Peter V.E. van den Berghe

Trace elements or micronutrients are essential dietary ingredients required in very small quantities for proper growth and development of an organism. Micronutrients comprise a broad group of chemical compounds, including several metals. Organisms rely on trace metals for many important physiological processes like mitochondrial respiration (copper and iron), transcription (copper and zinc), oxygen transport (iron), immunity (zinc) and many others. It is estimated that more than one billion people worldwide suffer from dietary trace metal deficiency, with moderate to severe clinical consequences. The necessity of these metals is further reflected by many disorders that involve metal biology. As examples, the common neurodegenerative disorders Alzheimer's disease and Parkinson's disease are characterized by high tissue levels of zinc, copper and iron [314]. Perturbations in iron homeostasis result in anemia and hemochromatosis [315]. Mutations in the P_{1B}-type ATPase *ATP7A* cause a systemic copper deficiency, resulting in the fatal X-linked neurodevelopmental disorder that is known as Menkes disease (MD) (OMIM 309400). Hepatolenticular copper accumulation in Wilson disease (WD) (OMIM 277900) is caused by mutations in *ATP7B* (homologue of *ATP7A*). These examples clearly illustrate that trace metal homeostasis needs to be balanced within a narrow range between toxicity and deficiency.

Copper homeostasis is a well-regulated process that has been extensively studied in the last two decades. Mammalian dietary copper absorption occurs mainly in the first part of the intestinal track [106]. Copper transporter (CTR) CTR1 is absolutely required for dietary copper absorption and is essential for cellular copper uptake [88, 89, 91, 93, 107]. The characterization of CTR1 as a high-affinity copper transporter marked the start of extensive studies on CTR1 structure, function and cellular localization [64, 85, 86, 88, 95, 96, 98-100, 105, 242, 244]. On the other hand, cellular copper export is equally important and is dependent on the copper-transporting P-type ATPases ATP7A and ATP7B [60, 137, 141, 147, 316]. In this thesis, I describe the use of a wide variety of biochemical and cell-biological approaches to unravel the molecular mechanisms of cellular copper uptake and export.

Monitoring cellular copper homeostasis

When studying copper metabolism, it is of utmost importance to have reliable functional copper transport assays. To study copper uptake and export in cells, we generated a novel transcription based reporter assay to monitor bio-available cytoplasmic copper (Chapter 3) (Figure 1). Metallothioneins (MT) are small proteins that bind heavy metals to prevent toxic accumulation of these metals [133, 249]. Copper binding to MT results in subsequent activation of the metal-responsive transcription factor-1 (MTF-1) to induce transcriptional activation of metal responsive genes like *MT* (Figure 1). This cell-intrinsic copper sensing system enables quantitative reporter induction in a saturable, copper-concentration-dependent manner. This was accompanied by concomitant copper-concentration dependent induction of MT transcription within the same timeframe (data not shown and [128]), indicating that this reporter measures bio-available copper without affecting intracellular copper concentrations. Using this reporter we were able to detect manipulations of the cellular copper transport machinery. On the one hand, expression of copper import proteins hCTR1 and hCTR2 markedly reduced the copper concentration necessary for full reporter induction (chapter 3 and 4). On the other hand, expression of copper export proteins ATP7B

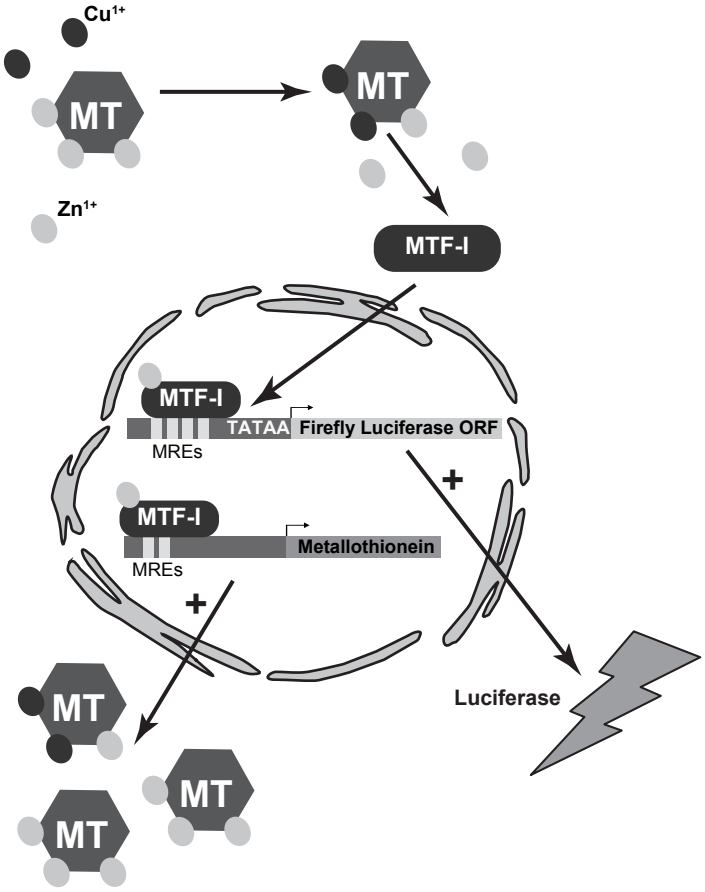

Figure 1. Novel transcription-based copper sensor: MRE-Luciferase reporter
The MRE-Luciferase reporter was constructed by introduction of four metal responsive elements (MREs) from the murine metallothionein (MT) 1A promotor in a Firefly luciferase vector with a minimal promotor. An increase of cytosolic copper (or zinc) results in zinc displacement from metallothioneins. This zinc pool activates the metal responsive transcription factor-I (MTF-I), which subsequently binds to MREs in the promoter region of specific genes like MT [133, 249]. This mechanism creates a positive feed-back loop to prevent toxic accumulation of metals by MT. This cell-intrinsic copper sensing mechanism also induces transcription of Firefly Luciferase when the MRE-Luciferase reporter is present in the cell. Hence, this reporter measures bio-available cytoplasmic copper.

and ATP7A reduced maximal reporter induction indicating that bio-available copper was exported (chapter 5 and data not shown). Expression of either copper import proteins or export proteins therefore had opposite effects on reporter induction, in concordance with the described functions of hCTR1 or ATP7B in literature. Expression of either hCTR1 or ATP7B containing inactivating mutations did not affect reporter induction, thereby precluding that the observed effects of hCTR1 and ATP7B on copper-dependent reporter induction was merely due to copper binding to these proteins. In addition, expression of the amino-terminal peptide of ATP7B, containing the six metal binding domains (MDBs) involved in copper binding did not affect copper-dependent reporter induction (data not shown). Taken together, these findings clearly show that the effects of hCTR1 and ATP7B

on MRE-Luciferase reporter induction required active copper transport.

The MRE-luciferase reporter has important advantages but also some limitations compared to previously existing and recently-developed methods to measure copper. Synthetic cell-permeable fluorescent copper sensors based on copper chelation like CTAP-1 and the Copper Sensor 1 [253, 317] have recently attracted attention. These sensors detect kinetically labile copper pools, which are not necessarily bio-available, and can potentially affect intracellular copper homeostasis by copper chelation. In contrast, the MRE-Luciferase reporter, as a functional assay, measures bio-available copper without affecting intracellular copper concentrations. Radioactive copper assays have been used in the past, but the applicability of this method is limited by the availability and the short half-life of the radioisotopes ($t_{½}$= 12.8 hrs for ^{64}Cu and $t_{½}$= 61.8 hrs for ^{67}Cu). Nevertheless, the MRE-Luciferase reporter represents cumulative copper load of cells in a period of 6-24 hrs, and therefore no information about copper uptake or export kinetics can be extracted. Detailed analysis of copper transport kinetics therefore requires radioactive copper assays.

Synchrotron X-ray fluorescence scanning allows spatial resolution of copper and other metals in cells with a detection limit of approximately 10^{-19} mol/μm^2 with a spatial resolution of 200 nm [317, 318]. However, this method cannot be used for copper transport kinetics and this technique requires very sophisticated and expensive equipment. A novel foster-resonance energy transfer (FRET)-based technique is a potential candidate to solve this problem. This ratiometric, genetically-encoded sensor is based on the copper-dependent protein-protein interaction between ATP7B and ATOX1 coupled to the FRET-pair CFP and YFP. The current sensor was surprisingly more sensitive to zinc than to copper [77, 319], and future experiments are therefore focused on modifications to change the specificity from zinc to copper (M. Merkx, personal communication). A major advantage of the FRET-sensor would be the addition of cellular signal peptides to measure copper in specific organelles or regions of interest in a cell. Both this sensor and our MRE-Luciferase reporter have the disadvantage that cells need to be transfected with these constructs to enable copper detection. This increases variability between experiments, and future experiments with these sensors would therefore greatly benefit from cell lines that stably express these sensors.

The protein-abundance of CCS, the copper chaperone for Cu/Zn superoxide dismutase (SOD1) [320], has been shown to be copper-responsive, and this feature has been applied to measure CCS as an indicator of cytoplasmic copper concentrations [321-323]. Although this approach also measures the availability of cytoplasmic copper for a biological process, similar to the MRE-Luciferase reporter, it is low-throughput and not quantitative.

One concern regarding the MRE-Luciferase reporter is the metal-specificity. As can be seen in Figure 1, the sensor is expected to be responsive to zinc in addition to copper. Indeed, reporter induction was also observed a zinc-concentration-dependent manner, and therefore the contribution of zinc-dependent induction should be carefully eliminated in experiments with this reporter. Experiments in chapter 3 revealed that it is indeed possible to eliminate the contribution of zinc to reporter induction.

Taken together, our novel transcription based copper sensor is a versatile tool that allows quantitative, sensitive and high-throughput assessment of changes in copper homeostasis. We anticipate several important future applications of this sensor. First, studies on zinc homeostasis might benefit from this reporter assay. Second, the high-throughput character

of this reporter renders this assay well-suited for functional genomic screens (e.g. using RNAi libraries) to detect and characterize novel proteins with a function in copper homeostasis. Ultimately, we propose to further develop this reporter as a diagnostic tool to detect aberrations of copper transport in patient cells compared to control cells.

Cellular copper import

Why do cells have two copper import proteins?

CTR1-dependent copper uptake is highly conserved in evolution, and appeared essential for cellular copper uptake in different organisms, including yeast, drosophila and mice. [83, 88, 89, 96, 113, 114, 263, 324], However, several independent observations indicate the presence of copper-uptake activity that is independent of CTR1. First, mouse embryonic fibroblasts (MEFs) isolated from the Ctr1 knockout mouse displayed a drastic decrease in high-affinity copper uptake, but a residual low-affinity copper uptake activity, amounting approximately 30% of control cells, could be detected [91]. Second, generation of intestine-specific Ctr1 knockout mice resulted in a systemic copper deficiency [93]. Strikingly however, intestinal hyperaccumulation of copper in these mice suggested that alternative copper uptake routes exist. Third, specific knockout of hepatic Ctr1 resulted only in a mild hepatic copper deficiency and reduced activity of cuproenzymes cytochrome C oxidase, SOD1, and the feroxidase ceruloplasmin (CP) [92]. Systemic copper homeostasis was only mildly affected, partly due to increased urinary copper excretion, and residual billiary copper excretion. This work suggested that Ctr1 does not represent the major or only copper import pathway in murine liver. We propose that CTR2 is the primary candidate for CTR1-independent copper uptake routes.

In the first functional studies done on hCTR2, it was shown that this transporter mediates copper uptake with low affinity compared to hCTR1 (chapter 3) [87]. This is supported by the absence of the aminoterminal Mets motifs in hCTR2, which are required for high-affinity copper uptake in hCTR1 [96]. However, copper transport affinity of hCTR2 cannot be measured directly using our reporter assay, and therefore characterization of hCTR2 using radioactive copper import assays is necessary to establish hCTR2-dependent uptake kinetics. Although hCTR2 is most likely a copper transporter with low affinity, it is also possible that the hCTR2-dependent reporter induction at relatively high copper concentrations is caused by its exclusive localization into endocytic organelles. Hence, endocytosis or delivery of intracellular copper pools to hCTR2, rather than transport affinity *per se*, could be limiting (Figure 2A). The localization of hCTR2 in lysosome-like organelles closely resembles the situation in yeast. Ctr6p, the hCTR2 orthologue in the fission yeast *Schizosaccharomyces pombe*, is localized in the vacuole [255], which is functionally equivalent to the mammalian lysosome. yCtr2p, the hCTR2 orthologue in *Saccharomyces cerevisia*, is also localized the vacuole and in involved in mobilization of copper from the vacuole to the cytosol [254]. However, it is currently unknown whether lysosomal copper is available for transport in mammalian cells. Lysosomal copper accumulation is observed in several animal models with hepatic copper overload [256-258], indicating the involvement of lysosomes in copper homeostasis, and suggesting that lysosomal copper concentrations might be high enough to allow low-affinity copper transport from the lysosomal lumen into the cytosol under certain

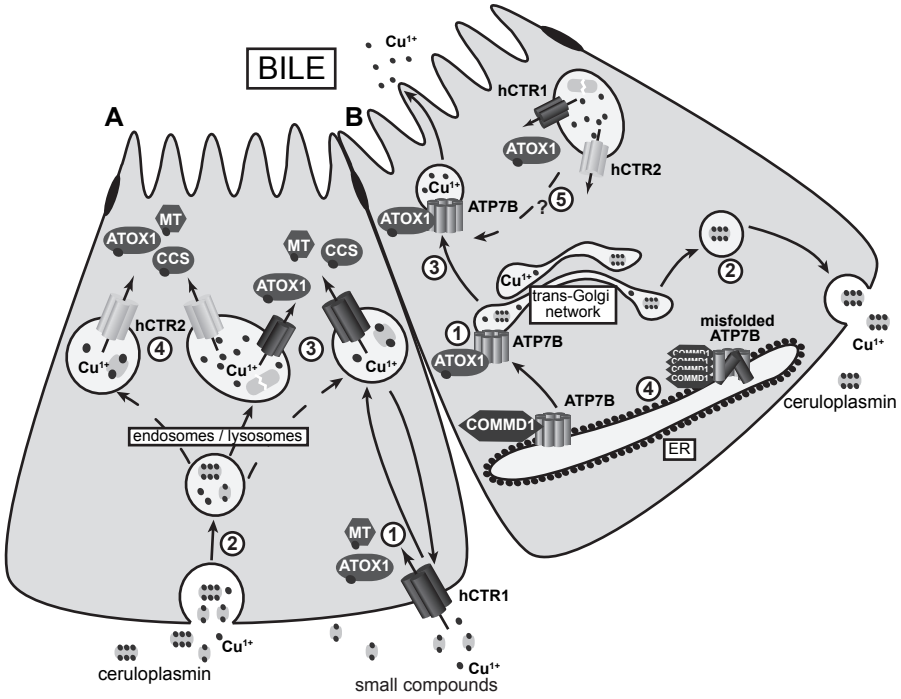

Figure 2. Hypothetical model for hepatic copper homeostasis
Hepatocytes acquire copper from the portal vein and hepatic arteries. (A) hepatocytes acquire copper from small compounds and ceruloplasmin. 1, one copper entry pathway is hCTR1 at the plasmamembrane, which can be internalized upon high copper concentrations. 2, Copper, small compounds and ceruloplasmin (CP) can be internalized by endocytosis and pinocytosis. CP can be degraded in the endocytic pathway, thereby releasing copper in the lysosomes. Copper in intracellular vesicles can be mobilized by either hCTR1 (3), hCTR2 (4) or both. Transported copper can bind to different copper chaperones for intracellular distribution. (B) 1, ATOX1 delivers copper to ATP7B in the trans-Golgi network (TGN), where ATP7B transports copper into the TGN. Here, copper can be incorporated in cuproenzymes like CP. 2, mature copper-containing CP is secreted for distribution throughout the body. 3, during copper excess, ATP7B can traffic towards the apical membrane for copper secretion into the bile. 4, newly synthesized ATP7B is subjected to folding and quality control in the ER. Misfolded proteins interacted more strongly with COMMD1. 5, Imported copper from hCTR1, hCTR2 or both can be delivered to different proteins in the cell, including ATP7B.

pathological conditions. In normal physiological conditions, lysosomal copper transport would require high local copper concentrations to compensate for the low affinity of hCTR2. The endocytic pathway has enormous intrinsic capacity to concentrate and specifically target cargo to lysosomes (reviewed by [325]). This implies that iterative organelle fusion between copper-loaded endocytic vesicles and hCTR2-containing vesicles could enable hCTR2-dependent copper uptake by elevating the copper concentration in these organelles. It is therefore tempting to speculate that such copper pools are available for hCTR2 (Figure 2A)

The existence of different copper pools in the blood also suggest that tissues have different copper uptake pathways. Albumin and α2-macroglobulin comprise the exchangeable copper pool in the blood, which presumably couples to hCTR1-dependent copper uptake [2, 19, 21, 22]. However, copper-containing CP represents the vast majority of non-exchangeable copper in the blood, therefore precluding a classic copper transport function of CP (reviewed

by [20]). CP is predominantly metabolized in the liver. Hepatic endothelial cells are able to transcytose CP, resulting in complete desialylation of CP and subsequent excretion into the space of Disse. Here, desialylated CP is endocytosed by hepatocytes by means of the asialoglycoprotein receptors [25, 26]. Following degradation of internalized ceruloplasmin in lysosomes, the copper is released and accessible for cellular copper uptake. CP has a half-life of approximately 5.5 days [326, 327], which means that 18% of the total CP pool per day is recycled in the liver. As CP-associated copper comprises approximately 90% of total copper in the blood, this indicates that approximately 1 mg of CP-bound copper is recycled by the liver per day. This pool could be (partly) subjected to lysosomal excretion in the bile [328], but the contribution of this process to total biliary copper excretion remains elusive. It is therefore tempting to speculate that this copper pool could be accessible for hCTR2-dependent copper uptake instead of hCTR1 (Figure 2A). Besides the liver, also the brain has a vast source of ceruloplasmin [329, 330]. Purkinje cells in the cerebellum are a source of CP in the brain [331], and a GPI-anchored splice variant of ceruloplasmin is expressed by astrocytes *[332, 333].* In conclusion, we speculate that mammals express two different copper uptake proteins, to allow independent and regulated uptake of different copper pools. Future research should focus on tissue specific knockout models for hCTR2 to investigate the biological function of this protein, and to directly test this hypothesis.

Oligomerization of copper transporters

One of the ongoing debates in CTR biology is the necessity of oligomerization for functional copper uptake. Biochemical analysis and electron microscopic crystallography revealed that hCTR1 subunits assemble in oligomeric complexes comprising three hCTR1 subunits [86, 87, 95, 99, 100] (chapter 4). Coexpression of hCTR1 M150I-M154I with hCTR1 WT did not affect oligomerization, expression or cellular localization, but protein function was inhibited in a *trans*-dominant fashion (chapter 4; Figure 4-6). This process is likely to be a default well-regulated process that essentially occurs in the ER (chapter 4). Together, these data provide strong biochemical and functional evidence that oligomerization of hCTR1 is required for functional high-affinity copper transport activity by permitting the formation of a copper permeable channel necessary for copper uptake (Figure 3). Experiments using hCTR2 indicated that oligomerization is a general characteristic for function copper uptake by CTR proteins. Despite the similar architecture of hCTR1 and hCTR2, hetero-oligomerization was not observed between hCTR1 and hCTR2 (preliminary data not shown). This is possibly due to the marked differences in the Aminotermini, Carboxytermini and intracellular loops between hCTR1 and hCTR2. The Aminotermini of hCTR1 can interact with themselves but not with the Aminoterminus of hCTR2, and this interaction might therefore preclude hetero-oligomerization [95]. One of the most intriguing questions that remain unanswered is how copper is transferred from the oligmeric Ctr1 to intracellular metallochaperones, and where in the cell this occurs. A remarkable difference between hCTR1 and hCTR2 is the absence in hCTR2 of three high-affinity copper ligands (His-Cys-His) in the Carboxyterminus of hCTR1 that might serve as a copper-binding site [98]. Interestingly, the cytosolic site of the second transmembrane region of hCTR2 contains a conserved Cys-His, which is possibly accessible from the cytosol and might provide a copper binding site similar to hCTR1. This could create specific targeting of copper transfer to

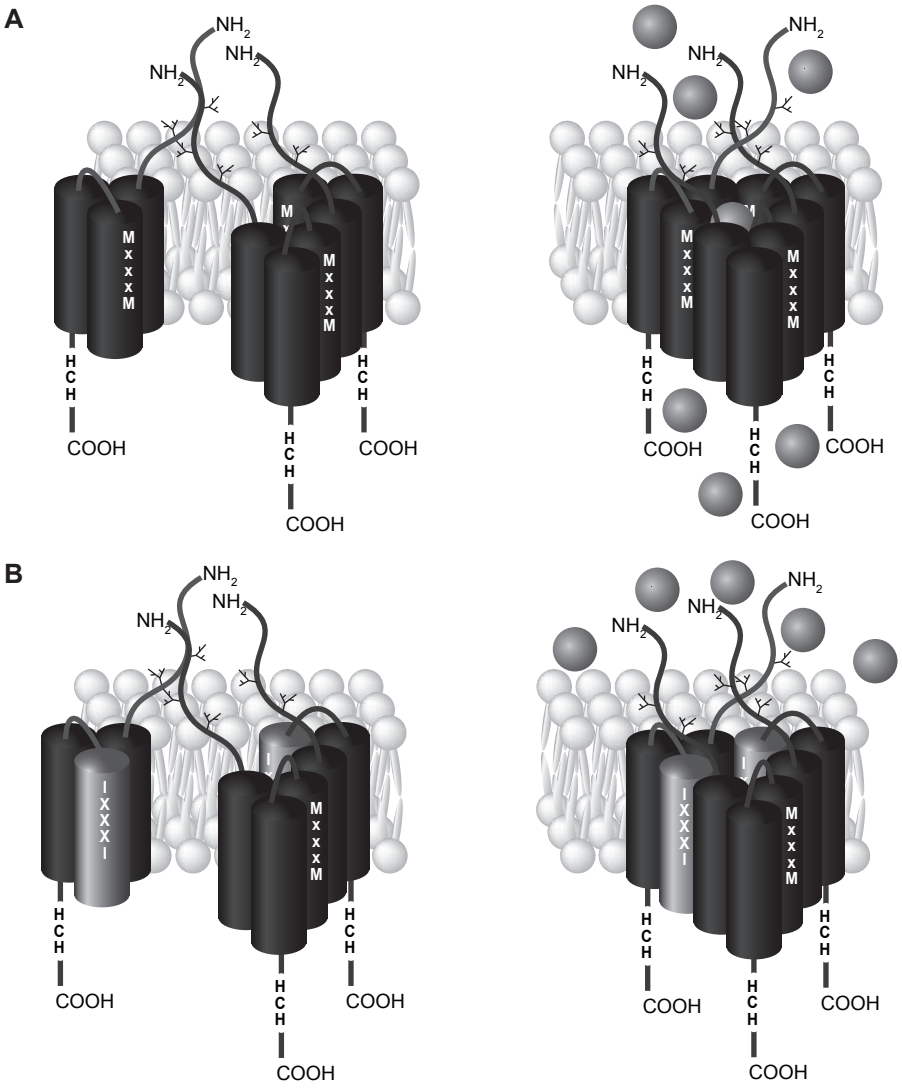

Figure 3. CTR oligomerization
(A) CTR1 is an integral membrane protein that contains three transmembrane regions with its glycosylated amino-terminus exposed in the extracytoplasmic lumen, whereas the carboxy-terminus protrudes into the cytosol [95, 97]. Evidence from literature and this thesis indicates that hCTR1 functions as a trimer to create an aqueous pore that is large enough to enable copper transport. (B) This complex requires M150I and M154I to coordinate copper in this pore, and introduction of one or more mutants that lack this methionine motif disrupts copper transport in a trans-dominant fashion (chapter 4).

copper chaperones. Copper from either hCTR1 or hCTR1 could have different cellular targets (Figure 2). It would be interesting to monitor ATP7B-dependent copper excretion, copper loading in SOD1 or copper binding to MT in the absence of hCTR1 or hCTR2 to discriminate between different intracellular copper transport pathways.

Cellular localization of copper transporters

Localization of the copper exporters ATP7A and ATP7B, and the copper import protein hCTR1 is copper dependent. ATP7A and ATP7B are localized in the TGN under basal copper conditions [60, 62, 137], but both proteins traffic to the periphery or to the plasma membrane when copper concentrations are increased [45, 137, 138, 140-142, 167, 195, 196, 197]. In this way, copper incorporation into the biosynthetic pathway during basal copper conditions is redirected to primary cellular copper excretion (Figure 2B). A small fraction of total hCTR1 in the cell appears at the plasma membrane [95, 105]. This hCTR1 pool is internalized upon increased copper concentrations, possibly as a means to reduce cellular copper uptake [64, 94]. However, the majority of hCTR1 is localized in intracellular organelles that markedly overlap with hCTR2, which is exclusively localized to intracellular organelles under steady state conditions (chapter 3). Comparison of hCTR1 and hCTR2 primary amino acid sequences revealed a conserved di-leucine motif in the Carboxyterminus of hCTR2 but not hCTR1 (Figure 1), a motif that is frequently involved in endocytosis of integral membrane proteins including ATP7A [63, 209]. This could explain the exclusive intracellular steady state localization of hCTR2.

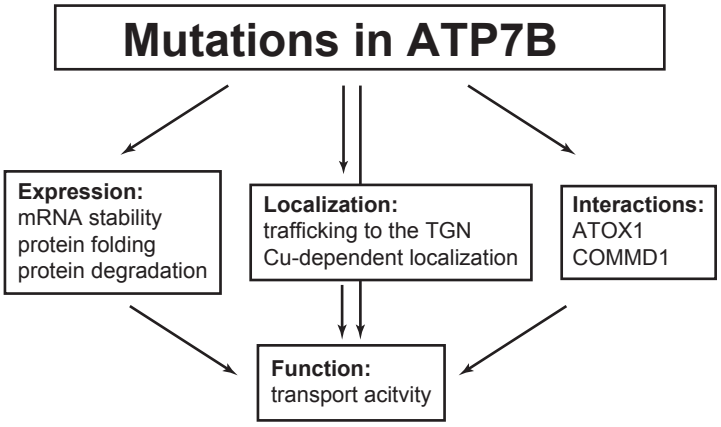

Figure 4. Molecular consequences of Wilson disease
Several molecular consequences caused by mutations in ATP7B potentially contribute to the Wilson disease phenotype. These processes are all putative targets for intervening therapies, like recovery of protein folding and expression by pharmacological chaperones.

Copper-dependent hCTR1 internalization and re-localization of ATP7A or ATP7B to the periphery suggests that common mechanisms may operate to relocalize copper transporters in order to prevent intracellular copper accumulation. Interestingly, concomitant trafficking of copper import and export proteins is also regulated in mammary and placenta tissue by hormones [31, 58, 200], but it is currently unknown whether the intracellular localization of hCTR2 is affected by these hormones. Together these observations suggest that intracellular signal transduction pathways regulate this localization and it is well possible that both hormones and high copper levels affect the same pathways. Inhibition of this apparent hormone-dependent trafficking of hCTR1, ATP7A, and ATP7B by specific inhibitors of cellular signal transduction cascades (kinase, phosphatase, ubiquitin modifiers and others) would therefore be an excellent starting point to unravel the underlying mechanisms of trafficking of these proteins.

Copper export and Wilson disease

Molecular consequences of Wilson disease mutations in ATP7B

Over 300 different mutations in the gene encoding *ATP7B* have been described, and most of these mutations are missense mutations [28], but most attempts to correlate the many different genotypes to the wide variety of clinical phenotypes failed [145, 146, 334]. This led us to propose that insight into genotype-clinical phenotype correlation could be enhanced by detailed characterization of the biochemical phenotypes associated with different mutations in *ATP7B* (chapter 5) (Figure 4) [145]. A surprisingly large number of the characterized WD mutations caused protein misfolding (six out of seven, chapter 5), including two of the most frequent mutations p.H1069Q and p.R778L [306]. Thus, protein misfolding appears to be a common mechanism for WD pathology, which hampers the possibility to make genotype-phenotype correlations with the present data.

COMMD1 is involved in protein folding

COMMD1 appears to have an important role in protein folding and quality control of nascent ATP7B [145]. COMMD1 was identified as the gene deleted in Bedlington terriers affected with hepatic copper toxicosis [145, 225, 229]. Previous studies have shown that COMMD1 interacts with the Aminoterminus of ATP7B, which contains the six consecutive MBDs important for copper-dependent regulation of protein localization and transport activity [71-77]. Most patient-associated mutations in this region of ATP7B, among them p.G85V, resulted in markedly increased binding of COMMD1 to full length ATP7B and to its individually expressed N-terminal region [217]. Furthermore, COMMD1 interacts more avidly with mutant ATP7B even when the mutated residue is not located within the N-terminal interaction domain (chapter 5) (Figure 2B). This observation was strictly correlated to those mutations that were associated with protein misfolding. We thus propose that ATP7B protein misfolding leads to a general effect on ATP7B structure, secondarily inducing increased COMMD1 binding. A common property of incompletely folded proteins is the solvent exposure of hydrophobic surfaces that are normally buried within the protein, and we suggest that COMMD1 associates with exposed hydrophobic domains on nascent ATP7B during its folding. This hypothesis would be consistent with previous studies that established extensive intramolecular interactions between the N-terminal domain and the large intracytoplasmic catalytic regions of ATP7B [187]. The regulation of protein folding by COMMD1 is further supported by the regulation of protein stability of the hypoxia-inducible factor-1α (HIF-1α). Here, COMMD1 competes with the heat shock protein HSP90, which is involved in correct folding of HIF-1α, for binding to the Aminoterminus of HIF-1α resulting in increased degradation of HIF-1α (van de Sluis et al., unpublished data). Interaction of HSP70 and HSP90 with WT and mutant ATP7B (preliminary data not shown) suggests that COMMD1 could affect quality control of ATP7B in a similar fashion by modulating the interaction of these heat shock proteins. Finally, as COMMD1 has been shown to interact with multiple E3 ubiquitin ligases [227, 235, 236, 335], we speculate that it may perform a regulatory function in the transition of protein (mis)folding to ubiquitin-mediated proteasomal degradation [235, 335]. Clearly, further studies should be done to assess the validity of this speculation.

Pharmacological chaperone treatment

Current treatment of WD patients comprises reduction of circulating copper with copper chelators and/or dietary zinc supplementation. Despite efficient treatment, 5% of all patients develop fulminant liver failure, and 10-50% of the patients have neurological deterioration [283, 284, 286]. Several pharmacological compounds, known as pharmacological folding chaperones, have recently become available, and were demonstrated to successfully restore protein expression and function of misfolded proteins associated with a number of hereditary diseases [289, 292, 308, 336]. Treatment with pharmacological chaperones 4-PBA and curcumin resulted in partial recovery of expression and subcellular localization for the most abundant Caucasian H1069Q mutation and very common Asian mutation R778L in ATP7B (chapter 5) [306]. Clinical treatment with pharmacological chaperones might therefore be feasible if indeed hepatic copper excretion can be improved. The observed residual copper export capacity of several ATP7B mutants would be in favor in this respect. Hence, the success of such strategies will be dependent on the amount of functional recovery that is necessary to relieve hepatic copper accumulation and copper excretion.

Misfolded proteins are detected by the quality control machinery in the ER, and misfolded proteins are targeted for ER-associated protein degradation (ERAD) [337]. This would explain the reduced expression of most of the misfolded WD mutations (chapter 5), which was supported by the increased proteasomal degradation of misfolded ATP7B G85V [217]. When ERAD fails, misfolded proteins start to accumulate and aggregate resulting in a condition known as ER-stress, which can ultimately result in cell death (reviewed by [338]). In WD, ER-stress might be a secondary effect of accumulation of mutant ATP7B, and therefore it is well possible that ER-stress has a significant contribution to WD pathology. Fortunately, the unfolded protein response (UPR) is a back-up mechanism that initiates transcription programs to resolve ER-stress [338]. Recent observations demonstrated that induction of the Heat shock response that promotes protein folding can partly relieve ER-stress [339]. Interestingly, obesity-induced ER-stress was reduced by treatment with pharmacological chaperones like 4-PBA, indicating that these chaperones affect both protein folding and ER-stress [340].

Treatment with pharmacological chaperones affects several pathways in the protein folding machinery. For instance, curcumin increases calcium concentrations in the ER thereby reducing the affinity of chaperone proteins to misfolded proteins [341]. 4-PBA induces heat shock protein expression [342], thereby improving protein folding and maybe also reducing ER-stress by induction of the heat shock response [339]. The strong association between COMMD1 and misfolded ATP7B suggested that COMMD1 is also affecting quality control of ATP7B (Figure 2B). Novel drug targeting this interaction might therefore provide a potential strategy to improve protein folding of COMMD1-associated proteins in the nearby future. Such strategies have proven their value as combination therapy with folding chaperones and proteasome inhibitors improved protein expression and function in two lysosomal storage disorders Gaucher disease and Tay-Sachs disease, respectively [289]. Future research should focus on novel therapeutic strategies to improve ATP7B folding by pharmacological chaperones to treat WD patients.

The applicability of pharmacological chaperone treatment should also be extended to

other copper related disorders. One such candidate is the fatal X-linked neurodevelopmental disorder Menkes disease (MD) that is caused by mutations in ATP7A (homologue of ATP7B). The MD mutations spectrum comprises deletions, nonsense mutations, frameshift mutations and missense mutations [343, 344] resulting in severe copper deficiency in patients with MD due to impaired dietary copper absorption [39-41]. Patients with classic MD have an average life-span of approximately three years, whereas patients with mild MD and OHS have an increased average life-span due to residual ATP7A activity [39-44]. The only (partial) effective treatment for MD is subcutaneous copper injections to resolve systemic copper deficiency [345]. Thus, a minor increase in circulating copper could already relieve some of the severe symptoms of MD, making MD an interesting target for pharmacological treatment. Future research on MD treatment could benefit greatly from the availability of relevant resources for MD. Routine diagnosis of MD comprises isolation of skin fibroblasts, which are tested for copper retention of radioactive copper (^{64}Cu) and export by pulse chase analysis [41]. The availability of these MD fibroblasts lines could be an excellent platform to test the applicability of pharmacological treatment for this disease.

Concluding remarks

In this thesis we aimed to improve our understanding of posttranslational regulation of cellular copper uptake and export. The systematic analysis of mutations in ATP7B and how these molecular consequences result in WD proved to be a very powerful approach to explore novel treatment strategies. A surprisingly large number of tested WD missense mutations resulted in misfolded proteins. Recovery of protein expression and localization are the first step to successfully restore ATP7B protein function in WD by pharmacological chaperones. However, successful recovery of protein function is the ultimate goal, but when successful, this treatment is a promising complementation of existing therapy, which might even extend to treatment of the related copper disorder MD. The addition of a novel copper sensor proved to be a valuable tool to successfully monitor cellular copper uptake and export, which resulted in the characterization of a novel copper uptake protein hCTR2 (chapter 3). The differences in subcellular localization together with structural differences between hCTR1 and hCTR2 suggest that hCTR1 and hCTR2 mobilize different copper pools to supply the cellular copper need. The next challenge will be to determine how, where, when and by which CTR protein these pools are used to acquire bio-available copper.

REFERENCES

1. Valko, M., H. Morris, and M.T. Cronin, *Metals, toxicity and oxidative stress.* Curr Med Chem, 2005. **12**(10): p. 1161-208.
2. Linder, M.C. and M. Hazegh-Azam, *Copper biochemistry and molecular biology.* Am J Clin Nutr, 1996. **63**(5): p. 797S-811S.
3. Lewis, K.O., *The nature and excretion of biliary copper in man.* Clin Sci, 1973. **45**(1): p. 133-4.
4. Lewis, K.O., *The nature of the copper complexes in bile and their relationship to the absorption and excretion of copper in normal subjects and in Wilson's disease.* Gut, 1973. **14**(3): p. 221-32.
5. Araya, M., et al., *Effects of chronic copper exposure during early life in rhesus monkeys.* Am J Clin Nutr, 2005. **81**(5): p. 1065-71.
6. August, D., M. Janghorbani, and V.R. Young, *Determination of zinc and copper absorption at three dietary Zn-Cu ratios by using stable isotope methods in young adult and elderly subjects.* Am J Clin Nutr, 1989. **50**(6): p. 1457-63.
7. Hunt, J.R. and R.A. Vanderpool, *Apparent copper absorption from a vegetarian diet.* Am J Clin Nutr, 2001. **74**(6): p. 803-7.
8. Johnson, P.E., D.B. Milne, and G.I. Lykken, *Effects of age and sex on copper absorption, biological half-life, and status in humans.* Am J Clin Nutr, 1992. **56**(5): p. 917-25.
9. Olivares, M., et al., *Age and copper intake do not affect copper absorption, measured with the use of 65Cu as a tracer, in young infants.* Am J Clin Nutr, 2002. **76**(3): p. 641-5.
10. Turnlund, J.R., *Human whole-body copper metabolism.* Am J Clin Nutr, 1998. **67**(5 Suppl): p. 960S-964S.
11. Turnlund, J.R., et al., *Copper absorption and retention in young men at three levels of dietary copper by use of the stable isotope 65Cu.* Am J Clin Nutr, 1989. **49**(5): p. 870-8.
12. Turnlund, J.R., et al., *A stable isotope study of copper absorption in young men: effect of phytate and alpha-cellulose.* Am J Clin Nutr, 1985. **42**(1): p. 18-23.
13. Turnlund, J.R., C.A. Swanson, and J.C. King, *Copper absorption and retention in pregnant women fed diets based on animal and plant proteins.* J Nutr, 1983. **113**(11): p. 2346-52.
14. Wapnir, R.A., *Copper absorption and bioavailability.* Am J Clin Nutr, 1998. **67**(5 Suppl): p. 1054S-1060S.
15. Varada, K.R., R.G. Harper, and R.A. Wapnir, *Development of copper intestinal absorption in the rat.* Biochem Med Metab Biol, 1993. **50**(3): p. 277-83.
16. Bronner, F. and J.H. Yost, *Saturable and nonsaturable copper and calcium transport in mouse duodenum.* Am J Physiol, 1985. **249**(1 Pt 1): p. G108-12.
17. Bauerly, K.A., S.L. Kelleher, and B. Lönnerdal, *Functional and molecular responses of suckling rat pups and human intestinal Caco-2 cells to copper treatment.* J Nutr Biochem, 2004. **15**(3): p. 155-62.
18. Bauerly, K.A., S.L. Kelleher, and B. Lönnerdal, *Effects of copper supplementation on copper absorption, tissue distribution, and copper transporter expression in an infant rat model.* Am J Physiol Gastrointest Liver Physiol, 2005. **288**(5): p. G1007-14.
19. Moriya, M., et al., *Copper Is Taken up Efficiently from Albumin and Alpha-2-Macroglobulin by Cultured Human Cells by More Than One Mechanism.* Am J Physiol Cell Physiol, 2008.
20. Hellman, N.E. and J.D. Gitlin, *Ceruloplasmin metabolism and function.* Annu Rev Nutr, 2002. **22**: p. 439-58.
21. Barrow, L. and M.S. Tanner, *Copper distribution among serum proteins in paediatric liver disorders and malignancies.* Eur J Clin Invest, 1988. **18**(6): p. 555-60.
22. Wirth, P.L. and M.C. Linder, *Distribution of copper among components of human serum.* J Natl Cancer Inst, 1985. **75**(2): p. 277-84.
23. Harris, Z.L., L.W. Klomp, and J.D. Gitlin, *Aceruloplasminemia: an inherited neurodegenerative disease with impairment of iron homeostasis.* Am J Clin Nutr, 1998. **67**(5 Suppl): p. 972S-977S.
24. Meyer, L.A., et al., *Copper transport and metabolism are normal in aceruloplasminemic mice.* J Biol Chem, 2001. **276**(39): p. 36857-61.
25. Omoto, E. and M. Tavassoli, *The role of endosomal traffic in the transendothelial transport of ceruloplasmin in the liver.* Biochem Biophys Res Commun, 1989. **162**(3): p. 1346-50.
26. Omoto, E. and M. Tavassoli, *Purification and characterization of ceruloplasmin receptors.* Trans Assoc Am Physicians, 1989. **102**: p. 170-5.
27. Ala, A., et al., *Wilson's disease.* Lancet, 2007. **369**(9559): p. 397-408.
28. Kenny, S. and D.W. Cox, *Wilson disease database: http://www.medicalgenetics.med.ualberta.ca/wilson/index.php*.
29. Hardman, B., et al., *Distinct functional roles for the Menkes and Wilson copper translocating P-type ATPases in human placental cells.* Cell Physiol Biochem, 2007. **20**(6): p. 1073-84.
30. Kuo, Y.M., J. Gitschier, and S. Packman, *Developmental expression of the mouse mottled and toxic milk genes suggests distinct functions for the Menkes and Wilson disease copper transporters.* Hum Mol Genet, 1997. **6**(7): p. 1043-9.
31. Michalczyk, A., et al., *ATP7B expression in human breast epithelial cells is mediated by lactational hormones.* J Histochem Cytochem, 2008. **56**(4): p. 389-99.
32. Walshe, J.M., *Wilson's disease; new oral therapy.* Lancet, 1956. **270**(6906): p. 25-6.
33. Brewer, G.J., et al., *Treatment of Wilson's disease with ammonium tetrathiomolybdate. I. Initial therapy in 17 neurologically affected patients.* Arch Neurol, 1994. **51**(6): p. 545-54.
34. Brewer, G.J., et al., *Initial therapy of patients with Wilson's disease with tetrathiomolybdate.* Arch Neurol, 1991. **48**(1): p. 42-7.
35. Brewer, G.J., V. Yuzbasiyan-Gurkan, and V. Johnson, *Treatment of Wilson's disease with zinc. IX: Response of serum lipids.* J Lab Clin Med, 1991. **118**(5): p. 466-70.
36. Danks, D.M., *Disorders of Copper transport*, in *The metabolic and molecular basis of inherited disease*, C.R. Scriver, et al., Editors. 1995, McGraw-Hill: New York. p. 2211-2235.
37. Gu, Y.H., et al., *A survey of Japanese patients with Menkes disease from 1990 to 2003: incidence and early signs before typical symptomatic onset, pointing the way to earlier diagnosis.* J Inherit Metab Dis, 2005. **28**(4): p. 473-8.
38. Tonnesen, T., W.J. Kleijer, and N. Horn, *Incidence of Menkes disease.* Hum Genet, 1991. **86**(4): p. 408-10.

39. Kaler, S.G., *Metabolic and molecular bases of Menkes disease and occipital horn syndrome.* Pediatr Dev Pathol, 1998. **1**(1): p. 85-98.
40. Mercer, J.F., *Menkes syndrome and animal models.* Am J Clin Nutr, 1998. **67**(5 Suppl): p. 1022S-1028S.
41. Tumer, Z. and N. Horn, *Menkes disease: underlying genetic defect and new diagnostic possibilities.* J Inherit Metab Dis, 1998. **21**(5): p. 604-12.
42. Danks, D.M., *The mild form of Menkes disease: progress report on the original case.* Am J Med Genet, 1988. **30**(3): p. 859-64.
43. Kaler, S.G., et al., *Occipital horn syndrome and a mild Menkes phenotype associated with splice site mutations at the MNK locus.* Nat Genet, 1994. **8**(2): p. 195-202.
44. Procopis, P., J. Camakaris, and D.M. Danks, *A mild form of Menkes steely hair syndrome.* J Pediatr, 1981. **98**(1): p. 97-9.
45. La Fontaine, S.L., et al., *Correction of the copper transport defect of Menkes patient fibroblasts by expression of the Menkes and Wilson ATPases.* J Biol Chem, 1998. **273**(47): p. 31375-80.
46. Sarkar, B., K. Lingertat-Walsh, and J.T. Clarke, *Copper-histidine therapy for Menkes disease.* J Pediatr, 1993. **123**(5): p. 828-30.
47. Nittis, T. and J.D. Gitlin, *Role of copper in the proteosome-mediated degradation of the multicopper oxidase hephaestin.* J Biol Chem, 2004. **279**(24): p. 25696-702.
48. Vulpe, C.D., et al., *Hephaestin, a ceruloplasmin homologue implicated in intestinal iron transport, is defective in the sla mouse.* Nat Genet, 1999. **21**(2): p. 195-9.
49. Yuan, D.S., et al., *The Menkes/Wilson disease gene homologue in yeast provides copper to a ceruloplasmin-like oxidase required for iron uptake.* Proc Natl Acad Sci U S A, 1995. **92**(7): p. 2632-6.
50. Abdel-Ghany, S.E., et al., *Two P-type ATPases are required for copper delivery in Arabidopsis thaliana chloroplasts.* Plant Cell, 2005. **17**(4): p. 1233-51.
51. Mendelsohn, B.A., et al., *Atp7a determines a hierarchy of copper metabolism essential for notochord development.* Cell Metab, 2006. **4**(2): p. 155-62.
52. Arguello, J.M., E. Eren, and M. Gonzalez-Guerrero, *The structure and function of heavy metal transport P1B-ATPases.* Biometals, 2007. **20**(3-4): p. 233-48.
53. Lutsenko, S., E.S. LeShane, and U. Shinde, *Biochemical basis of regulation of human copper-transporting ATPases.* Arch Biochem Biophys, 2007. **463**(2): p. 134-48.
54. Gonzalez-Guerrero, M. and J.M. Arguello, *Mechanism of Cu+-transporting ATPases: soluble Cu+ chaperones directly transfer Cu+ to transmembrane transport sites.* Proc Natl Acad Sci U S A, 2008. **105**(16): p. 5992-7.
55. Gonzalez-Guerrero, M., et al., *Structure of the Two Transmembrane Cu+ Transport Sites of the Cu+-ATPases.* J Biol Chem, 2008. **283**(44): p. 29753-9.
56. Paynter, J.A., et al., *Expression of the Menkes gene homologue in mouse tissues lack of effect of copper on the mRNA levels.* FEBS Lett, 1994. **351**(2): p. 186-90.
57. Vulpe, C., et al., *Isolation of a candidate gene for Menkes disease and evidence that it encodes a copper-transporting ATPase.* Nat Genet, 1993. **3**(1): p. 7-13.
58. Kelleher, S.L. and B. Lönnerdal, *Mammary gland copper transport is stimulated by prolactin through alterations in Ctr1 and Atp7A localization.* Am J Physiol Regul Integr Comp Physiol, 2006. **291**(4): p. R1181-91.
59. Nyasae, L., et al., *Dynamics of endogenous ATP7A (Menkes protein) in intestinal epithelial cells: copper-dependent redistribution between two intracellular sites.* Am J Physiol Gastrointest Liver Physiol, 2007. **292**(4): p. G1181-94.
60. Petris, M.J., et al., *Ligand-regulated transport of the Menkes copper P-type ATPase efflux pump from the Golgi apparatus to the plasma membrane: a novel mechanism of regulated trafficking.* EMBO J, 1996. **15**(22): p. 6084-95.
61. Setty, S.R., et al., *Cell-specific ATP7A transport sustains copper-dependent tyrosinase activity in melanosomes.* Nature, 2008. **454**(7208): p. 1142-6.
62. Yamaguchi, Y., et al., *Biochemical characterization and intracellular localization of the Menkes disease protein.* Proc Natl Acad Sci U S A, 1996. **93**(24): p. 14030-5.
63. Francis, M.J., et al., *Identification of a di-leucine motif within the C terminus domain of the Menkes disease protein that mediates endocytosis from the plasma membrane.* J Cell Sci, 1999. **112 (Pt 11)**: p. 1721-32.
64. Petris, M.J., et al., *Copper-stimulated endocytosis and degradation of the human copper transporter, hCtr1.* J Biol Chem, 2003. **278**(11): p. 9639-46.
65. Ravia, J.J., et al., *Menkes Copper ATPase (Atp7a) is a novel metal-responsive gene in rat duodenum, and immunoreactive protein is present on brush-border and basolateral membrane domains.* J Biol Chem, 2005. **280**(43): p. 36221-7.
66. Monty, J.F., et al., *Copper exposure induces trafficking of the menkes protein in intestinal epithelium of ATP7A transgenic mice.* J Nutr, 2005. **135**(12): p. 2762-6.
67. Nose, Y., E.M. Rees, and D.J. Thiele, *Structure of the Ctr1 copper trans'PORE'ter reveals novel architecture.* Trends Biochem Sci, 2006. **31**(11): p. 604-7.
68. Rae, T.D., et al., *Undetectable intracellular free copper: the requirement of a copper chaperone for superoxide dismutase.* Science, 1999. **284**(5415): p. 805-8.
69. Prohaska, J.R. and A.A. Gybina, *Intracellular copper transport in mammals.* J Nutr, 2004. **134**(5): p. 1003-6.
70. O'Halloran, T.V. and V.C. Culotta, *Metallochaperones, an intracellular shuttle service for metal ions.* J Biol Chem, 2000. **275**(33): p. 25057-60.
71. Arnesano, F., et al., *Characterization of the binding interface between the copper chaperone Atx1 and the first cytosolic domain of Ccc2 ATPase.* J Biol Chem, 2001. **276**(44): p. 41365-76.
72. Hamza, I., et al., *Interaction of the copper chaperone HAH1 with the Wilson disease protein is essential for copper homeostasis.* Proc Natl Acad Sci USA, 1999. **96**(23): p. 13363-8.
73. Larin, D., et al., *Characterization of the interaction between the Wilson and Menkes disease proteins and the cytoplasmic copper*

chaperone, HAH1p. J Biol Chem, 1999. **274**(40): p. 28497-504.
74. Portnoy, M.E., et al., *Structure-function analyses of the ATX1 metallochaperone.* J Biol Chem, 1999. **274**(21): p. 15041-5.
75. Pufahl, R.A., et al., *Metal ion chaperone function of the soluble Cu(I) receptor Atx1.* Science, 1997. **278**(5339): p. 853-6.
76. Strausak, D., et al., *Kinetic analysis of the interaction of the copper chaperone Atox1 with the metal binding sites of the Menkes protein.* J Biol Chem, 2003. **278**(23): p. 20821-7.
77. van Dongen, E.M., L.W. Klomp, and M. Merkx, *Copper-dependent protein-protein interactions studied by yeast two-hybrid analysis.* Biochem Biophys Res Commun, 2004. **323**(3): p. 789-95.
78. Arguello, J.M. and M. Gonzalez-Guerrero, *Cu+ -ATPases brake system.* Structure, 2008. **16**(6): p. 833-4.
79. Hamza, I., et al., *The metallochaperone Atox1 plays a critical role in perinatal copper homeostasis.* Proc Natl Acad Sci USA, 2001. **98**(12): p. 6848-52.
80. Hamza, I., J. Prohaska, and J.D. Gitlin, *Essential role for Atox1 in the copper-mediated intracellular trafficking of the Menkes ATPase.* Proc Natl Acad Sci USA, 2003. **100**(3): p. 1215-20.
81. Dancis, A., et al., *Molecular characterization of a copper transport protein in S. cerevisiae: an unexpected role for copper in iron transport.* Cell, 1994. **76**(2): p. 393-402.
82. Kampfenkel, K., et al., *Molecular characterization of a putative Arabidopsis thaliana copper transporter and its yeast homologue.* J Biol Chem, 1995. **270**(47): p. 28479-86.
83. Knight, S.A., et al., *A widespread transposable element masks expression of a yeast copper transport gene.* Genes Dev, 1996. **10**(15): p. 1917-29.
84. Zhou, B. and J. Gitschier, *hCTR1: a human gene for copper uptake identified by complementation in yeast.* Proc Natl Acad Sci USA, 1997. **94**(14): p. 7481-6.
85. Eisses, J.F. and J.H. Kaplan, *Molecular characterization of hCTR1, the human copper uptake protein.* J Biol Chem, 2002. **277**(32): p. 29162-71.
86. Lee, J., et al., *Biochemical characterization of the human copper transporter Ctr1.* J Biol Chem, 2002. **277**(6): p. 4380-7.
87. van den Berghe, P.V., et al., *Human copper transporter 2 is localized in late endosomes and lysosomes and facilitates cellular copper uptake.* Biochem J, 2007. **407**(1): p. 49-59.
88. Kuo, Y.M., et al., *The copper transporter CTR1 provides an essential function in mammalian embryonic development.* Proc Natl Acad Sci USA, 2001. **98**(12): p. 6836-41.
89. Lee, J., J.R. Prohaska, and D.J. Thiele, *Essential role for mammalian copper transporter Ctr1 in copper homeostasis and embryonic development.* Proc Natl Acad Sci USA, 2001. **98**(12): p. 6842-7.
90. Haremaki, T., et al., *Vertebrate Ctr1 coordinates morphogenesis and progenitor cell fate and regulates embryonic stem cell differentiation.* Proc Natl Acad Sci USA, 2007. **104**(29): p. 12029-34.
91. Lee, J., M.J. Petris, and D.J. Thiele, *Characterization of mouse embryonic cells deficient in the ctr1 high affinity copper transporter. Identification of a Ctr1-independent copper transport system.* J Biol Chem, 2002. **277**(43): p. 40253-9.
92. Kim, H., et al., *Deletion of Hepatic Ctr1 Reveals Its Function in Copper Acquisition and Compensatory Mechanisms for Copper Homeostasis.* Am J Physiol Gastrointest Liver Physiol, 2008.
93. Nose, Y., B.E. Kim, and D.J. Thiele, *Ctr1 drives intestinal copper absorption and is essential for growth, iron metabolism, and neonatal cardiac function.* Cell Metab, 2006. **4**(3): p. 235-44.
94. Guo, Y., et al., *Identification of methionine-rich clusters that regulate copper-stimulated endocytosis of the human Ctr1 copper transporter.* J Biol Chem, 2004. **279**(17): p. 17428-33.
95. Klomp, A.E., et al., *The Aminoterminus of the human copper transporter 1 (hCTR1) is localized extracellularly, and interacts with itself.* Biochem J, 2003. **370**(Pt 3): p. 881-9.
96. Puig, S., et al., *Biochemical and genetic analyses of yeast and human high affinity copper transporters suggest a conserved mechanism for copper uptake.* J Biol Chem, 2002. **277**(29): p. 26021-30.
97. Maryon, E.B., S.A. Molloy, and J.H. Kaplan, *O-linked glycosylation at threonine 27 protects the copper transporter hCTR1 from proteolytic cleavage in mammalian cells.* J Biol Chem, 2007. **282**(28): p. 20376-87.
98. Eisses, J.F. and J.H. Kaplan, *The mechanism of copper uptake mediated by human CTR1: a mutational analysis.* J Biol Chem, 2005. **280**(44): p. 37159-68.
99. Aller, S.G., et al., *Eukaryotic CTR copper uptake transporters require two faces of the third transmembrane domain for helix packing, oligomerization, and function.* J Biol Chem, 2004. **279**(51): p. 53435-41.
100. Aller, S.G. and V.M. Unger, *Projection structure of the human copper transporter CTR1 at 6-A resolution reveals a compact trimer with a novel channel-like architecture.* Proc Natl Acad Sci USA, 2006. **103**(10): p. 3627-32.
101. Russ, W.P. and D.M. Engelman, *The GxxxG motif: a framework for transmembrane helix-helix association.* J Mol Biol, 2000. **296**(3): p. 911-9.
102. Senes, A., M. Gerstein, and D.M. Engelman, *Statistical analysis of amino acid patterns in transmembrane helices: the GxxxG motif occurs frequently and in association with beta-branched residues at neighboring positions.* J Mol Biol, 2000. **296**(3): p. 921-36.
103. Liou, J., et al., *Live-cell imaging reveals sequential oligomerization and local plasma membrane targeting of stromal interaction molecule 1 after Ca2+ store depletion.* Proc Natl Acad Sci U S A, 2007. **104**(22): p. 9301-6.
104. Laffray, S., et al., *Dissociation and trafficking of rat GABAB receptor heterodimer upon chronic capsaicin stimulation.* Eur J Neurosci, 2007. **25**(5): p. 1402-16.
105. Klomp, A.E., et al., *Biochemical characterization and subcellular localization of human copper transporter 1 (hCTR1).* Biochem J, 2002. **364**(Pt 2): p. 497-505.
106. Linder, M.C., *Biochemistry of Copper*. 1991: Springer; 1 edition (Oct 31 1991).
107. Kuo, Y.M., et al., *Copper transport protein (Ctr1) levels in mice are tissue specific and dependent on copper status.* J Nutr, 2006. **136**(1): p. 21-6.

108. Zimnicka, A.M., E.B. Maryon, and J.H. Kaplan, *Human copper transporter hCTR1 mediates basolateral uptake of copper into enterocytes: implications for copper homeostasis.* J Biol Chem, 2007. **282**(36): p. 26471-80.
109. Bertinato, J., et al., *Ctr2 is partially localized to the plasma membrane and stimulates copper uptake in COS-7 cells.* Biochem J, 2008. **409**(3): p. 731-40.
110. Gunshin, H., et al., *Cloning and characterization of a mammalian proton-coupled metal-ion transporter.* Nature, 1997. **388**(6641): p. 482-8.
111. Canonne-Hergaux, F., et al., *The Nramp2/DMT1 iron transporter is induced in the duodenum of microcytic anemia mk mice but is not properly targeted to the intestinal brush border.* Blood, 2000. **96**(12): p. 3964-70.
112. Southon, A., et al., *Malvolio is a copper transporter in Drosophila melanogaster.* J Exp Biol, 2008. **211**(Pt 5): p. 709-16.
113. Turski, M.L. and D.J. Thiele, *Drosophila Ctr1A functions as a copper transporter essential for development.* J Biol Chem, 2007. **282**(33): p. 24017-26.
114. Zhou, H., K.M. Cadigan, and D.J. Thiele, *A copper-regulated transporter required for copper acquisition, pigmentation, and specific stages of development in Drosophila melanogaster.* J Biol Chem, 2003. **278**(48): p. 48210-8.
115. Arredondo, M., et al., *DMT1, a physiologically relevant apical Cu1+ transporter of intestinal cells.* Am J Physiol, Cell Physiol, 2003. **284**(6): p. C1525-30.
116. Fleming, M.D., et al., *Nramp2 is mutated in the anemic Belgrade (b) rat: evidence of a role for Nramp2 in endosomal iron transport.* Proc Natl Acad Sci USA, 1998. **95**(3): p. 1148-53.
117. Beaumont, C., et al., *Two new human DMT1 gene mutations in a patient with microcytic anemia, low ferritinemia, and liver iron overload.* Blood, 2006. **107**(10): p. 4168-70.
118. Iolascon, A., et al., *Microcytic anemia and hepatic iron overload in a child with compound heterozygous mutations in DMT1 (SCL11A2).* Blood, 2006. **107**(1): p. 349-54.
119. Mims, M.P., et al., *Identification of a human mutation of DMT1 in a patient with microcytic anemia and iron overload.* Blood, 2005. **105**(3): p. 1337-42.
120. Ohgami, R.S., et al., *The Steap proteins are metalloreductases.* Blood, 2006. **108**(4): p. 1388-94.
121. McKie, A.T., et al., *An iron-regulated ferric reductase associated with the absorption of dietary iron.* Science, 2001. **291**(5509): p. 1755-9.
122. Wyman, S., et al., *Dcytb (Cybrd1) functions as both a ferric and a cupric reductase in vitro.* FEBS Lett, 2008. **582**(13): p. 1901-6.
123. Rees, E.M. and D.J. Thiele, *Identification of a vacuole-associated metalloreductase and its role in Ctr2-mediated intracellular copper mobilization.* J Biol Chem, 2007. **282**(30): p. 21629-38.
124. Mena, N.P., et al., *Hepcidin inhibits apical iron uptake in intestinal cells.* Am J Physiol Gastrointest Liver Physiol, 2008. **294**(1): p. G192-8.
125. Nicolas, G., et al., *Lack of hepcidin gene expression and severe tissue iron overload in upstream stimulatory factor 2 (USF2) knockout mice.* Proc Natl Acad Sci U S A, 2001. **98**(15): p. 8780-5.
126. Pigeon, C., et al., *A new mouse liver-specific gene, encoding a protein homologous to human antimicrobial peptide hepcidin, is overexpressed during iron overload.* J Biol Chem, 2001. **276**(11): p. 7811-9.
127. Leary, S.C., D.R. Winge, and P.A. Cobine, *"Pulling the plug" on cellular copper: The role of mitochondria in copper export.* Biochim Biophys Acta, 2008.
128. Muller, P., et al., *Gene expression profiling of liver cells after copper overload in vivo and in vitro reveals new copper-regulated genes.* J Biol Inorg Chem, 2007. **12**(4): p. 495-507.
129. Lee, J., et al., *Isolation of a murine copper transporter gene, tissue specific expression and functional complementation of a yeast copper transport mutant.* Gene, 2000. **254**(1-2): p. 87-96.
130. Yuzbasiyan-Gurkan, V., et al., *Treatment of Wilson's disease with zinc: X. Intestinal metallothionein induction.* J Lab Clin Med, 1992. **120**(3): p. 380-6.
131. Irato, P. and V. Albergoni, *Interaction between copper and zinc in metal accumulation in rats with particular reference to the synthesis of induced-metallothionein.* Chem Biol Interact, 2005. **155**(3): p. 155-64.
132. Santon, A., et al., *Effect and possible role of Zn treatment in LEC rats, an animal model of Wilson's disease.* Biochim Biophys Acta, 2003. **1637**(1): p. 91-7.
133. Zhang, B., et al., *Activity of metal-responsive transcription factor 1 by toxic heavy metals and H2O2 in vitro is modulated by metallothionein.* Mol Cell Biol, 2003. **23**(23): p. 8471-85.
134. Gonzalez, B.P., et al., *Zinc supplementation decreases hepatic copper accumulation in LEC rat: a model of Wilson's disease.* Biol Trace Elem Res, 2005. **105**(1-3): p. 117-34.
135. Klein, D., et al., *Association of copper to metallothionein in hepatic lysosomes of Long-Evans cinnamon (LEC) rats during the development of hepatitis [se e comments].* Eur J Clin Invest, 1998. **28**(4): p. 302-10.
136. Klein, D., et al., *Binding of Cu to metallothionein in tissues of the LEC rat with inherited abnormal copper accumulation.* Arch Toxicol, 1997. **71**(5): p. 340-3.
137. Hung, I.H., et al., *Biochemical characterization of the Wilson disease protein and functional expression in the yeast Saccharomyces cerevisiae.* J Biol Chem, 1997. **272**(34): p. 21461-6.
138. Bartee, M.Y. and S. Lutsenko, *Hepatic copper-transporting ATPase ATP7B: function and inactivation at the molecular and cellular level.* Biometals, 2007. **20**(3-4): p. 627-37.
139. Fanni, D., et al., *Expression of ATP7B in normal human liver.* Eur J Histochem, 2005. **49**(4): p. 371-8.
140. Guo, Y., et al., *NH2-terminal signals in ATP7B Cu-ATPase mediate its Cu-dependent anterograde traffic in polarized hepatic cells.* Am J Physiol Gastrointest Liver Physiol, 2005. **289**(5): p. G904-16.
141. Roelofsen, H., et al., *Copper-induced apical trafficking of ATP7B in polarized hepatoma cells provides a mechanism for biliary copper excretion.* Gastroenterology, 2000. **119**(3): p. 782-93.

142. Cater, M.A., et al., *ATP7B mediates vesicular sequestration of copper: insight into biliary copper excretion.* Gastroenterology, 2006. **130**(2): p. 493-506.
143. Schaefer, M., et al., *Hepatocyte-specific localization and copper-dependent trafficking of the Wilson's disease protein in the liver.* Am J Physiol, 1999. **276**(3 Pt 1): p. G639-46.
144. Petris, M.J. and J.F. Mercer, *The Menkes protein (ATP7A; MNK) cycles via the plasma membrane both in basal and elevated extracellular copper using a Carboxyterminal di-leucine endocytic signal.* Hum Mol Genet, 1999. **8**(11): p. 2107-15.
145. de Bie, P., et al., *Molecular pathogenesis of Wilson and Menkes disease: correlation of mutations with molecular defects and disease phenotypes.* J Med Genet, 2007. **44**(11): p. 673-88.
146. Stapelbroek, J.M., et al., *The H1069Q mutation in ATP7B is associated with late and neurologic presentation in Wilson disease: results of a meta-analysis.* J Hepatol, 2004. **41**(5): p. 758-63.
147. Payne, A.S. and J.D. Gitlin, *Functional expression of the menkes disease protein reveals common biochemical mechanisms among the copper-transporting P-type ATPases.* J Biol Chem, 1998. **273**(6): p. 3765-70.
148. Camakaris, J., et al., *Gene amplification of the Menkes (MNK; ATP7A) P-type ATPase gene of CHO cells is associated with copper resistance and enhanced copper efflux.* Hum Mol Genet, 1995. **4**(11): p. 2117-23.
149. Katano, K., et al., *The copper export pump ATP7B modulates the cellular pharmacology of carboplatin in ovarian carcinoma cells.* Mol Pharmacol, 2003. **64**(2): p. 466-73.
150. La Fontaine, S., et al., *Functional analysis and intracellular localization of the human menkes protein (MNK) stably expressed from a cDNA construct in Chinese hamster ovary cells (CHO-K1).* Hum Mol Genet, 1998. **7**(8): p. 1293-300.
151. Hung, Y.H., et al., *Purification and membrane reconstitution of catalytically active Menkes copper-transporting P-type ATPase (MNK; ATP7A).* Biochem J, 2007. **401**(2): p. 569-79.
152. Voskoboinik, I., et al., *ATP-dependent copper transport by the Menkes protein in membrane vesicles isolated from cultured Chinese hamster ovary cells.* FEBS Lett, 1998. **435**(2-3): p. 178-82.
153. Voskoboinik, I., et al., *Functional studies on the Wilson copper P-type ATPase and toxic milk mouse mutant.* Biochem Biophys Res Commun, 2001. **281**(4): p. 966-70.
154. Kuhlbrandt, W., *Biology, structure and mechanism of P-type ATPases.* Nat Rev Mol Cell Biol, 2004. **5**(4): p. 282-95.
155. Banci, L., et al., *The different intermolecular interactions of the soluble copper-binding domains of the menkes protein, ATP7A.* J Biol Chem, 2007. **282**(32): p. 23140-6.
156. Banci, L., et al., *Solution structure and intermolecular interactions of the third metal-binding domain of ATP7A, the Menkes disease protein.* J Biol Chem, 2006. **281**(39): p. 29141-7.
157. Banci, L., et al., *An NMR study of the interaction between the human copper(I) chaperone and the second and fifth metal-binding domains of the Menkes protein.* FEBS J, 2005. **272**(3): p. 865-71.
158. Banci, L., et al., *Solution structure and backbone dynamics of the Cu(I) and apo forms of the second metal-binding domain of the Menkes protein ATP7A.* Biochemistry, 2004. **43**(12): p. 3396-403.
159. DeSilva, T.M., G. Veglia, and S.J. Opella, *Solution structures of the reduced and Cu(I) bound forms of the first metal binding sequence of ATP7A associated with Menkes disease.* Proteins, 2005. **61**(4): p. 1038-49.
160. Jensen, P.Y., et al., *Investigation of the copper binding sites in the Menkes disease protein, ATP7A. SSIEM Award. Society of the Study of Inborn Errors of Metabolism.* J Inherit Metab Dis, 1998. **21**(3): p. 195-8.
161. Jones, C.E., et al., *Structure and metal binding studies of the second copper binding domain of the Menkes ATPase.* J Struct Biol, 2003. **143**(3): p. 209-18.
162. Myari, A., et al., *Copper(I) interaction with model peptides of WD6 and TM6 domains of Wilson ATPase: regulatory and mechanistic implications.* J Inorg Biochem, 2004. **98**(9): p. 1483-94.
163. DiDonato, M., et al., *Expression, purification, and metal binding properties of the N-terminal domain from the wilson disease putative copper-transporting ATPase (ATP7B).* J Biol Chem, 1997. **272**(52): p. 33279-82.
164. Lutsenko, S., et al., *N-terminal domains of human copper-transporting adenosine triphosphatases (the Wilson's and Menkes disease proteins) bind copper selectively in vivo and in vitro with stoichiometry of one copper per metal-binding repeat.* J Biol Chem, 1997. **272**(30): p. 18939-44.
165. Cater, M.A., et al., *Intracellular trafficking of the human Wilson protein: the role of the six N-terminal metal-binding sites.* Biochem J, 2004. **380**(Pt 3): p. 805-13.
166. Cater, M.A., S. La Fontaine, and J.F. Mercer, *Copper binding to the N-terminal metal-binding sites or the CPC motif is not essential for copper-induced trafficking of the human Wilson protein (ATP7B).* Biochem J, 2007. **401**(1): p. 143-53.
167. Forbes, J.R. and D.W. Cox, *Copper-dependent trafficking of Wilson disease mutant ATP7B proteins.* Hum Mol Genet, 2000. **9**(13): p. 1927-35.
168. Forbes, J.R., G. Hsi, and D.W. Cox, *Role of the copper-binding domain in the copper transport function of ATP7B, the P-type ATPase defective in Wilson disease.* J Biol Chem, 1999. **274**(18): p. 12408-13.
169. Goodyer, I.D., et al., *Characterization of the Menkes protein copper-binding domains and their role in copper-induced protein relocalization.* Hum Mol Genet, 1999. **8**(8): p. 1473-8.
170. Greenough, M., et al., *Signals regulating trafficking of Menkes (MNK; ATP7A) copper-translocating P-type ATPase in polarized MDCK cells.* Am J Physiol Cell Physiol, 2004. **287**(5): p. C1463-71.
171. Huster, D. and S. Lutsenko, *The distinct roles of the N-terminal copper-binding sites in regulation of catalytic activity of the Wilson's disease protein.* J Biol Chem, 2003. **278**(34): p. 32212-8.
172. Mercer, J.F., et al., *Copper-induced trafficking of the cU-ATPases: a key mechanism for copper homeostasis.* Biometals, 2003. **16**(1): p. 175-84.
173. Petris, M.J., et al., *Copper-regulated trafficking of the Menkes disease copper ATPase is associated with formation of a phosphorylated catalytic intermediate.* J Biol Chem, 2002. **277**(48): p. 46736-42.
174. Strausak, D., et al., *The role of GMXCXXC metal binding sites in the copper-induced redistribution of the Menkes protein.* J Biol Chem,

1999. **274**(16): p. 11170-7.

175. Voskoboinik, I., et al., *The regulation of catalytic activity of the menkes copper-translocating P-type ATPase. Role of high affinity copper-binding sites.* J Biol Chem, 2001. **276**(30): p. 28620-7.
176. Mandal, A.K. and J.M. Arguello, *Functional roles of metal binding domains of the Archaeoglobus fulgidus Cu(+)-ATPase CopA.* Biochemistry, 2003. **42**(37): p. 11040-7.
177. Mandal, A.K., et al., *Identification of the transmembrane metal binding site in Cu+-transporting PIB-type ATPases.* J Biol Chem, 2004. **279**(52): p. 54802-7.
178. Cobbold, C., et al., *The Menkes disease ATPase (ATP7A) is internalized via a Rac1-regulated, clathrin- and caveolae-independent pathway.* Hum Mol Genet, 2003. **12**(13): p. 1523-33.
179. Albers, R.W., *Biochemical aspects of active transport.* Annu Rev Biochem, 1967. **36**: p. 727-56.
180. Post, R.L., C. Hegyvary, and S. Kume, *Activation by adenosine triphosphate in the phosphorylation kinetics of sodium and potassium ion transport adenosine triphosphatase.* J Biol Chem, 1972. **247**(20): p. 6530-40.
181. Toyoshima, C., H. Nomura, and T. Tsuda, *Lumenal gating mechanism revealed in calcium pump crystal structures with phosphate analogues.* Nature, 2004. **432**(7015): p. 361-8.
182. Bingham, M.J., A. Burchell, and H.J. McArdle, *Identification of an ATP-dependent copper transport system in endoplasmic reticulum vesicles isolated from rat liver.* J Physiol, 1995. **482 (Pt 3)**: p. 583-7.
183. Dijkstra, M., et al., *Adenosine triphosphate-dependent copper transport in isolated rat liver plasma membranes.* J Clin Invest, 1995. **95**(1): p. 412-6.
184. Efremov, R.G., et al., *Molecular modelling of the nucleotide-binding domain of Wilson's disease protein: location of the ATP-binding site, domain dynamics and potential effects of the major disease mutations.* Biochem J, 2004. **382**(Pt 1): p. 293-305.
185. Dmitriev, O., et al., *Solution structure of the N-domain of Wilson disease protein: distinct nucleotide-binding environment and effects of disease mutations.* Proc Natl Acad Sci U S A, 2006. **103**(14): p. 5302-7.
186. Morgan, C.T., et al., *The distinct functional properties of the nucleotide-binding domain of ATP7B, the human copper-transporting ATPase: analysis of the Wilson disease mutations E1064A, H1069Q, R1151H, and C1104F.* J Biol Chem, 2004. **279**(35): p. 36363-71.
187. Tsivkovskii, R., B.C. MacArthur, and S. Lutsenko, *The Lys1010-Lys1325 fragment of the Wilson's disease protein binds nucleotides and interacts with the N-terminal domain of this protein in a copper-dependent manner.* J Biol Chem, 2001. **276**(3): p. 2234-42.
188. Klomp, L.W., et al., *Identification and functional expression of HAH1, a novel human gene involved in copper homeostasis.* J Biol Chem, 1997. **272**(14): p. 9221-6.
189. Banci, L., et al., *Understanding copper trafficking in bacteria: interaction between the copper transport protein CopZ and the N-terminal domain of the copper ATPase CopA from Bacillus subtilis.* Biochemistry, 2003. **42**(7): p. 1939-49.
190. Multhaup, G., et al., *Interaction of the CopZ copper chaperone with the CopA copper ATPase of Enterococcus hirae assessed by surface plasmon resonance.* Biochem Biophys Res Commun, 2001. **288**(1): p. 172-7.
191. Radford, D.S., et al., *CopZ from Bacillus subtilis interacts in vivo with a copper exporting CPx-type ATPase CopA.* FEMS Microbiol Lett, 2003. **220**(1): p. 105-12.
192. Yatsunyk, L.A. and A.C. Rosenzweig, *Cu(I) binding and transfer by the N terminus of the Wilson disease protein.* J Biol Chem, 2007. **282**(12): p. 8622-31.
193. Achila, D., et al., *Structure of human Wilson protein domains 5 and 6 and their interplay with domain 4 and the copper chaperone HAH1 in copper uptake.* Proc Natl Acad Sci U S A, 2006. **103**(15): p. 5729-34.
194. Walker, J.M., et al., *The N-terminal metal-binding site 2 of the Wilson's Disease Protein plays a key role in the transfer of copper from Atox1.* J Biol Chem, 2004. **279**(15): p. 15376-84.
195. Huster, D., et al., *Defective cellular localization of mutant ATP7B in Wilson's disease patients and hepatoma cell lines.* Gastroenterology, 2003. **124**(2): p. 335-45.
196. Yang, X.L., et al., *Two forms of Wilson disease protein produced by alternative splicing are localized in distinct cellular compartments.* Biochem J, 1997. **326 (Pt 3)**: p. 897-902.
197. La Fontaine, S., et al., *Effect of the toxic milk mutation (tx) on the function and intracellular localization of Wnd, the murine homologue of the Wilson copper ATPase.* Hum Mol Genet, 2001. **10**(4): p. 361-70.
198. Francis, M.J., et al., *A Golgi localization signal identified in the Menkes recombinant protein.* Hum Mol Genet, 1998. **7**(8): p. 1245-52.
199. Hardman, B., et al., *Expression, localisation and hormone regulation of the human copper transporter hCTR1 in placenta and choriocarcinoma Jeg-3 cells.* Placenta, 2006. **27**(9-10): p. 968-77.
200. Hardman, B., et al., *Hormonal regulation of the Menkes and Wilson copper-transporting ATPases in human placental Jeg-3 cells.* Biochem J, 2007. **402**(2): p. 241-50.
201. Harada, M., et al., *The Wilson disease protein ATP7B resides in the late endosomes with Rab7 and the Niemann-Pick C1 protein.* Am J Pathol, 2005. **166**(2): p. 499-510.
202. Harada, M., et al., *Wilson disease protein ATP7B is localized in the late endosomes in a polarized human hepatocyte cell line.* Int J Mol Med, 2003. **11**(3): p. 293-8.
203. Harada, M., et al., *Copper does not alter the intracellular distribution of ATP7B, a copper-transporting ATPase.* Biochem Biophys Res Commun, 2000. **275**(3): p. 871-6.
204. Hernandez, S., et al., *ATP7B copper-regulated traffic and association with the tight junctions: copper excretion into the bile.* Gastroenterology, 2008. **134**(4): p. 1215-23.
205. Hubbard, A.L. and L.T. Braiterman, *Could ATP7B export Cu(I) at the tight junctions and the apical membrane?* Gastroenterology, 2008. **134**(4): p. 1255-7.
206. Schaefer, M. and J.D. Gitlin, *Genetic disorders of membrane transport. IV. Wilson's disease and Menkes disease.* Am J Physiol, 1999. **276**(2 Pt 1): p. G311-4.

207. Braiterman, L.T., et al., *Apical targeting and Golgi retention signals reside within a 9 amino acid sequence in the copper-ATPase, ATP7B.* Am J Physiol Gastrointest Liver Physiol, 2008.
208. Schaefer, M., et al., *Localization of the Wilson's disease protein in human liver.* Gastroenterology, 1999. **117**(6): p. 1380-5.
209. Petris, M.J., et al., *A Carboxyterminal di-leucine is required for localization of the Menkes protein in the trans-Golgi network.* Hum Mol Genet, 1998. **7**(13): p. 2063-71.
210. Lane, C., et al., *Studies on endocytic mechanisms of the Menkes copper-translocating P-type ATPase (ATP7A; MNK). Endocytosis of the Menkes protein.* Biometals, 2004. **17**(1): p. 87-98.
211. Clarke, D.M., T.W. Loo, and D.H. MacLennan, *Functional consequences of mutations of conserved amino acids in the beta-strand domain of the Ca2(+)-ATPase of sarcoplasmic reticulum.* J Biol Chem, 1990. **265**(24): p. 14088-92.
212. Vanderwerf, S.M., et al., *Copper specifically regulates intracellular phosphorylation of the Wilson's disease protein, a human copper-transporting ATPase.* J Biol Chem, 2001. **276**(39): p. 36289-94.
213. Vanderwerf, S.M. and S. Lutsenko, *The Wilson's disease protein expressed in Sf9 cells is phosphorylated.* Biochem Soc Trans, 2002. **30**(4): p. 739-41.
214. Schlief, M.L., A.M. Craig, and J.D. Gitlin, *NMDA receptor activation mediates copper homeostasis in hippocampal neurons.* J Neurosci, 2005. **25**(1): p. 239-46.
215. Schlief, M.L., et al., *Role of the Menkes copper-transporting ATPase in NMDA receptor-mediated neuronal toxicity.* Proc Natl Acad Sci USA, 2006. **103**(40): p. 14919-24.
216. Richardson, D.R. and Y. Suryo Rahmanto, *Differential regulation of the Menkes and Wilson disease copper transporters by hormones: an integrated model of metal transport in the placenta.* Biochem J, 2007. **402**(2): p. e1-3.
217. de Bie, P., et al., *Distinct Wilson's disease mutations in ATP7B are associated with enhanced binding to COMMD1 and reduced stability of ATP7B.* Gastroenterology, 2007. **133**(4): p. 1316-26.
218. Sanokawa-Akakura, R., et al., *A novel role for the immunophilin FKBP52 in copper transport.* J Biol Chem, 2004. **279**(27): p. 27845-8.
219. McLaughlin, S.H., H.W. Smith, and S.E. Jackson, *Stimulation of the weak ATPase activity of human hsp90 by a client protein.* J Mol Biol, 2002. **315**(4): p. 787-98.
220. Lim, C.M., et al., *Copper-dependent interaction of dynactin subunit p62 with the N terminus of ATP7B but not ATP7A.* J Biol Chem, 2006. **281**(20): p. 14006-14.
221. Lim, C.M., et al., *Copper-dependent interaction of glutaredoxin with the N termini of the copper-ATPases (ATP7A and ATP7B) defective in Menkes and Wilson diseases.* Biochem Biophys Res Commun, 2006. **348**(2): p. 428-36.
222. Stephenson, S.E., et al., *A single PDZ domain protein interacts with the Menkes copper ATPase, ATP7A. A new protein implicated in copper homeostasis.* J Biol Chem, 2005. **280**(39): p. 33270-9.
223. Schroer, T.A., *Dynactin.* Annu Rev Cell Dev Biol, 2004. **20**: p. 759-79.
224. van de Sluis, B., et al., *Refined genetic and comparative physical mapping of the canine copper toxicosis locus.* Mamm Genome, 2000. **11**(6): p. 455-60.
225. van De Sluis, B., et al., *Identification of a new copper metabolism gene by positional cloning in a purebred dog population.* Hum Mol Genet, 2002. **11**(2): p. 165-73.
226. van de Sluis, B.J., et al., *Genetic mapping of the copper toxicosis locus in Bedlington terriers to dog chromosome 10, in a region syntenic to human chromosome region 2p13-p16.* Hum Mol Genet, 1999. **8**(3): p. 501-7.
227. van de Sluis, B., et al., *Increased activity of hypoxia-inducible factor 1 is associated with early embryonic lethality in Commd1 null mice.* Mol Cell Biol, 2007. **27**(11): p. 4142-56.
228. Narindrasorasak, S., et al., *Characterization and copper binding properties of human COMMD1 (MURR1).* Biochemistry, 2007. **46**(11): p. 3116-28.
229. Tao, T.Y., et al., *The copper toxicosis gene product Murr1 directly interacts with the Wilson disease protein.* J Biol Chem, 2003. **278**(43): p. 41593-6.
230. Burstein, E., et al., *A novel role for XIAP in copper homeostasis through regulation of MURR1.* EMBO J, 2004. **23**(1): p. 244-54.
231. Maine, G.N., et al., *COMMD1 expression is controlled by critical residues that determine XIAP binding.* Biochem J, 2009. **417**(2): p. 601-9.
232. Spee, B., et al., *Functional consequences of RNA interference targeting COMMD1 in a canine hepatic cell line in relation to copper toxicosis.* Anim Genet, 2007. **38**(2): p. 168-70.
233. Burstein, E., et al., *COMMD proteins, a novel family of structural and functional homologs of MURR1.* J Biol Chem, 2005. **280**(23): p. 22222-32.
234. de Bie, P., et al., *The many faces of the copper metabolism protein MURR1/COMMD1.* J Hered, 2005. **96**(7): p. 803-11.
235. Maine, G.N. and E. Burstein, *COMMD proteins and the control of the NF kappa B pathway.* Cell Cycle, 2007. **6**(6): p. 672-6.
236. Maine, G.N., et al., *COMMD1 promotes the ubiquitination of NF-kappaB subunits through a cullin-containing ubiquitin ligase.* EMBO J, 2007. **26**(2): p. 436-47.
237. Culotta, V.C., et al., *Intracellular pathways of copper trafficking in yeast and humans.* Adv Exp Med Biol, 1999. **448**: p. 247-54.
238. Himelblau, E. and R.M. Amasino, *Delivering copper within plant cells.* Curr Opin Plant Biol, 2000. **3**(3): p. 205-10.
239. Casareno, R.L., D. Waggoner, and J.D. Gitlin, *The copper chaperone CCS directly interacts with copper/zinc superoxide dismutase.* J Biol Chem, 1998. **273**(37): p. 23625-8.
240. Mercer, J.F., et al., *Isolation of a partial candidate gene for Menkes disease by positional cloning.* Nat Genet, 1993. **3**(1): p. 20-5.
241. Petris, M.J., *The SLC31 (Ctr) copper transporter family.* Pflugers Arch, 2004. **447**(5): p. 752-5.
242. Eisses, J.F., Y. Chi, and J.H. Kaplan, *Stable plasma membrane levels of hCTR1 mediate cellular copper uptake.* J Biol Chem, 2005. **280**(10): p. 9635-9.

243. Pena, M.M., J. Lee, and D.J. Thiele, *A delicate balance: homeostatic control of copper uptake and distribution.* J Nutr, 1999. **129**(7): p. 1251-60.
244. Puig, S. and D.J. Thiele, *Molecular mechanisms of copper uptake and distribution.* Current opinion in chemical biology, 2002. **6**(2): p. 171-80.
245. Mosmann, T., *Rapid colorimetric assay for cellular growth and survival: application to proliferation and cytotoxicity assays.* J Immunol Methods, 1983. **65**(1-2): p. 55-63.
246. Westin, G., et al., *OVEC, a versatile system to study transcription in mammalian cells and cell-free extracts.* Nucleic Acids Res, 1987. **15**(17): p. 6787-98.
247. de Bie, P., et al., *Characterization of COMMD protein-protein interactions in NF-kappaB signalling.* Biochem J, 2006. **398**(1): p. 63-71.
248. Shibata, T., A.J. Giaccia, and J.M. Brown, *Development of a hypoxia-responsive vector for tumor-specific gene therapy.* Gene Ther, 2000. **7**(6): p. 493-8.
249. Palmiter, R.D., *Regulation of metallothionein genes by heavy metals appears to be mediated by a zinc-sensitive inhibitor that interacts with a constitutively active transcription factor, MTF-1.* Proc Natl Acad Sci U S A, 1994. **91**(4): p. 1219-23.
250. Murphy, B.J., et al., *Activation of metallothionein gene expression by hypoxia involves metal response elements and metal transcription factor-1.* Cancer Res, 1999. **59**(6): p. 1315-22.
251. Poss, K.D. and S. Tonegawa, *Reduced stress defense in heme oxygenase 1-deficient cells.* Proc Natl Acad Sci U S A, 1997. **94**(20): p. 10925-30.
252. Bianchi, L., L. Tacchini, and G. Cairo, *HIF-1-mediated activation of transferrin receptor gene transcription by iron chelation.* Nucleic Acids Res, 1999. **27**(21): p. 4223-7.
253. Zeng, L., et al., *A selective turn-on fluorescent sensor for imaging copper in living cells.* J Am Chem Soc, 2006. **128**(1): p. 10-1.
254. Rees, E.M., J. Lee, and D.J. Thiele, *Mobilization of intracellular copper stores by the ctr2 vacuolar copper transporter.* J Biol Chem, 2004. **279**(52): p. 54221-9.
255. Bellemare, D.R., et al., *Ctr6, a vacuolar membrane copper transporter in Schizosaccharomyces pombe.* J Biol Chem, 2002. **277**(48): p. 46676-86.
256. Sternlieb, I., et al., *Lysosomal defect of hepatic copper excretion in Wilson's disease (hepatolenticular degeneration).* Gastroenterology, 1973. **64**(1): p. 99-105.
257. Terada, K., et al., *Biliary excretion of copper in LEC rat after introduction of copper transporting P-type ATPase, ATP7B.* FEBS Lett, 1999. **448**(1): p. 53-6.
258. Haywood, S., et al., *Pathobiology of copper-induced injury in Bedlington terriers: ultrastructural and microanalytical studies.* Anal Cell Pathol, 1996. **10**(3): p. 229-41.
259. MacDiarmid, C.W., L.A. Gaither, and D. Eide, *Zinc transporters that regulate vacuolar zinc storage in Saccharomyces cerevisiae.* Embo J, 2000. **19**(12): p. 2845-55.
260. Kim, B.E., et al., *Zn2+-stimulated endocytosis of the mZIP4 zinc transporter regulates its location at the plasma membrane.* J Biol Chem, 2004. **279**(6): p. 4523-30.
261. Wang, F., et al., *Zinc-stimulated endocytosis controls activity of the mouse ZIP1 and ZIP3 zinc uptake transporters.* J Biol Chem, 2004. **279**(23): p. 24631-9.
262. Touret, N., et al., *Dynamic traffic through the recycling compartment couples the metal transporter Nramp2 (DMT1) with the transferrin receptor.* J Biol Chem, 2003. **278**(28): p. 25548-57.
263. Dancis, A., et al., *The Saccharomyces cerevisiae copper transport protein (Ctr1p). Biochemical characterization, regulation by copper, and physiologic role in copper uptake.* J Biol Chem, 1994. **269**(41): p. 25660-7.
264. Spencer, R.H. and D.C. Rees, *The alpha-helix and the organization and gating of channels.* Annu Rev Biophys Biomol Struct, 2002. **31**: p. 207-33.
265. Corbeil, R.R. and S.R. Searle, *Restricted maximum likelihood (REML) estimation of variance components in the mixed model.* Technometrics, 1976. **18**: p. 31-38.
266. De Feo, C.J., S.G. Aller, and V.M. Unger, *A structural perspective on copper uptake in eukaryotes.* Biometals, 2007. **20**(3-4): p. 705-16.
267. Barwe, S.P., et al., *Janus model of the Na,K-ATPase beta-subunit transmembrane domain: distinct faces mediate alpha/beta assembly and beta-beta homo-oligomerization.* J Mol Biol, 2007. **365**(3): p. 706-14.
268. Horschitz, S., T. Lau, and P. Schloss, *Glycine residues G338 and G342 are important determinants for serotonin transporter dimerisation and cell surface expression.* Neurochem Int, 2008. **52**(4-5): p. 770-5.
269. Kim, S., et al., *Transmembrane glycine zippers: physiological and pathological roles in membrane proteins.* Proc Natl Acad Sci U S A, 2005. **102**(40): p. 14278-83.
270. Penna, A., et al., *The CRAC channel consists of a tetramer formed by Stim-induced dimerization of Orai dimers.* Nature, 2008. **456**(7218): p. 116-20.
271. Cairo, E.R., et al., *Impaired routing of wild type FXYD2 after oligomerisation with FXYD2-G41R might explain the dominant nature of renal hypomagnesemia.* Biochim Biophys Acta, 2008. **1778**(2): p. 398-404.
272. Hosaka, Y., et al., *Function, subcellular localization and assembly of a novel mutation of KCNJ2 in Andersen's syndrome.* J Mol Cell Cardiol, 2003. **35**(4): p. 409-15.
273. Hou, Z. and L.H. Matherly, *Oligomeric structure of the human reduced folate carrier: Identification of homo-oligomers and dominant-negative effects on carrier expression and function.* J Biol Chem, 2008.
274. Jones, H.M., K.L. Hamilton, and D.C. Devor, *Role of an S4-S5 linker lysine in the trafficking of the Ca(2+)-activated K(+) channels IK1 and SK3.* J Biol Chem, 2005. **280**(44): p. 37257-65.
275. Lopez-Gimenez, J.F., et al., *The alpha1b-adrenoceptor exists as a higher-order oligomer: effective oligomerization is required for receptor maturation, surface delivery, and function.* Mol Pharmacol, 2007. **71**(4): p. 1015-29.

276. MacKinnon, R., *Determination of the subunit stoichiometry of a voltage-activated potassium channel.* Nature, 1991. **350**(6315): p. 232-5.
277. Palty, R., et al., *Single alpha-domain constructs of the Na+/Ca2+ exchanger, NCLX, oligomerize to form a functional exchanger.* Biochemistry, 2006. **45**(39): p. 11856-66.
278. Wang, C., et al., *An alternative splicing product of the murine trpv1 gene dominant negatively modulates the activity of TRPV1 channels.* J Biol Chem, 2004. **279**(36): p. 37423-30.
279. Yerushalmi, H., M. Lebendiker, and S. Schuldiner, *Negative dominance studies demonstrate the oligomeric structure of EmrE, a multidrug antiporter from Escherichia coli.* J Biol Chem, 1996. **271**(49): p. 31044-8.
280. Davis, A.V. and T.V. O'Halloran, *A place for thioether chemistry in cellular copper ion recognition and trafficking.* Nat Chem Biol, 2008. **4**(3): p. 148-51.
281. Hill, V.A., C.A. Seymour, and P.S. Mortimer, *Pencillamine-induced elastosis perforans serpiginosa and cutis laxa in Wilson's disease.* Br J Dermatol, 2000. **142**(3): p. 560-1.
282. Medici, V., L. Rossaro, and G.C. Sturniolo, *Wilson disease--a practical approach to diagnosis, treatment and follow-up.* Dig Liver Dis, 2007. **39**(7): p. 601-9.
283. Brewer, G.J., et al., *Worsening of neurologic syndrome in patients with Wilson's disease with initial penicillamine therapy.* Arch Neurol, 1987. **44**(5): p. 490-3.
284. Brewer, G.J., et al., *Treatment of Wilson disease with ammonium tetrathiomolybdate: IV. Comparison of tetrathiomolybdate and trientine in a double-blind study of treatment of the neurologic presentation of Wilson disease.* Arch Neurol, 2006. **63**(4): p. 521-7.
285. Hoogenraad, T.U., *Paradigm shift in treatment of Wilson's disease: zinc therapy now treatment of choice.* Brain Dev, 2006. **28**(3): p. 141-6.
286. Medici, V., et al., *Diagnosis and management of Wilson's disease: results of a single center experience.* J Clin Gastroenterol, 2006. **40**(10): p. 936-41.
287. Roberts, E.A. and M.L. Schilsky, *Diagnosis and treatment of Wilson disease: an update.* Hepatology, 2008. **47**(6): p. 2089-111.
288. Czlonkowska, A., et al., *Wilson's disease-cause of mortality in 164 patients during 1992-2003 observation period.* J Neurol, 2005. **252**(6): p. 698-703.
289. Mu, T.W., et al., *Chemical and biological approaches synergize to ameliorate protein-folding diseases.* Cell, 2008. **134**(5): p. 769-81.
290. Lim, M., et al., *Modulation of deltaF508 cystic fibrosis transmembrane regulator trafficking and function with 4-phenylbutyrate and flavonoids.* Am J Respir Cell Mol Biol, 2004. **31**(3): p. 351-7.
291. Singh, O.V., H.B. Pollard, and P.L. Zeitlin, *Chemical rescue of deltaF508-CFTR mimics genetic repair in cystic fibrosis bronchial epithelial cells.* Mol Cell Proteomics, 2008. **7**(6): p. 1099-110.
292. Wang, X., et al., *Chemical and biological folding contribute to temperature-sensitive DeltaF508 CFTR trafficking.* Traffic, 2008. **9**(11): p. 1878-93.
293. Vandesompele, J., et al., *Accurate normalization of real-time quantitative RT-PCR data by geometric averaging of multiple internal control genes.* Genome Biol, 2002. **3**(7): p. RESEARCH0034.
294. Krieger, E., G. Koraimann, and G. Vriend, *Increasing the precision of comparative models with YASARA NOVA--a self-parameterizing force field.* Proteins, 2002. **47**(3): p. 393-402.
295. Banci, L., et al., *Metal binding domains 3 and 4 of the Wilson disease protein: solution structure and interaction with the copper(I) chaperone HAH1.* Biochemistry, 2008. **47**(28): p. 7423-9.
296. Hooft, R.W., et al., *Errors in protein structures.* Nature, 1996. **381**(6580): p. 272.
297. Konagurthu, A.S., et al., *MUSTANG: a multiple structural alignment algorithm.* Proteins, 2006. **64**(3): p. 559-74.
298. Notredame, C., D.G. Higgins, and J. Heringa, *T-Coffee: A novel method for fast and accurate multiple sequence alignment.* J Mol Biol, 2000. **302**(1): p. 205-17.
299. El-Sheikh, A.A., et al., *Functional role of arginine 375 in transmembrane helix 6 of multidrug resistance protein 4 (MRP4/ABCC4).* Mol Pharmacol, 2008. **74**(4): p. 964-71.
300. Bennett-Lovsey, R.M., et al., *Exploring the extremes of sequence/structure space with ensemble fold recognition in the program Phyre.* Proteins, 2008. **70**(3): p. 611-25.
301. Jones, D.T., *GenTHREADER: an efficient and reliable protein fold recognition method for genomic sequences.* J Mol Biol, 1999. **287**(4): p. 797-815.
302. Negahm, F. and S. Bibudhendra, *Insights into the mechanism of copper transport by the Wilson and Menkes disease copper-transporting ATPases.* Inorganica Chimica Acta, 2002. **339**: p. 179-187.
303. Canutescu, A.A., A.A. Shelenkov, and R.L. Dunbrack, Jr., *A graph-theory algorithm for rapid protein side-chain prediction.* Protein Sci, 2003. **12**(9): p. 2001-14.
304. Krieger, E., et al., *Making optimal use of empirical energy functions: force-field parameterization in crystal space.* Proteins, 2004. **57**(4): p. 678-83.
305. Rodriguez-Granillo, A., E. Sedlak, and P. Wittung-Stafshede, *Stability and ATP binding of the nucleotide-binding domain of the Wilson disease protein: effect of the common H1069Q mutation.* J Mol Biol, 2008. **383**(5): p. 1097-111.
306. Kumar, S., et al., *Analysis of most common mutations R778G, R778L, R778W, I1102T and H1069Q in Indian Wilson disease patients: correlation between genotype/phenotype/copper ATPase activity.* Mol Cell Biochem, 2007. **294**(1-2): p. 1-10.
307. Wang, Y., et al., *Modulating the folding of P-glycoprotein and cystic fibrosis transmembrane conductance regulator truncation mutants with pharmacological chaperones.* Mol Pharmacol, 2007. **71**(3): p. 751-8.
308. Hayashi, H. and Y. Sugiyama, *4-phenylbutyrate enhances the cell surface expression and the transport capacity of wild-type and mutated bile salt export pumps.* Hepatology, 2007. **45**(6): p. 1506-16.
309. Rubenstein, R.C. and P.L. Zeitlin, *A pilot clinical trial of oral sodium 4-phenylbutyrate (Buphenyl) in deltaF508-homozygous cystic fibrosis patients: partial restoration of nasal epithelial CFTR function.* Am J Respir Crit Care Med, 1998. **157**(2): p. 484-90.

310. Brusilow, S.W., *Phenylacetylglutamine may replace urea as a vehicle for waste nitrogen excretion.* Pediatr Res, 1991. **29**(2): p. 147-50.
311. Maestri, N.E., et al., *Prospective treatment of urea cycle disorders.* J Pediatr, 1991. **119**(6): p. 923-8.
312. Garcia-Alloza, M., et al., *Curcumin labels amyloid pathology in vivo, disrupts existing plaques, and partially restores distorted neurites in an Alzheimer mouse model.* J Neurochem, 2007. **102**(4): p. 1095-104.
313. Gondcaille, C., et al., *Phenylbutyrate up-regulates the adrenoleukodystrophy-related gene as a nonclassical peroxisome proliferator.* J Cell Biol, 2005. **169**(1): p. 93-104.
314. Barnham, K.J. and A.I. Bush, *Metals in Alzheimer's and Parkinson's diseases.* Curr Opin Chem Biol, 2008. **12**(2): p. 222-8.
315. Edison, E.S., A. Bajel, and M. Chandy, *Iron homeostasis: new players, newer insights.* Eur J Haematol, 2008. **81**(6): p. 411-24.
316. Holzer, A.K., G.H. Manorek, and S.B. Howell, *Contribution of the major copper influx transporter CTR1 to the cellular accumulation of cisplatin, carboplatin, and oxaliplatin.* Mol Pharmacol, 2006. **70**(4): p. 1390-4.
317. Yang, L., et al., *Imaging of the intracellular topography of copper with a fluorescent sensor and by synchrotron x-ray fluorescence microscopy.* Proc Natl Acad Sci U S A, 2005. **102**(32): p. 11179-84.
318. Finney, L., et al., *X-ray fluorescence microscopy reveals large-scale relocalization and extracellular translocation of cellular copper during angiogenesis.* Proc Natl Acad Sci U S A, 2007. **104**(7): p. 2247-52.
319. van Dongen, E.M., et al., *Ratiometric fluorescent sensor proteins with subnanomolar affinity for Zn(II) based on copper chaperone domains.* J Am Chem Soc, 2006. **128**(33): p. 10754-62.
320. Culotta, V.C., et al., *The copper chaperone for superoxide dismutase.* J Biol Chem, 1997. **272**(38): p. 23469-72.
321. Bertinato, J., M. Iskandar, and M.R. L'Abbe, *Copper deficiency induces the upregulation of the copper chaperone for Cu/Zn superoxide dismutase in weanling male rats.* J Nutr, 2003. **133**(1): p. 28-31.
322. Caruano-Yzermans, A.L., T.B. Bartnikas, and J.D. Gitlin, *Mechanisms of the copper-dependent turnover of the copper chaperone for superoxide dismutase.* J Biol Chem, 2006. **281**(19): p. 13581-7.
323. Prohaska, J.R., M. Broderius, and B. Brokate, *Metallochaperone for Cu,Zn-superoxide dismutase (CCS) protein but not mRNA is higher in organs from copper-deficient mice and rats.* Arch Biochem Biophys, 2003. **417**(2): p. 227-34.
324. Pena, M.M., S. Puig, and D.J. Thiele, *Characterization of the Saccharomyces cerevisiae high affinity copper transporter Ctr3.* J Biol Chem, 2000. **275**(43): p. 33244-51.
325. Ballabio, A. and V. Gieselmann, *Lysosomal disorders: From storage to cellular damage.* Biochim Biophys Acta, 2008.
326. Gitlin, D. and C.A. Janeway, *Turnover of the copper and protein moieties of ceruloplasmin.* Nature, 1960. **185**: p. 693.
327. Sternlieb, I., et al., *The Incorporation of Copper into Ceruloplasmin in Vivo: Studies with Copper and Copper.* J Clin Invest, 1961. **40**(10): p. 1834-40.
328. Gross, J.B., Jr., et al., *Biliary copper excretion by hepatocyte lysosomes in the rat. Major excretory pathway in experimental copper overload.* J Clin Invest, 1989. **83**(1): p. 30-9.
329. Klomp, L.W., et al., *Ceruloplasmin gene expression in the murine central nervous system.* J Clin Invest, 1996. **98**(1): p. 207-15.
330. Klomp, L.W. and J.D. Gitlin, *Expression of the ceruloplasmin gene in the human retina and brain: implications for a pathogenic model in aceruloplasminemia.* Hum Mol Genet, 1996. **5**(12): p. 1989-96.
331. Barnes, N., et al., *The copper-transporting ATPases, menkes and wilson disease proteins, have distinct roles in adult and developing cerebellum.* J Biol Chem, 2005. **280**(10): p. 9640-5.
332. Jeong, S.Y. and S. David, *Glycosylphosphatidylinositol-anchored ceruloplasmin is required for iron efflux from cells in the central nervous system.* J Biol Chem, 2003. **278**(29): p. 27144-8.
333. Patel, B.N., R.J. Dunn, and S. David, *Alternative RNA splicing generates a glycosylphosphatidylinositol-anchored form of ceruloplasmin in mammalian brain.* J Biol Chem, 2000. **275**(6): p. 4305-10.
334. Riordan, S.M. and R. Williams, *The Wilson's disease gene and phenotypic diversity.* J Hepatol, 2001. **34**(1): p. 165-71.
335. van de Sluis, B., et al., *COMMD1: a novel protein involved in the proteolysis of proteins.* Cell Cycle, 2007. **6**(17): p. 2091-8.
336. Robben, J.H., et al., *Rescue of vasopressin V2 receptor mutants by chemical chaperones: specificity and mechanism.* Mol Biol Cell, 2006. **17**(1): p. 379-86.
337. Vembar, S.S. and J.L. Brodsky, *One step at a time: endoplasmic reticulum-associated degradation.* Nat Rev Mol Cell Biol, 2008. **9**(12): p. 944-57.
338. Zhang, K. and R.J. Kaufman, *From endoplasmic-reticulum stress to the inflammatory response.* Nature, 2008. **454**(7203): p. 455-62.
339. Liu, Y. and A. Chang, *Heat shock response relieves ER stress.* EMBO J, 2008. **27**(7): p. 1049-59.
340. Ozcan, L., et al., *Endoplasmic reticulum stress plays a central role in development of leptin resistance.* Cell Metab, 2009. **9**(1): p. 35-51.
341. Egan, M.E., et al., *Curcumin, a major constituent of turmeric, corrects cystic fibrosis defects.* Science, 2004. **304**(5670): p. 600-2.
342. Choo-Kang, L.R. and P.L. Zeitlin, *Induction of HSP70 promotes DeltaF508 CFTR trafficking.* Am J Physiol Lung Cell Mol Physiol, 2001. **281**(1): p. L58-68.
343. Moller, L.B., et al., *Identification and analysis of 21 novel disease-causing amino acid substitutions in the conserved part of ATP7A.* Hum Mutat, 2005. **26**(2): p. 84-93.
344. Tumer, Z., L. Birk Moller, and N. Horn, *Screening of 383 unrelated patients affected with Menkes disease and finding of 57 gross deletions in ATP7A.* Hum Mutat, 2003. **22**(6): p. 457-64.
345. Sherwood, G., B. Sarkar, and A.S. Kortsak, *Copper histidinate therapy in Menkes' disease: prevention of progressive neurodegeneration.* J Inherit Metab Dis, 1989. **12 Suppl 2**: p. 393-6.

SUMMARY

Posttranslational regulation of copper transporters

Peter V.E. van den Berghe

The transition metal copper is a versatile cofactor for many redox-active enzymes that perform essential functions. This same redox-activity allows the generation of toxic reactive oxygen species (ROS). To maintain copper homeostasis, organisms have evolved intricate mechanisms, performed by highly conserved proteins, to balance copper uptake, distribution and export on the systemic and cellular level. In this thesis, I describe biochemical and functional studies aimed at unraveling the mechanisms that regulate cellular copper uptake and export in relation to the molecular pathogenesis of Wilson disease, a hereditary copper overload disorder.

Regulation of dietary copper absorption is an important process in copper homeostasis. In **chapter 1** we review the role of distinct proteins involved in dietary copper uptake. We distinguish the subsequent steps between apical copper import by enterocytes and excretion into the portal circulation, and we discuss the regulation of dietary copper uptake during physiological and pathophysiological conditions. In **chapter 2,** we introduce our current knowledge of the regulation of copper excretion from the body. Regulation of copper excretion is equally important compared to regulation of copper intake, as is illustrated by the severe copper overload in patients with Wilson disease, in which hepatobiliary copper excretion is severely affected. Indeed, cellular copper export is mediated by the P_{1B}-type ATPasesATP7B, which is mutated in patients with Wilson disease, and by its closest homologue, ATP7A; the protein mutated in Menkes disease. In **chapter 2** we specifically review the posttranslational regulation of copper export by ATP7A and ATP7B with respect to protein structure, regulation of ATPase activity, copper-dependent and copper-independent trafficking, and the role of modifications and interacting proteins.

To enable monitoring changes in cellular copper homeostasis, we started our experiments by developing a novel transcription-based copper sensor based on a cell-intrinsic copper sensing mechanism. Copper binding to metallothioneins (MT) and subsequent activation of the metal-responsive transcription factor-1 (MTF-1) induces transcriptional activation of metal responsive genes. We developed the MRE (metal-responsive element)-Luciferase reporter, which contains four MREs from the mouse MT-1A promoter upstream of the firefly luciferase open reading frame (**chapter 3**). This enabled us to monitor bio-available copper in a copper-concentration-dependent manner. This MRE-Luciferase reporter allows quantitative, sensitive and high-throughput assessment of changes in cellular copper homeostasis.

In **chapters 3 and 4**, we focus on cellular copper import by the copper transporter (CTR) protein family. The human high-affinity copper transporter 1 (hCTR1) is required for intestinal copper absorption, and is essential for cellular copper uptake. In **chapter 3** we showed that the MRE–luciferase reporter was activated in a copper-dependent manner, and maximally induced at 1 μM $CuCl_2$, when hCTR1 was expressed, consistent with previous estimations of the transport affinity of hCTR1 (K_m approximately 1-5 μM). Electron microscopic crystallography of recombinant hCTR1 had revealed that hCTR1 subunits assemble in oligomeric complexes comprising three hCTR1 subunits, but whether this trimeric structure is necessary for copper transport was unknown. In **chapter 4**, we therefore characterized hCTR1 oligomerization and assessed the role of oligomerization in functional copper uptake. Co-immunoprecipitation of wild type (WT) hCTR1 with different epitope tags indicated that hCTR1 subunits interact in a copper independent

manner. hCTR1-dependent copper uptake, measured by the MRE-Luciferase reporter, was completely abolished by conversion of two highly conserved methionine residues in the second transmembrane helix of hCTR1 into isoleucines (hCTR1 M150I-M154I). Co-expression of hCTR1 M150I-M154I with WT hCTR1 did not affect oligomerization, expression or cellular localization of WT hCTR1, but WT hCTR1-dependent copper uptake was inhibited in a dominant fashion. Taken together, these data provide biochemical and functional evidence that oligomerization of hCTR1 is required for high-affinity copper transport activity by permitting the formation of a permeable channel necessary for copper uptake.

Several observations have indicated the existence of hCTR1-independent copper uptake pathways. In **chapters 3 and 4,** we characterized the homologous human CTR2 (hCTR2) as a *bona fide* copper uptake protein, and showed that it exhibits both differences and similarities to hCTR1. One significant difference between hCTR1 and hCTR2 is their subcellular localization. hCTR1 was localized at the plasma membrane and in intracellular organelles in a dynamic and regulated fashion. In contrast to hCTR1, hCTR2 was exclusively localized in late endosomes and lysosomes, which is in concordance with the localization of its yeast orthologue. Hence, we speculate that hCTR2 enables mobilization of copper from lysosomal copper pools in analogy with the function of CTR2 in yeast. Our data in **chapter 3** suggest that hCTR1 and hCTR2 also have distinct copper transport affinities. Expression of wild type hCTR2 significantly induced MRE-luciferase expression at 40-100 μM $CuCl_2$, whereas hCTR1-induced reporter activation occurred at much lower copper concentrations. Similar to hCTR1, chemical cross-linking of hCTR2 resulted in high-molecular-mass complexes containing hCTR2. Co-immunoprecipitation of hCTR2-vsvG and hCTR2-FLAG suggested that hCTR2 forms multimeric complexes, like hCTR1 (**chapter 3**). In addition, co-expression of WT hCTR2 with a methionine to isoleucine mutant of hCTR2 dominantly inhibited the hCTR2-dependent copper uptake (**chapter 4**). Apparently, oligomerization is a common characteristic for CTR proteins, which is required for CTR-dependent copper uptake in general. However, the structural differences together with the differences in subcellular localization between hCTR1 and hCTR2 suggest that cells have evolved separate copper uptake pathways that allow copper mobilization from different copper pools. Future research should focus on the regulation of copper acquisition from these copper pools and their contribution to copper homeostasis.

As has been mentioned above, hepatic copper excretion is mediated by ATP7B. Mutations in the gene encoding *ATP7B* result in the autosomal recessive copper overload disorder Wilson disease (WD). WD patients suffer from toxic copper accumulation in the liver and basal ganglia, and treatment is focused on reduction of circulating copper by dietary zinc supplementation or copper chelation. Despite treatment, a significant number of patients have neurological deterioration. In **chapter 5**, we investigated the possibility that defects arising from some WD mutations are ameliorated by drug treatment aimed at improvement of protein folding and restoration of protein function. To this end, we systematically characterized the molecular consequences of distinct *ATP7B* missense mutations associated with WD. Homology modeling of these different mutations suggested that most mutations result in misfolded ATP7B proteins. Consistent with these observations, almost all tested mutations resulted in reduced ATP7B protein expression, whereas mRNA

abundance was unaffected. Furthermore, physiological localization of ATP7B to the *trans*-Golgi network was abrogated, and mutant ATP7B was retained in the endoplasmic reticulum instead. However, increased expression and normalization of localization after culturing cells at 30°C suggested that these proteins were indeed misfolded. Four distinct mutations exhibited residual copper export capacity, which suggests that improved expression of these mutants could restore ATP7B expression in these patients. Interestingly, treatment with pharmacological chaperones curcumin and 4-phenylbutyrate (4-PBA), a clinically approved compound, partially restored expression and localization of most ATP7B mutants.

In conclusion, systematic analysis of patient mutations proved to be a valuable approach to unravel the molecular consequences of these disease-causing mutations and to explore novel treatment strategies. The surprisingly large number of WD mutations that result in protein misfolding indicates that pharmacological chaperone-treatment to improve protein folding, localization and function might actually improve clinical management of a significant proportion of WD-patients in the future.

NEDERLANDSE SAMENVATTING

Posttranslationele regulatie van kopertransporters

Peter V.E. van den Berghe

Koper is een belangrijke co-factor in verschillende redox-actieve enzymen, die essentiële functies in het lichaam uitvoeren. Helaas kan koper ook ernstige schade berokkenen doordat dit metaal betrokken is bij de vorming van vrije radicalen. Daarom is een strikte regulatie van de koperhuishouding van groot belang. Evolutionaire ontwikkelingen hebben een ingewikkeld systeem van sterk geconserveerde eiwitten voortgebracht, waardoor organismen in staat zijn om koperopname, koperdistributie en koperuitscheiding in balans te houden op cel- en lichaamsniveau. In dit proefschrift beschrijf ik biochemische en functionele studies, die gedaan zijn om inzicht te krijgen in de regulatie van cellulaire koperopname en koperexcretie, zowel onder fysiologische omstandigheden, als bij de ziekte van Wilson, een erfelijke koperstapelingsziekte.

Regulatie van koperopname vanuit de voeding is een belangrijke stap in koperhomeostase. In **hoofdstuk 1** hebben we een overzicht gegeven van de verschillende eiwitten die betrokken zijn bij koperopname in de darm. We onderscheiden daarbij de opeenvolgende stappen tussen koperopname vanuit het darmlumen in de darmcel, intracellulaire koperdistributie en koperexport vanuit de darmcel naar de bloedbaan. Tevens bediscussiëren we de regulatie van koperopname vanuit uit de voeding in fysiologische en pathofysiologische omstandigheden. In **hoofdstuk 2** introduceren we de huidige kennis van de regulatie van de koperuitscheiding uit het lichaam. De regulatie van de koperexcretie is net zo belangrijk als regulatie van de opname van koper uit het voedsel. Dit wordt nadrukkelijk geïllustreerd door de koperstapeling in de levers van patiënten met de ziekte van Wilson, waarin het proces van koperexcretie uit het lichaam is verstoord. De cellulaire koperexport is afhankelijk van de P_{1B}-type ATPases ATP7B, dat is gemuteerd in patiënten met de ziekte van Wilson, en van het homologe eiwit ATP7A; het eiwit gemuteerd in de ziekte van Menkes. In **hoofdstuk 2** bediscussiëren we specifiek de posttranslationele regulatie van ATP7A en ATP7B met betrekking tot de eiwitstructuur, de regulatie van ATPase activiteit, koperafhankelijke en koperonafhankelijke veranderingen in intracellulaire locatie, en de functie van modificaties en eiwit-eiwit interacties.

Om veranderingen in koperhomeostase te volgen hebben we een nieuwe kopersensor ontwikkeld, die is gebaseerd op de celintrinsieke mechanismen waarop koperconcentraties worden gedetecteerd. Koper kan binden aan metallothioneïnes (MT´s), waardoor de metaalresponsieve transcriptiefactor 1 (MTF-1) wordt geactiveerd. Vervolgens induceert MTF-1 de transcriptie van metaalresponsieve genen door te binden aan metaalresponsieve elementen (MRE´s) in promotorgebieden van deze genen, zoals MT's. Onze MRE-Luciferase reporter bevat vier van deze MRE's uit de promotor van het muizen *Mt-1a* gen, die in een vector met het Luciferase gen uit de vuurvlieg zijn gekloneerd (**hoofdstuk 3**). Hierdoor waren we in staat om de relatie tussen de extracellulaire koperconcentratie en de biologisch beschikbare hoeveelheid koper in de cel te detecteren. Samengevat maakt deze MRE-luciferase reporter gevoelige, kwantitatieve en groots opgezette analyse van koperhomeostase mogelijk.

In de **hoofdstukken 3 en 4** ligt de focus op cellulaire koperopname door de kopertransporter (CTR)-eiwitfamilie. De humane hoogaffiniteit-kopertransporter 1 (hCTR1) is van groot belang bij koperopname in de darm en is essentieel voor cellulaire koperopname. In **hoofdstuk 3** hebben we aangetoond dat in cellen, die recombinant hCTR1 tot expressie brengen, de MRE-Luciferase reporter maximaal werd geïnduceerd

bij een extracellulaire koperconcentratie van 1 µM $CuCl_{2.}$. Dit is in overeenstemming met de geschatte kopperaffiniteit van hCTR1 (K_m ongeveer 1-5 µM). Met behulp van elektronmicroscopische kristallografie van recombinant hCTR1 was eerder al aangetoond dat monomere hCTR1 polypeptide ketens een oligomeer complex vormen bestaande uit drie hCTR1 monomere eenheden. Omdat deze resultaten geen uitsluitsel geven over het belang van trimeervorming voor de functie van hCTR1, hebben we in **hoofdstuk 4** de rol van oligomerisatie van hCTR1 met betrekking tot functionele koperopname verder onderzocht. Co-immunoprecipitatie van wildtype (WT) hCTR1 met verschillende gefuseerde epitopen toonde aan dat hCTR1 eenheden onafhankelijk van koper aan elkaar konden binden. De hCTR1-afhankelijk inductie van de MRE-Luciferase reporter was volledig teniet gedaan door twee sterk geconserveerde methionine residuen in de tweede transmembraan helix van hCTR1 te muteren in isoleucines (hCTR1 M150I-M154I). Co-expressie van WT hCTR1 en hCTR1 M150I-M154I veranderde niets aan de binding tussen hCTR1 moleculen of aan de cellulaire positie. Alleen de hCTR1-afhankelijke koperopname was op een dominante manier gereduceerd. Door deze biochemische en functionele observaties concluderen we dat oligomerisatie van hCTR1 moleculen essentieel is voor hoogaffiniteit kopertransport, waarbij er een koperpermeabel kanaal wordt gevormd dat kopertransport mogelijk maakt.

Daarnaast zijn er ook indicaties in de literatuur voor CTR1-onafhankelijk koperopnameroutes in de cel. In de **hoofdstukken 3 en 4** hebben we de homologe kopertransporter humaan CTR2 (hCTR2) gekarakteriseerd als een *bonafide* koperopname-eiwit, dat zowel overeenkomsten als verschillen met hCTR1 heeft. Een significant verschil tussen hCTR1 en hCTR2 was de subcellulaire locatie. hCTR1 bevond zich op een dynamische en gereguleerde manier zowel op de plasmamembraan als in intracellulaire organellen. hCTR2 werd echter exclusief gelokaliseerd in endosomen en lysosomen, wat overeenkomt met de locatie van Ctr2 in gist. Naar aanleiding van dit onderzoek speculeren we dat hCTR2, in analogie met de functie in gist, een rol speelt in het mobiliseren van koper uit lysosomale kopervoorraden. De data in **hoofdstuk 3** suggereert dat er duidelijke verschillen in kopperaffiniteit zijn tussen hCTR1 en hCTR2. Expressie van WT hCTR2 veroorzaakte een significante koperafhankelijke inductie van de MRE-Luciferase reporter bij een extracellulaire koperconcentratie van 40-100 µM $CuCl_2$, terwijl expressie van recombinant hCTR1 maximale reporter inductie teweeg bracht bij lagere extracellulaire koperconcentraties. Door eiwitten, die in een complex zitten, op chemische wijze covalent aan elkaar te verbinden, konden we aantonen dat hCTR2 in hoogmoleculaire complexen voorkwam. Vervolgens hebben we met behulp van co-immunoprecipitatie aangetoond dat hCTR2 monomere eenheden, net als hCTR1, aan elkaar konden binden (**hoofdstuk 3**). Ook de hCTR2 afhankelijke koperopname werd op een dominante wijze gereduceerd door de twee geconserveerde methionines te muteren in isoleucines (**hoofdstuk 4**). Blijkbaar is oligomerisatie van CTR-moleculen een algemeen kenmerk van CTR. De verschillen in de subcellulaire locaties van hCTR1 en hCTR2 suggereert echter dat cellen gescheiden routes hebben ontwikkeld om koper uit verschillende kopervoorraden te mobiliseren. Verder onderzoek zal daarom moeten uitwijzen hoe kopertransport uit deze kopervoorraden wordt gereguleerd en hoe dit uiteindelijk bijdraagt aan koperhomeostase.

Zoals hierboven beschreven, is de cellulaire koperexport uit de lever afhankelijk van ATP7B. De ziekte van Wilson (WD) is een autosomaal recessieve koperstapelingsziekte,

die wordt veroorzaakt door mutaties in het gen dat codeert voor ATP7B. Patiënten met WD lijden aan schadelijke koperstapeling in de lever en de basale ganglia. Tegenwoordig worden deze patiënten behandeld door de hoeveelheid circulerend koper te reduceren met zinksupplementen in de voeding en het gebruik van koperchelatoren. Desondanks vindt er bij een significant aantal patiënten een verslechtering van de neurologische symptomen plaats. In **hoofdstuk 5** onderzochten we of we de defecten in ATP7B in WD patiënten konden verhelpen met medicijnen die de eiwitvouwing verbeteren. Daarom hebben we als eerste systematisch de moleculaire gevolgen van verschillende ziekteveroorzakende mutaties in *ATP7B* onderzocht. Uit modelering van deze mutaties op basis van homologie met andere eiwitten bleek dat de meeste van deze mutaties de eiwitvouwing van ATP7B sterk beïnvloedden. Deze bevinding werd ondersteund door de lage ATP7B eiwitexpressie en normale mRNA expressie, die het gevolg waren van de meeste mutaties in ATP7B. Een groot aantal mutanten van ATP7B bleek in het endoplasmatisch reticulum te worden vastgehouden in plaats van getransporteerd te worden naar het *trans*-Golgi netwerk. Door cellen bij 30°C te kweken, bleken zowel de expressie als de intracellulaire locatie van de meeste gemuteerde ATP7B eiwitten aanzienlijk genormaliseerd te zijn. Deze waarnemingen vormden een sterke aanwijzing voor verkeerde eiwitvouwing. Vier verschillende ATP7B-mutanten vertoonden residuale koperexportcapaciteit, zodat een verbetering van de eiwitexpressie al voldoende zou kunnen zijn om de kopertransportfunctie bij patiënten met deze varianten van ATP7B te herstellen. Het was daarom interessant, dat behandeling met de farmacologische chaperones curcumin en het voor de kliniek goedgekeurde 4-phenylbutyraat (4-PBA), de eiwitexpressie en locatie voor de meeste ATP7B mutanten kon verbeteren.

Samengevat is de systematische analyse van de verschillende ATP7B-mutanten een waardevolle aanpak gebleken, omdat we hierdoor in staat waren om de consequenties op eiwitniveau van deze mutaties in kaart te brengen en nieuwe behandelingsmethoden uit te testen. Een verrassend groot aantal mutaties bij patiënten met de ziekte van Wilson resulteerde in een verkeerde vouwing van ATP7B. Hierdoor kan behandeling van deze patiënten met farmacologische chaperones in de toekomst misschien uitkomst bieden door vouwing, positionering en functie van ATP7B in deze patiënten te verbeteren.

SAMENVATTING VOOR DE LEEK

Van sluizencomplex tot kopertransporters

Peter V.E. van den Berghe

Tijdens mijn promotieonderzoek heb ik onderzoek gedaan aan kopertransport. De eerste vraag die meteen opkomt is: "Waarom koper, dat gebruik je toch voor elektrische bedrading, koken en mooie beeldjes?" Koper is een metaal, dat het lichaam nodig heeft voor een aantal belangrijke processen. Ieder mens moet zuurstof inademen, maar zonder koper zouden wij het zuurstof niet kunnen gebruiken. Koper speelt daarom een belangrijke rol in de hersenen en koper is ook van essentieel belang voor het krijgen van een mooie bruine huidskleur in de zomer. Wanneer te weinig koper opgenomen kan worden uit het voedsel ontstaat er een tekort aan koper. Dit gebeurt in patiënten met de ziekte van Menkes, een erfelijke ziekte waarbij kinderen lijden aan een chronisch kopertekort. Hierdoor ontwikkelen deze kinderen sterke afwijkingen in de hersenen en overlijden ze meestal binnen drie jaar na de geboorte. Het gebruik van koper heeft ook een keerzijde, omdat koper erg schadelijk kan zijn. Een andere erfelijke aandoening, de ziekte van Wilson, is een ziekte waarbij mensen niet in staat zijn om koper uit de lever uit te scheiden. Dit leidt tot schadelijke koperophoping in de lever, waardoor deze patiënten ernstige leverafwijkingen krijgen. Hieruit blijkt dat het lichaam een goed georganiseerd systeem nodig heeft om koper in het lichaam op te nemen, op te slaan, maar ook om koper weer uit te scheiden. Daarom hebben lichaamscellen een complex systeem van eiwitten ontwikkeld, die koperopname en koperuitscheiding reguleren. Eiwitten kunnen worden gezien als een soort machines of onderdelen van machines in de cel. Ik heb mij de afgelopen vier jaar verdiept in de functie van de eiwitten die betrokken zijn bij het kopertransport.

De voorkant van mijn proefschrift heeft voor mij een dubbele betekenis. Aan de ene kant is dit de plek waar ik ben geboren en getogen. Aan de andere kant symboliseert het oude sluizencomplex in Hansweert de functie van zowel koperopname- en koperuitscheidingseiwitten. Deze eiwitten zijn namelijk een soort kopersluizen. De sluisdeur die betrokken is bij koperopname noemen we hCTR1. Uit onderzoek van anderen bleek dat een hCTR1-sluizencomplex uit meerdere (drie) hCTR1-sluisdeuren bestaat, maar het was onduidelijk of de vorming van een sluizencomplex met meerder hCTR1 eiwitten ook daadwerkelijk noodzakelijk was voor koperopname. Tijdens mijn onderzoek heb ik voor de eerste keer aangetoond, dat het hCTR1-sluizencomplex alleen werkt als het uit meerdere functionele hCTR1-sluisdeuren bestaat. Tijdens mijn onderzoek heb ik hCTR2 als een tweede koperopname-eiwit gekarakteriseerd. hCTR2 werkt bij hogere koperconcentraties dan hCTR1. Verder komt hCTR1 zowel aan de buitenkant van de cel als in compartimenten binnenin de cel voor, terwijl hCTR2 uitsluitend in compartimenten binnenin de cel voorkomt. Deze compartimenten zou men kunnen zien als kopervoorraden die de cel kan aanspreken wanneer dit nodig is. De verschillende locaties in de cel van hCTR1 en hCTR2 suggereert dat cellen verschillende koperopname routes hebben ontwikkeld om koper uit verschillende kopervoorraden te verplaatsen. Verder onderzoek zal daarom moeten uitwijzen hoe kopertransport uit deze kopervoorraden wordt gereguleerd en hoe dit uiteindelijk bijdraagt aan de koperhuishouding.

Koperuitscheiding vanuit de cel kan evengoed als een sluizencomplex worden voorgesteld, waarbij het eiwit ATP7B de kopersluis vormt. Omdat koperuitscheiding een proces is dat energie kost, kan ATP7B dus worden voorgesteld als een kopersluis die als het ware benzine nodig heeft om koper de cel uit te pompen. In patiënten met de ziekten van Wilson kan ATP7B geen koper uit de lever pompen. Het bleek dat de sluisdeuren of de benzinemotor

bij de ziekte van Wilson vaak verkeerd in elkaar worden gezet. Hierdoor komt ATP7B niet op de juiste plek in de cel of is de motor kapot of geblokkeerd. Deze foutjes kan de cel helaas niet zelf oplossen, maar er zijn bepaalde medicijnen die deze foutjes gedeeltelijke kunnen verhelpen. Dit soort medicijnen helpt bij het correct in elkaar zetten van de sluisdeuren. Tijdens ons onderzoek bleek dat de twee stoffen Curcumin en 4-phenylbutyraat in staat waren om sommige van de foutjes in ATP7B, die bij patiënten voorkomen, gedeeltelijk te herstellen. Dit biedt dus mogelijk nieuwe behandelingsmethoden voor patiënten met de ziekte van Wilson. Er is dus verder onderzoek nodig om uit te zoeken of we deze medicijnen in de toekomst ook daadwerkelijk in patiënten met de ziekte van Wilson kunnen gebruiken.

DANKWOORD

Beste lezer,

Als jochie uit Zeeland heeft het grootste gedeelte van mijn jeugd zich op en om het water afgespeeld. Ik ben vlak bij de oude sluizen in Hansweert geboren en dit sluizencomplex is een mooie metafoor voor mijn onderzoek naar kopertransport. Na jaren ploeteren en zwoegen is mijn proefschrift eindelijk klaar. Als ik terugkijk kom ik tot de conclusie dat promoveren lang niet zo leuk zou zijn geweest zonder al mijn leuke vrienden en collega's om me heen. Daarom wil ik mijn laatste paar pagina's gebruiken om deze mensen te bedanken. De afgelopen viereneenhalf jaar heb ik lief en leed gedeeld met de mensen van de afdeling metabole en endocriene ziekten. De afdeling is inmiddels zo groot geworden dat mijn dankwoord onleesbaar wordt als ik al die mensen persoonlijk ga bedanken. Daarom aan alle AIO's, stafmedewerkers, postdoc's, analisten en andere medewerkers: bedankt voor de leuke tijd! Daarnaast wil ik een aantal mensen in het bijzonder bedanken.

In de eerste plaats Leo klomp, mijn co-promotor. Leo, we kennen elkaar sinds het begin van mijn studie medische biologie in Utrecht, en eigenlijk zijn we elkaar steeds weer tegengekomen. In de laatste viereneenhalf jaar is onze samenwerking enorm toegenomen doordat ik als AIO in jouw lab aan de slag ging. Ik waardeer het heel erg dat je me de ruimte hebt gegeven om me te ontwikkelen als een zelfstandige onderzoeker, zodat ik nu ook vol vertrouwen de volgende stap in mijn carrière kan zetten. Daarnaast heb ik altijd smakelijk kunnen lachen om jouw woordenwisselingen met je computer tijdens het maken van presentaties.

Beste Ruud, als mijn promotor was je vooral op de achtergrond bezig, maar vanaf de zijlijn hield je altijd wel een oogje in het zeil. Ik vind het echt heel erg knap dat je van iedereen weet waar hij of zij mee bezig is en er dan ook nog iets zinnigs over weet te zeggen. Het is echt heel erg bijzonder hoe je op zo een rustige, charismatische wijze leiding geeft aan de afdeling.

Als het dan eindelijk zo ver is dat de promotie voor de deur staat, dan moet je ook eens gaan nadenken over de keuze van de paranimfen. De eerste keuze was eigenlijk de gemakkelijkste. Erwin, als mijn enige en kleine broertje vind ik het ontzettend fijn dat je naast me staat op het moment van mijn verdediging. Ik heb enorm veel bewondering voor alles wat je doet en ik heb heel veel respect voor de manier waarop je keihard werkt om te bereiken wat je voor ogen hebt. Ik wens je al het geluk van de wereld toe met je vriendinnetje Dominique.

Mijn tweede paranimfje komt uit het lab, maar omdat er zoveel leuke mensen op het lab rondlopen was dit een wat lastigere keuze. Lieve Willianne, ik ben erg blij dat jij mijn paranimfje bent als laatste der Mohikanen van de eens zo omvangrijke kopergroep. Vaak was ik weer stomverbaasd door de enorme bergen werk die jij wist te verzetten en door het excessieve geweld dat ik af en toe te verduren kreeg.

Mijn interesse voor het wetenschappelijk onderzoek werd goed aangewakkerd tijdens mijn wetenschappelijke stages. Sander, jij hebt me tijdens mijn eerste stage geholpen bij mijn babystapjes in het lab. Jeff, jouw onmetelijke energie en enthousiasme gaven voor mij de doorslag om daarna als AIO aan de bak te gaan.

Ik weet dat ik ontzettend kan mopperen, klagen en altijd mijn mening klaar heb over de gang van zaken in en om het lab, maar ik heb echt veel waardering voor de analisten die

ondanks dit alles de afdeling goed draaiende houden en hierdoor de AIO's en postdocs veel werk uit handen nemen.

Een groot deel van het denk-, mopper-, zeur-, lach-, schrijf-, discussie- en brainstormwerk vond plaats in de AIO-kamer, waar toevallig ook de meeste (ex-)collega's uit de kopergroep "woonden". In wissellende bezetting waren dit mensen waar ik erg veel mee optrok en erg veel aan heb gehad. Lieve Patricia, ik heb ontzettend veel bewondering voor jouw doorzettingsvermogen en ambitie. Vanaf het prille begin stortte jij vaak je hart uit over alle futiliteiten die je weer op konden winden zoals jouw liefdesleven of dat van anderen. Hoewel je misschien niet altijd alles vertelde. Prim (of priemel voor intimi), als mijn drinkmaatje waren onze bonte avonturen een welkome afleiding op het dagelijkse lableven. Ik kan nog steeds smakelijk lachen om de blinde paniek die jou af en toe overmande als iets niet helemaal ging zoals verwacht. Bart, sorry dat we altijd zo een drukte op de kamer maakten. Jouw drive en de fijne discussies waren altijd een goede motivatie om me in nieuwe dingen vast te bijten. Toen het aandeel kopermensen in de AIO-kamer drastisch was afgenomen, werd de kamer langzamerhand bevolkt door een wat rustiger, maar zeker niet minder leuk publiek. Stan, Gemma, Henk en Raffaella: bedankt voor de gezellige werksfeer op onze kamer en dat jullie me altijd lekker lieten uitrazen als ik het weer eens ergens niet mee eens was.

Als AIO ga je toch het meest om met de mensen die in het zelfde schuitje zitten. De borrels en sociale uitstapjes met de AIO's (Wendy, Patrica, Prim, Lieke, Sjaac, Olivier, Leyla, Ellen, Yuan, Gemma, Hannelie, Henk en Sabine) waren vaak een mooi platform voor het uitwisselen van de nieuwste labroddels en frustraties. Alleen jammer dat de borrelcommissie en het filmavondinitiatief uiteindelijk een zachte dood zijn gestorven. Saskia, ik ben erg blij dat je me af en toe weer even met mijn beide benen op de grond wist te zetten.

De mensen die mij nauwlettend in de gaten hebben gehouden tijdens mijn doldwaze NVH-avonturen weten dat ik niet altijd even blij was met de doktertjes. Toch moet het van mijn hart dat onze labdokters Janneke, Henk, Sabine en Hannelie puike exemplaren zijn die zich goed staande weten te houden binnen ons onderzoekswereldje.

Vrouwtje theelepel is mijn labpartner in crime gebleken. Lieke, ik verbaas me er keer op keer weer over hoe onbedwingbaar nieuwsgierig jij kunt zijn. Na ons voortdurend gekibbel als een getrouwd stel tijdens ons harde pipetteerwerk kan ik Bart eigenlijk alleen maar succes wensen in jullie echte huwelijk. Jij was natuurlijk niet de enige persoon in het befaamde U-tje Peter en Co., want Dennis was een rotsvast onderdeel van de practical joke terreur die ons lab jaren lang heeft geteisterd.

Het lab kreeg ineens veel meer fleur toen de mediterrane schonen het lab betraden. The average noise level in the lab increased significantly with several decibels, and poor Prim suffered from the superlative of the practical lab joke after the arrival of the smallest Greek lady I have ever seen. My dear Alexandra, I really enjoyed our mutual interest in good food, drinking and dancing. I value your friendship greatly and I really miss you in the lab.

Ciao bella Raffaella, you are such a lovely noisy lady, I really like your "angry" behavior when you are passionate about the things in your life and work. I am impressed by your ability to pick up only Dutch slang like FF kaike and boeiuh …

Monique, het was altijd een verademing wanneer jij weer antwoord wist op een of ander praktisch of logistiek probleem. Daarnaast is het echt wonderbaarlijk hoe onze eigen Truus de mier alle touwtjes strak in handen heeft. Beste Truus, ik heb altijd dankbaar gebruikgemaakt

van al je hulp. Margriet, ik weet dat ik niet de gemakkelijkste was om mee samen te werken, omdat ik weer eens een onmogelijk statistisch model had bedacht. Ontzettend bedankt voor alle hulp bij mijn statistische vraagstukken. Inge, bedankt voor de opbouwende kritiek in werkbesprekingen en voor je hulp bij mijn samenvatting.

Het begeleiden van studenten en het helpen van mensen heb ik altijd een dankbare taak gevonden tijdens mijn werk in het lab. Het was dan ook erg leuk en uitdagend om mijn twee studenten Ellen en Reinoud de fijne kneepjes van het onderzoek bij te brengen. Ik heb hier erg veel van geleerd en ik hoop dat dit wederzijds is. Daarnaast was het een luxe, dat Ellen van Beurden (en indirect Helga) mij ondersteunde bij een aantal van mijn experimenten.

Naast alle labmensen en de gezelligheid op het lab is mijn sociale leven minsten net zo belangrijk. Theo, Pat, Joene en Robbie: als vijfde wiel aan de wagen heb ik altijd ontzettend genoten van de stamppot en drink-, concert- en festivaluitspattingen die vast op het programma stonden. Alvast mijn excuses voor het feit dat ik van plan ben om geen iPod's meer stuk te maken. Genoeg is genoeg zullen we maar zeggen. Robbie, bedankt dat je me in al die tijd niet van de muur hebt laten donderen.

De salsafeestjes met alle salsavriendjes en -vriendinnetjes waren een welkome afleiding op het alledaagse lableven. Lieve Annewytske, ik vind je echt top en ik hoop dat we onze goede gesprekken met overmatig wijngebruik nog lang kunnen voortzetten.

Richard, ik vind het ontzettend tof dat we sinds de kleuterschool beste vrienden zijn. Sorry, dat ik je heel vroeger nog wel eens achternazat. Ik waardeer het echt heel erg dat we elkaar er nooit op aankijken op de soms wat lange tijd tussen onze afspraken en dat het altijd is zoals vanouds, zoals het hoort.

Deo en Jose jullie zijn van die zeldzaam bijzondere mensen die er altijd zijn in zowel de leuke als de minder leuke tijden. Ik ben echt heel erg blij dat ik jullie tot mijn directe vriendenkring mag rekenen.

Lieve Silvia, het afgelopen jaar was echt heel bijzonder. Ik had van tevoren nooit verwacht dat ik zo ontzettend verliefd op jou zou worden. Door jou had ik die o zo belangrijke zeldzame momentjes van rust en ontspanning. Daarnaast vind ik het echt heel knap dat je zoveel begrip en geduld had in deze toch wel lastige periode met veel stress en weinig tijd. Ik ben echt heel erg blij met je en hoop dat we nog heel lang van elkaar kunnen blijven genieten!

Lieve pa en ma, van jullie heb ik de belangrijkste lessen geleerd die ik in de afgelopen 29 jaar heb kunnen leren. Door jullie beiden weet ik dat niets vanzelf komt en dat er altijd mensen zijn die onvoorwaardelijk om je geven, mensen die sterk genoeg zijn om te blijven en niet voor de problemen weglopen. Ik ben jullie enorm dankbaar voor alle steun en interesse. Ik ben erg trost op het feit dat jullie samen alles de baas blijven en van het leven genieten. Ik hou van jullie.

CURRICULUM VITAE & PUBLICATIONS

Peter van den Berghe werd geboren op 3 januari 1980 te Reimerswaal. Na het behalen van zijn VWO diploma in 1998 aan het sint Willibrord College te Goes, begon hij in september van dat jaar aan zijn opleiding Medische Biologie aan de Universiteit Utrecht. Voor zijn studie heeft hij in 2003 zijn bijvak stage afgerond binnen de Functional Genomics groep van Prof. Dr. Ronald Plasterk in het Hubrecht Laboratorium te Utrecht onder begeleiding van Dr. Sander van der Linden. Tijdens deze stage heeft hij meegewerkt aan een genome-wide RNAi-screen in de nematode *Caenorhabditis elegans*. Daarna volgde hij in 2003 zijn hoofdvakstage binnen de afdeling Immunotherapie in het Wilhelmina Kinderziekenhuis te Utrecht onder de begeleiding van Dr. Jeffrey Beekman en Dr. Jeanette Leusen. Hier werkte hij aan de interactie tussen het eiwit Filamine A en de hoogaffiniteitreceptor voor immunogolbulines, FcγRI. Het doctoraal diploma medische biologie werd behaald op 24 april 2004 en in september van dat jaar is hij begonnen als Assistent in Opleiding binnen de afdeling Metabole en Endocriene ziekten in het Wilhelmina Kinderziekenhuis, onderdeel van het Universitair Medische Centrum Utrecht onder begeleiding van Dr. Leo Klomp en Prof. Dr. Ruud Berger. De resultaten van zijn onderzoek zijn beschreven in dit proefschrift.

Peter van den Berghe was born on Januari 3rd in 1980 in Reimerswaal, the Netherlands. He attended the sint Willibrord College secondary school in Goes, the Neterlands, after which he started to study Medical Biology at the Utrecht University, the Netherlands in 1998. He finished his minor practical training rotation in 2003 at the Functional Genomics group of Prof. Dr. Ronald Plasterk in the Hubrecht Laboratory in Utrecht, the Netherlands, under supervision of Dr. Sander van der Linden, where he performed a genome-wide RNAi screen in the nematode *Caenorhabditis elegans*. In 2003, he started his second practical training rotation at the department of Immunotherapy in the Wilhelmina Children's Hospital in Utrecht, under supervision of Dr. Jeffrey Beekman and Dr. Jeanette Leusen, where he studied the interaction between Filamin A and the high-affinity immunoglobulin receptor FcγRI. After graduating as MSc. in Medical Biology on April 24th 2004, he started as a PhD student at the department of Metabolic and Endocrine Disease in the Wilhelmina Children's Hospital of the University Medical Center Utrecht, under supervision of Dr. Leo Klomp and Prof. Dr. Ruud Berger. The results of his research are described in this thesis.

List of Publications

Beekman JM, van der Poel CE, van der Linden JA, van den Berg DL, **van den Berghe PV**, van de Winkel JG, Leusen JH. Filamin A stabilizes Fc gamma RI surface expression and prevents its lysosomal routing. J. Immunol. 2008 Mar 15;180(6):3938-45.

de Bie P, van de Sluis B, Burstein E, **van de Berghe PV**, Muller P, Berger R, Gitlin JD, Wijmenga C, Klomp LW. Distinct Wilson's disease mutations in ATP7B are associated with enhanced binding to COMMD1 and reduced stability of ATP7B. Gastroenterology. 2007 Oct;133(4):1316-26. Epub 2007 Jul 25.

v**an den Berghe PV**, Folmer DE, Malingré HE, van Beurden E, Klomp AE, van de Sluis B, Merkx M, Berger R, Klomp LW. Human copper transporter 2 is localized in late endosomes and lysosomes and facilitates cellular copper uptake. Biochem. J. 2007 Oct 1;407(1):49-59.

Simmer F, Moorman C, van der Linden AM, Kuijk E, **van den Berghe PV**, Kamath RS, Fraser AG, Ahringer J, Plasterk RH. Genome-wide RNAi of C. elegans using the hypersensitive rrf-3 strain reveals novel gene functions. PLoS Biol. 2003 Oct;1(1):E12. Epub 2003 Oct 13.